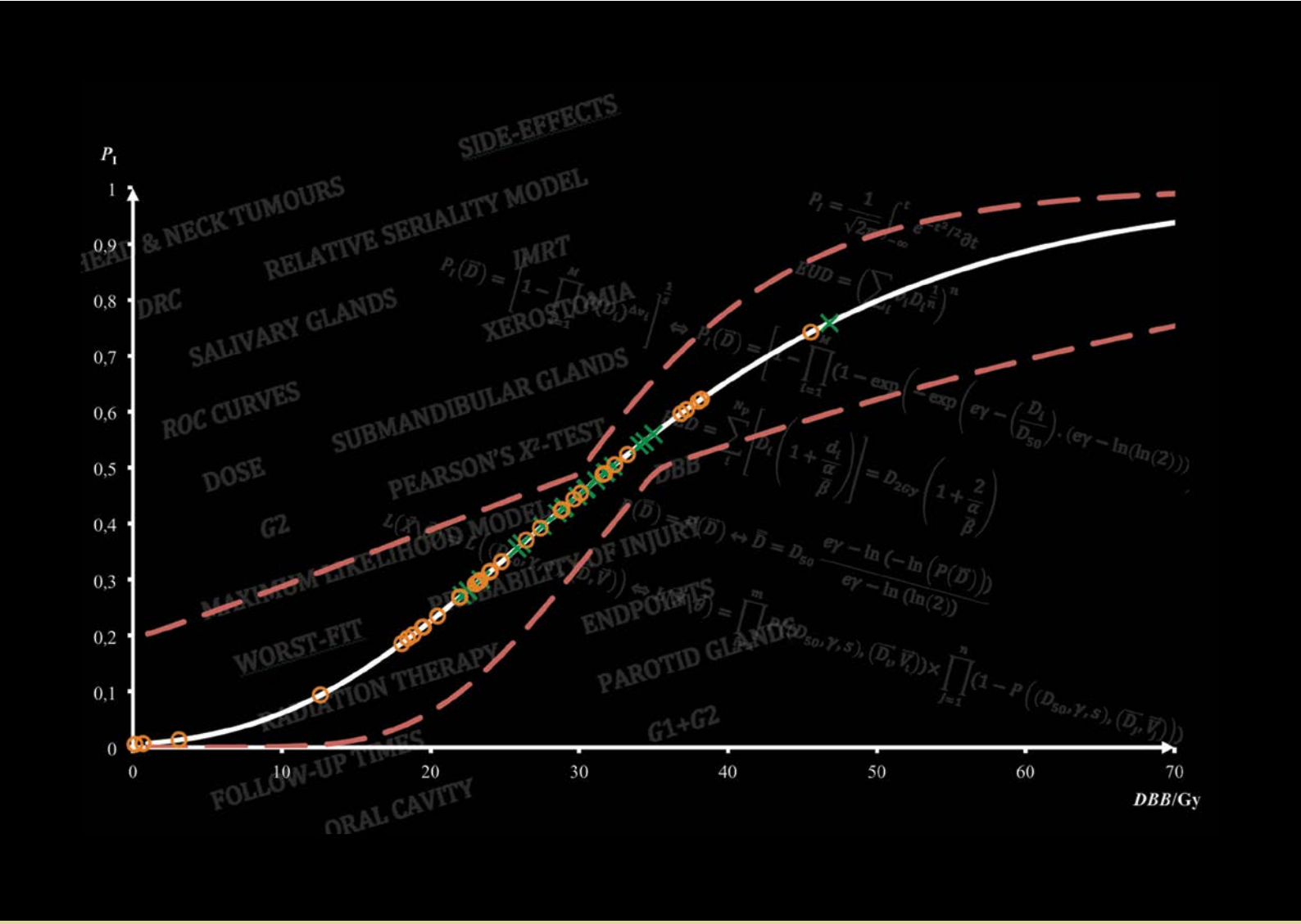

Cláudia de Melo Rocha Peixoto Xavier

DERIVATION OF DOSE-RESPONSE PARAMETERS FOR XEROSTOMIA IN HEAD AND NECK TUMOUR PATIENTS TREATED WITH RADIATION THERAPY

Dissertation presented to the Department of Physics
at Coimbra University to accomplish the academic degree
of Master in Biomedical Engineering

July 2014

· U C ·

Universidade de Coimbra

• U C •

FCTUC FACULDADE DE CIÊNCIAS
E TECNOLOGIA
UNIVERSIDADE DE COIMBRA

Cláudia de Melo Rocha Peixoto Xavier

Derivation of dose-response parameters for xerostomia in head and neck tumour patients treated with radiation therapy

Dissertation presented to the Department of Physics at Coimbra University to accomplish the academic degree of Master in Biomedical Engineering.

Supervisors:

Brígida da Costa Ferreira, *Ph.D.*

Panayiotis Mavroidis, *Ph.D.*

Maria do Carmo Lopes, *Ph.D.*

Coimbra, 2014

This work was developed in collaboration with:

Instituto Português de Oncologia Francisco Gentil – E.P.E

Universidade de Aveiro

Cancer Therapy and Research Center at the University of Texas Health Science Center at San Antonio Texas

Acknowledgments

This passed year was a journey, which was marked by every single person that passed through and contributed in many different ways to it. Due to that, it is only fair to start by paying my sincere acknowledgments to them.

In USA, more specifically in San Antonio, Texas I want to start by acknowledging Doctor Niko Papanikolaou, professor and chief at the Medical Physics Division in CTRC at UTHSCSA, for receiving me so well and making me fill welcome in CTCR. To Doctor Panayiotis Mavroidis, my supervisor in CTRC, my genuine acknowledgment for giving me this great opportunity, for helping make it happen and for all the support given to me during my stay in San Antonio. To Carolina and Nina, assistants in CTRC, thank you for being tireless helping me with all the bureaucratic documents and for everything else I have needed before and during my stay there. To Mr. Shawn, thank you for bringing such joy to my "one million dollars" lunch breaks and for teaching me that even if the heart is not that happy there is always a reason to smile. To the Martinez family, my heartfelt acknowledgment for all the help, support and for treating me as a member of the family, you will always be in my heart. And to Sanne Strijker, my "Siamese twin" in San Antonio and friend for life, thank you for all the moments shared, help, care and for turning my passage through San Antonio so memorable to the point where I will never forget it and want to go back.

In Portugal, I want to give my acknowledgments to the radiation oncologist Leila Khouri from the Radiation Therapy Department of IPOCFG for all the availability provided throughout the course of this project. To Doctor Maria do Carmo Lopes, director of the Medical Physics Department at IPOCFG, for receiving me at IPOCFG and for the always-present time for me in your so busy schedule. To Tiago Ventura for all the constructive criticism, help and good disposition. To Doctor Paulo Crespo, for the availability provided. To professor Miguel Morgado, coordinator of the course Biomedical Engineering at FCTUC, for all the help and support given through this entire project and for all the dedication showed to all the students at the Physics Department. To my godmother, Doctor Maria José Capelo, for always believing in me and for all the help.

I also want to give my honest acknowledgments to people without whom my life would not be so filled and lived, my friends, specifically to Margarida, my colleague of battle and my support through this hole year, and to Rita C. for sharing the "Thesis breaks" with me and all types of encouragement.

I want to give a special acknowledgment to Doctor Brígida Ferreira, my supervisor at IPOCFG, that without knowing helped made a huge dream of mine come true (studying in USA), that believed in me and in my competences even when I dough them, that guided me tirelessly through all this project and that always helped and supported me. Thank you for everything, I will never forget you and everything you did for me.

At last but not least, I want to give my acknowledgments to my hole family for all the support you gave me before and during my journey, specially to my brother for not throwing me from the 7th floor window when I bothered him with my worries and problems, and to my parents to whom I owe everything: support, love, care, etc. Thank you for giving me all that I have needed, for wanting the best for me and for supporting my dreams.

None of this would be possible without my parents and therefore I dedicate my Master Thesis to you both, Lólia and Nuno Xavier.

"All we are is the result of
all we have thought"

- Buddha

Abstract

Purpose: To derive dose-response parameters for the radiation therapy side-effect xerostomia in head and neck tumour patients treated at *IPOCFG*.

Methods and Materials: A total of 302 patients with head and neck tumours treated with Intensity Modulated Radiation Therapy (*IMRT*) were included in this study. Acute and late xerostomia evaluated according to the guidelines established by the Radiation Therapy Oncology Group and the European Organization for Research and Treatment of Cancer (*RTOG/EORTC*) were studied. *DRC* were derived for the Relative Seriality model at the follow-up times: 7 weeks, 3, 7, 12, 18 and 24 months. The incidence of complications was determined by dividing the patients into: Grade 0 (*G*0, complication-free) vs. Grade 2 (*G*2, moderate severity) and *G*0 vs. *G*1+*G*2 (mild+moderate). The dose that irradiated the contralateral parotid, the ipsilateral parotid, both parotids and all salivary glands was used to establish dose-response relations. Goodness of the fit was evaluated using the *ROC* curve, Pearson's X^2-test and Worst-fit methods.

Results: The values of D_{50}, γ and s for xerostomia *G*2 at the follow-up times of 12, 18 and 24 months considering the dose that irradiated the contralateral parotid were 38.6, 0.707, $1x10^{-4}$; 51.7, 0.444, $1x10^{-4}$; and 48.3, 0.685, $1x10^{-4}$, respectively. Similarly, for the sum of the parotids these were 39.2, 0.730, $1x10^{-4}$; 54.2, 0.468, $1x10^{-4}$; and 51.7, 0.633, $1x10^{-4}$, respectively. Statistical analysis showed that the derived Relative Seriality model quantifying xerostomia *G*2 based on the dose that irradiated the contralateral parotids and the sum of the parotids has a reasonable-good quality (range 0.6-0.7) while the model derived quantifying *G*1+*G*2 xerostomia only reached reasonable quality (~0.6).

Conclusions: Using the derived parameters for the Relative Seriality model, a better prediction of the probability of xerostomia *G*2 may be made compared to xerostomia *G*1+*G*2. The best radiobiological parameters were found using the dose irradiating the contralateral parotids and sum of the parotids, for the follow-up times of 12, 18 and

24 months. To minimize the probability of xerostomia the dose in the parotids should be below 28Gy.

Xerostomia, Salivary glands, Dose-response curves, Relative Seriality model, Head and neck tumours.

Resumo

Objetivo: Derivação de parâmetros dose-resposta para efeitos secundário da radioterapia, xerostomia, em doentes com tumores de cabeça e pescoço tratados no *IPOCFG*.

Métodos e Materiais: Um total de 302 pacientes com tumores de cabeça e pescoço, tratados com Radioterapia de Intensidade Modulada (*IMRT*), foram incluídos neste estudo. O efeito secundário estudado foi xerostomia aguda e tardia, avaliadas segundo as recomendações do Radiation Therapy Oncology Group e da European Organization for Research and Treatment of Cancer (*RTOG/EORTC*). Foram derivadas curvas de dose-resposta para o modelo Relative Seriality para os períodos de follow-up: 7 semanas, 3, 7, 12, 18 e 24 meses. A incidência de complicações foi determinada através da divisão dos doentes em: Grau 0 (*G*0, sem complicações) vs. Grau 2 (*G*2, severidade moderada) e *G*0 vs. *G*1+*G*2 (suave+moderada). Para estabelecer as relações de dose-efeito, foi considerada a dose fornecida na parótida contra-lateral, parótida ipsilateral, soma das parótidas e glândulas salivares. A qualidade do ajuste foi avaliada através dos métodos: curvas *ROC*, Pearson's X^2-test e Worst-fit.

Resultados: Os valores de D_{50}, γ e s para a xerostomia *G*2 nos períodos de follow-up de 12,18 e 24 meses considerando a dose fornecida na parótida contra-lateral foram 38.6, 0.707, $1x10^{-4}$; 51.7, 0.444, $1x10^{-4}$; e 48.3, 0.685, $1x10^{-4}$, respetivamente. Para a soma das parótidas estes foram 39.2, 0.730, $1x10^{-4}$; 54.2, 0.468, $1x10^{-4}$; e 51.7, 0.633, $1x10^{-4}$, respetivamente. A análise estatística do modelo demonstrou que o modelo Relative Seriality para xerostomia *G*2 considerando a dose fornecida nas parótidas contra-laterais e soma das parótidas tem uma qualidade razoável-boa (intervalo de 0.6 a 0.7) enquanto que o modelo derivado para quantificar a xerostomia *G*1+*G*2 só atingiu uma qualidade razoável (aproximadamente 0.6).

Conclusões: Usando os parâmetros derivados para o modelo Reltive Seriality, pode ser feita uma melhor previsão da probabilidade de xerostomia *G*2, do que para xerostomia *G*1+*G*2. Os melhores parâmetros rádio-biológicos foram obtidos através

da utilização da dose que irradiou as parótidas contra-laterais e soma das parótidas para os períodos de follow-up de 12, 18 e 24 meses. De forma a minimizar a probabilidade de xerostomia, a dose administrada às parótidas deve ser inferior a 28Gy.

Xerostomia, Glândulas salivares, Curvas dose-resposta, Modelo Relative Seriality, Tumores de cabeça e pescoço.

Contents

List of Figures

List of Tables

Acronyms & Abbreviations

3D	*Tri-dimensional*
3D-CRT	*Tri-dimensional Conformal Radiation Therapy*
ART	*Adaptive Radiation Therapy*
AUC	*Area Under the Curve*
BED	*Biologically Effective Dose*
CBCT	*Cone-Beam Computed Tomography*
CI	*Confidence Interval*
CT	*Computed Tomography*
CTV	*Clinical Target Volume*
dIMRT	*Direct Intensity Modulated Radiation Therapy*
DBB (or $\overline{\overline{D}}$)	*Biologically Effective Uniform Dose*
DRC	*Dose-Response Curves*
DVH	*Dose-Volume Histogram*
EORTC	European Organization for Research and Treatment of Cancer
FPR	*False Positive Ratio*
GTV	*Gross Tumour Volume*
H&N	*Head And Neck*
ICRU	International Commission on Radiation Units and Measurements
IMRT	*Intensity Modulated Radiation Therapy*
IPOCFG	Instituto Português de Oncologia de Coimbra Francisco Gentil
MLC	*Multi-leaf Collimator*
OAR	*Organs At Risk*
P_I	*Probability of Injury*

PRT	*Planning Risk Volume*
PTV	*Planning Target Volume*
rIMRT	*Rapid Intensity Modulated Radiation Therapy*
ROC	*Receiver Operating Characteristic*
RT	*Radiation Therapy*
RTOG	Radiation Therapy Oncology Group
TPR	*True Positive Ratio*

CHAPTER 1: Introduction

1.1 Theoretical Framework

In 1895 a big discovery marked the health sector when Roentgen discovered the x-rays. X-rays started being used to treat skin lesions in a very short time. However, the physical effects of the radiation beams in tissues were not yet known. The outcome of the first treated patients wasn't as good as expected due to inability to control the cancer and the large morbidity. In 1897 Henri Becquerel discovered the radioactivity, which was further studied by Marie and Pierre Curie in 1898, giving rise to the discovery of two radioactive elements: radium and polonium. Suppositions that radium rays could be used to treat diseases lead to studies about the biological effects of the radiation beams in tissues and to improvements in the delivery of the radiation. In 1928 R. Wideroe showed that electrons can be accelerated in a tube through the application of a certain radio frequency voltage in separated sections of the tube so that when arriving to a gap they would be accelerated with the double of the energy. This idea was applied to the construction of electron linear accelerators, which became clinically available in 1950. Yet, with x-rays beams high doses in normal tissues and tumours were still being delivered. Subsequently, in 1965 Takahashi S. created the multi-leaf collimator. This is composed by a set of independent leaves that move into pre-defined segments controlling the shape of the beam [1-4].

The goal of radiation therapy consists on the control/reduction of the tumour and minimizing the damages in normal tissues. To achieve that goal, a plan is made for the patient to maximize the irradiation of the tumour while protecting the organs at risk that surround the tumour. Depending on the radiosensitivity of the patient and the dose delivered, the irradiation of healthy tissues may lead to the development of side-effects. For patients with head and neck tumours important organs at risk are the parotid glands and oral cavity, whose irradiation above the tolerance may cause complications like, xerostomia, mucositis and earing loss.

1.2 Aim

The aim of this master thesis consisted in the derivation of the dose-response parameters of the Relative Seriality model for the radiation therapy side-effect: xerostomia. The clinical data from head and neck tumour cases treated with radiation therapy at *IPOCFG* since 2007 were used in this study. The goodness of the fit of the derived models was evaluated through a statistical analysis using the methods: Receiving Operator Characteristic curve, Pearson's X^2-test and Worst-fit. A comparison with the parameters published in literature was also made.

1.3 Organization of the Dissertation

This thesis was divided into six chapters:

- **CHAPTER 1: Introduction** – this chapter presented a theoretical framework of this thesis and its main goal;
- **CHAPTER 2: H&N Radiation Therapy** – in this chapter the basics of the radiation therapy for head and neck tumours are presented. The concept of Image-Guided Radiation Therapy is discussed and some radiobiological dose-response models are introduced;
- **CHAPTER 3: Materials & Methods** –this chapter is divided into two parts. The first part presents the criteria for patient selection and treatment details. The second part describes the statistical methods used to evaluate the goodness of the fit of the Relative Seriality model;
- **CHAPTER 4: Results** – here the results obtained are presented. This chapter is composed by three sections: $G0$ vs. $G2$, $G0$ vs. $G1+G2$ and the comparison between mean dose values and Biological Effective Uniform Dose values;
- **CHAPTER 5: Discussion** – in this chapter the results are discussed. Dose-response curves derived for different structures and time periods are compared;
- **CHAPTER 6: Conclusions** – summarizes the conclusions achieved through this study and future studies are proposed.

CHAPTER 2: H&N Radiation Therapy

2.1 Target Volumes & Organs at Risk

There are several imaging means for the diagnosis of oncological problems as, e.g. the Magnetic Resonance Imaging (*MRI*), the Positron Emission Tomography (*PET*) and the Computed Tomography (*CT*) scan, which allow diagnosis. After a patient has been diagnosed, he will be forwarded to an oncological institution where a multi-disciplinary board will decide the proper care (Figure 1). Generally in 50% of the patients radiation therapy is recommended.

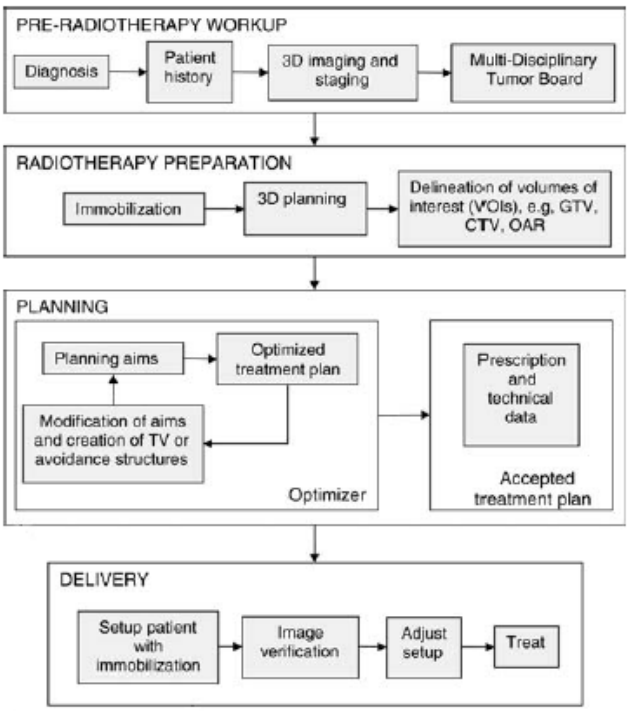

Figure 1 – Workflow of radiation therapy [5].

Most of radiation therapy treatments are delivered in multiple fractions. In head and neck tumour cases an immobilization mask is made to guarantee that the patient will reproduce the position of the planning *CT* through all the fractions of the radiation therapy treatment (Figure 2).

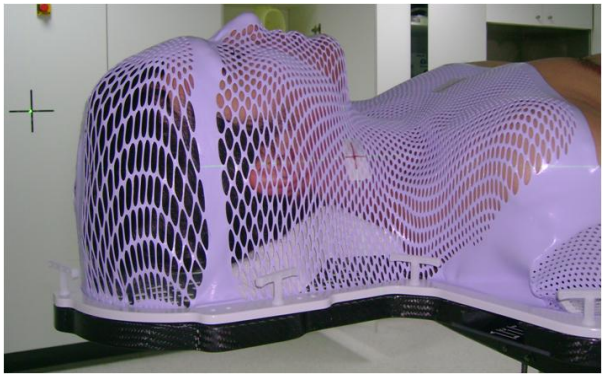

Figure 2 – Immobilization mask used to treat head and neck tumour cases at *IPOCFG* [courtesy of *IPOCFG*].

In the planning *CT* scan the physician will outline the target volumes and the organs at risk. For the delineation of the target volume and organs at risk a strict set of guidelines must be followed (Figure 3) [5,6]:

- Gross Tumour Volume (*GTV*) – perceptible extent and location of the primary tumour. For those patients that had previously done a complete surgical resection (postoperative), there is no *GTV*;
- Clinical Target Volume (*CTV*) – volume that contains the *GTV* and a margin that takes into account microscopic disease;
- Planning Target Volume (*PTV*) – volume containing the *GTV*, *CTV* and a margin around the *CTV* that accounts for variations and inaccuracies due to organ motion and setup errors in order to ensure that the *CTV* receives the prescribed dose;
- Organs at Risk (*OAR*) – normal tissues that constrain the dose prescribed to the tumour. These organs may have different classifications depending on their functional organization. These may be (Figure 4):
    - Serial – if a functional sub-unit of the chain receives a radiation dose above the tolerance organ functionality is lost (e.g. spinal cord);
    - Parallel – the functional sub-units of the organ are independent thus, if only one small volume of the organ is damaged it won't affect organ function (e.g. parotid glands);
    - Mixed – tissues that have functional sub-units with both behaviours (serial and parallel).

Due to internal organ motion and setup uncertainties a margin around the organs at risk may be used, the Planning Risk Volume (*PRV*) [7].

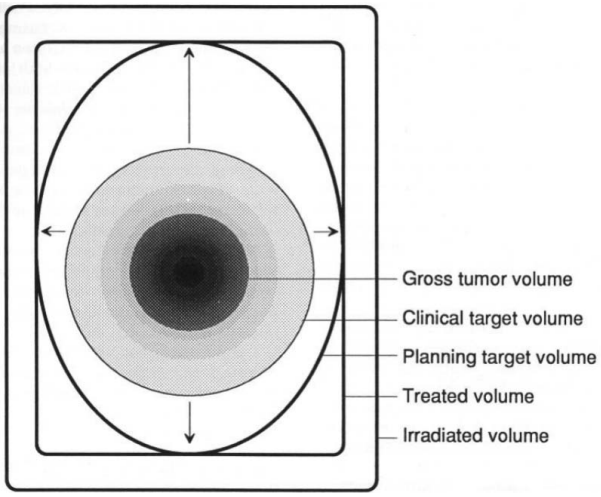

Figure 3 – Target volumes (*GTV*, *CTV* and *PTV*), treated volume and volume irradiated [8].

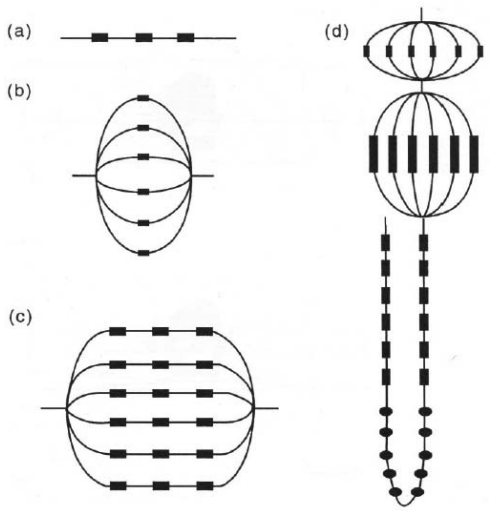

Figure 4 – Tissue organization structures: (a) serial, (b) parallel, (c) serial-parallel and (d) mixed [7].

For head and neck tumours the most important organs at risk are the spinal cord, brainstem, parotid glands, oral cavity, mandible, thyroid, optical nerves, oesophagus, pharynx, larynx, brachial plexus, etc. (Figure 5). Irradiation of these structures above the tolerance dose may cause complications such as patient paralysis, xerostomia, mucositis, osteoradionecrois, hypothryrodism, blindness, etc.

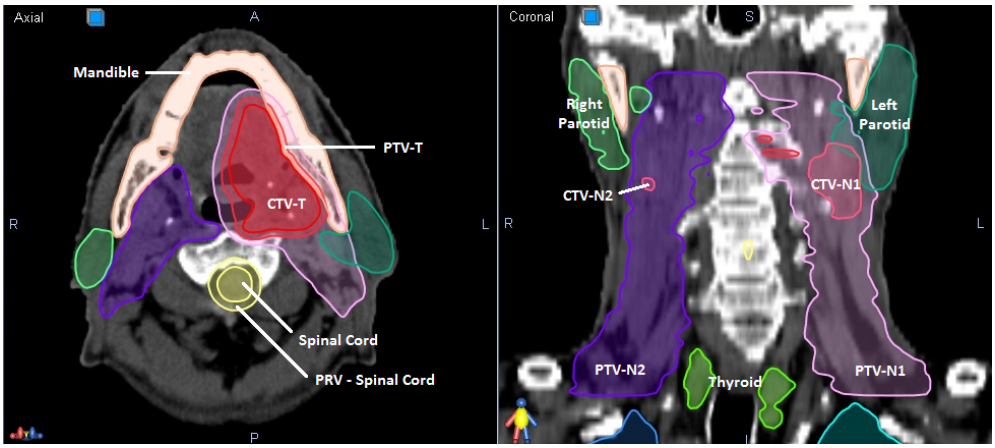

Figure 5 – Two slices of a *CT* scan (axial on the left and coronal on the right) from a patient treated at *IPOCFG*. In this patient the organs at risk delineated were: mandible, spinal cord and margin – *PRV*-spinal cord –, thyroid, parotid glands and the target volumes to be treated (*PTV-T*: primary tumour; *CTV-N1* and *N2*: adenopathies; *PTV-N1* and *N2*: regions with a small probability of disease) [courtesy of *IPOCFG*].

2.2 Salivary Glands

The salivary glands can be divided in two groups: the *minor* salivary glands which are hundreds spread all over the oral cavity (lips, cheeks, palate, floor of the mouth and part of the tongue) and oropharynx; and the *major* salivary glands, which include both parotids, submandibular and sublingual glands (Figure 6). The parotid glands are located in the preauricular region and posterior area of the mandible, and the submandibular glands are positioned beneath the floor of mouth along the interior of the mandible. The sublingual glands are anterior at the submandibular glands [9,10].

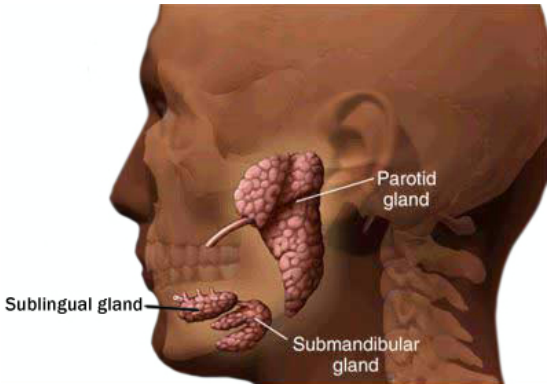

Figure 6 - *Major* salivary glands [10].

Each salivary gland secretes fluids that when mixed originate the saliva. The saliva has several roles as, for example, lubrication and protections of the oral tissues, facilitating speech and aiding the digestion of food. These are all functions important to maintain a good quality of life.

For patients with head and neck cancers one of the most important acute and late side effects of radiation therapy is usually related to a dysfunction in the salivary glands called xerostomia. This dysfunction consists on a reduction on the saliva production leading to oral dryness, thick/sticky saliva and difficulties in speech, chewing or swallowing [11,12].

Radiation therapy side effects may be considered early or late if those occurred 6 months before or after the start of radiation therapy treatment, respectively. The side effects are usually graded according to their severity where for example *G*0 corresponds to complication-free and *G*4 corresponds to severe/irreversible complications (Table 1).

Table 1 – Acute and late radiation endpoints for xerostomia according to *RTOG/EORTC* guidelines [13].

Severity	Endpoints	
	Acute	Late
***G*0**	• None	• None
***G*1**	• Slight disgeusia • Mild xerostomia	• Slight xerostomia • Good response to stimulation
***G*2**	• Severe disgeusia • Moderate xerostomia	• Bad response to stimulation Moderate xerostomia
***G*3**	-	• Complete xerostomia • No response to stimulation
***G*4**	• Gland necrosis	• Fibrosis

2.3 Treatment Planning

The third step in the workflow of radiation therapy, after structure delineation, is the treatment planning. This may be made by the physicist or dosimetrist in the Treatment Planning System (Figure 1).

Today the most common form of radiation therapy is 3D Conformal Radiation Therapy, which is generally based on forward planning. In this case, during plan optimization the beams number, directions, energy and shapes are manually defined by the planner until a good dose distribution is obtained. This is a trial and error

process where all these variables are continuously changed to improve plan quality. When an adequate dose distribution is obtained the physician will then evaluate the plan and approve the treatment. The evaluation of plan quality is based on dose statistics, dose-volume histograms (*DVH*) and 3D dose distributions. Dose-volume histograms quantify the percentage of volume that receives a certain dose value, both for organs at risk and target volumes (Figure 7) [5].

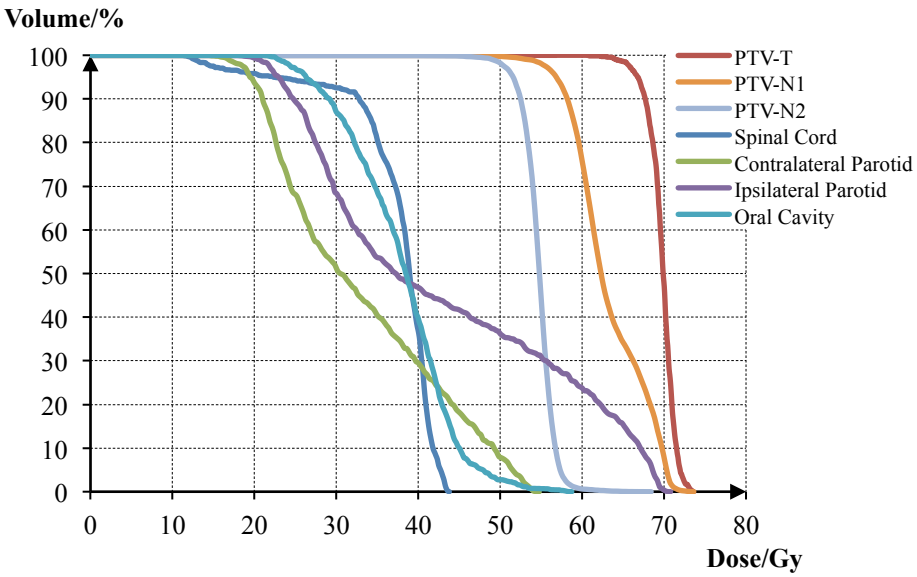

Figure 7 – Example of dose-volume histograms for target volumes (*PTV-T*, *PTV-N1* and *PTV-N2*) and organs at risk (spinal cord, contralateral parotid, ipsilateral parotid and oral cavity).

2.4 *RT* Techniques

3D Conformal Radiation Therapy - *3D-CRT* - is a technique that uses uniform fields. The irradiation beams can be delivered from several directions: axial or non-coplanar (Figure 8 - a). In the example of the figure, due to the uniformity of the beams, both tumour and spinal cord, are receiving the same dose limiting the prescription dose to the tumour.

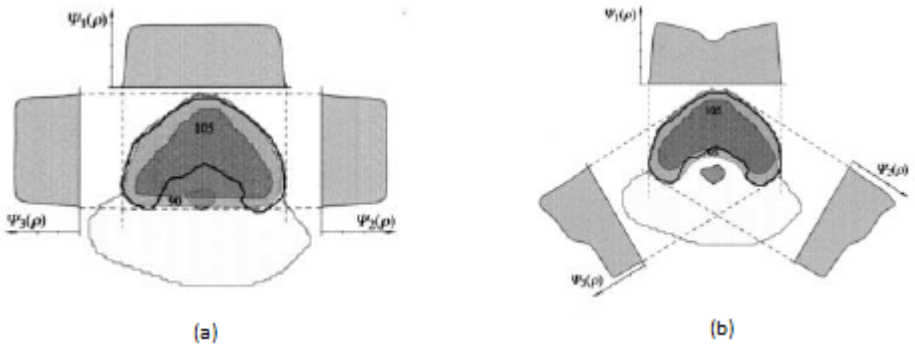

Figure 8 - (a) 3D Conformal *RT* technique using uniform beams and (b) *IMRT* technique using non-uniform beams [14].

Today, 3D conformal *RT* is performed using a multi-leaf collimator (*MLC*). The *MLC* is a device made of tungsten leaves that move independently from each other. These may be used to block normal tissues that are thus protected from the radiation beams (Figure 9). The movements of the multi-leaf collimator are computer-controlled thus precisely delivering the treatment plan [14,15].

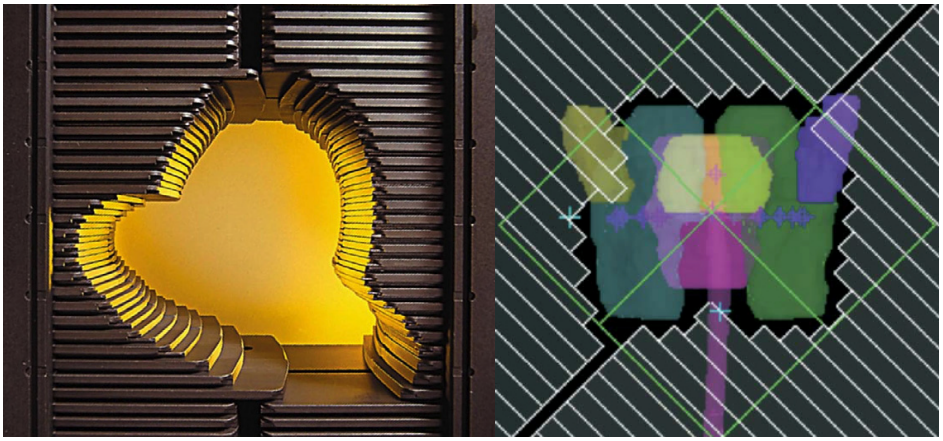

Figure 9 – Example of a Multi-leaf collimator (left) and *MLC* leaves positioned to protect both parotids from the radiation beam (right) [15,16].

Evolutions on external beam radiation therapy led to Intensity Modulated Radiation Therapy – *IMRT* - (Figure 8- b). Intensity modulated beams allow shaping the 3D dose distribution to concave tumour shapes and produce steep dose gradients in the target boundaries, thus significantly protecting the organs at risk compared to 3D conformal radiation therapy. Thus target volume coverage and the sparing of the organs at risk are improved. Generally *IMRT* dose distributions are obtained using inverse treatment planning. In inverse optimization, after setting the desired clinical

objectives, for example the prescription dose in the target volumes and tolerance dose for the organs at risk, the inverse optimization algorithm will determine the fluency map that will produce the desired dose distribution [17-20].

The most common methods of delivery of *IMRT* are [15]:

- Step-and-shoot or segmented – the collimator moves to a certain position and the radiation beam is switch on. When finished the irradiation the collimator will assume the next position until all segments are delivered (Figure 10);
- Dynamic – based on a continue irradiation while the leaves of the collimator move continuously.

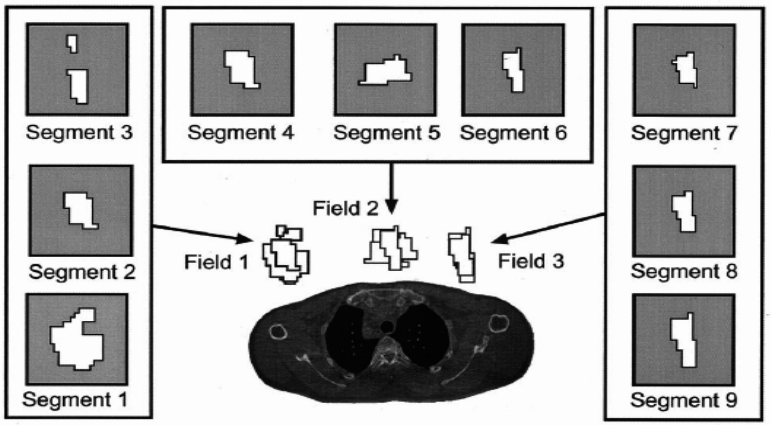

Figure 10 – Example of a nine segments delivery by step-and-shoot method [21].

Image-Guided Radiation Therapy is a technique that allows to verify patient positioning while positioned in the treatment table. Two types of images can be acquired [22,23]:

- 2D Portal images – the patient is irradiated with a very low dose from two orthogonal directions, one anterior and one lateral. This will create 2D images that will be compared with the corresponding *CT* planning image;
- Megavoltage Cone-Beam *CT* – the linear accelerator rotates around the patient allowing the creation of a 3D image. This image is then compared with the planning *CT* and informs the position of the patient relatively to the isocenter. The cone-beam *CT* is normally used in more demanding treatment techniques (Figure 11).

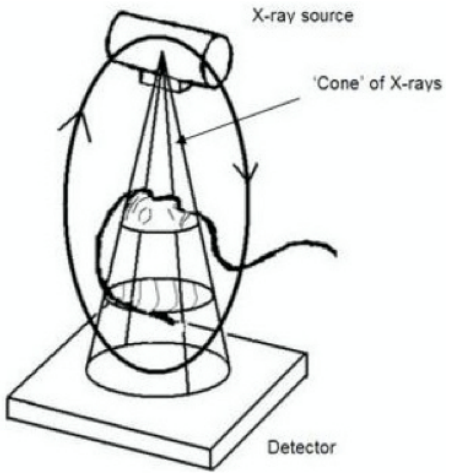

Figure 11 – Megavoltage Cone-Beam *CT* [24].

2.5 Dose-Response Models

Dose-response models describe tissue response to radiation allowing to quantify cell survival rates and consequently the probability of tumour control or complications. Cellular death is proportional to the dose value that irradiates a certain tissue and depending on the dose delivered the tissues may be able to repair. To increase the repair of the normal tissues, radiation therapy is delivered in several fractions. The Linear-Quadratic Model assumes that the time between fractions is enough to repair sub-lethal damage. It describes the cellular survival rate (s) versus the delivered dose (D = number of fractions × dose per fraction):

$$s = e^{-(\alpha D + \beta D^2)}$$

where α/β quantifies the sensibility to fractionation related to the capacity of repair. Cells with a fast cellular cycle, e.g. skin or tumours, will express earlier effects, which translates into a high values of α/β. α/β=10 is normally used to describe those tissues. In other hand, tissues with a slow cellular cycle will manifest mostly late side-effects and generally have low α/β, i.e., α/β~3 (Figure 12).

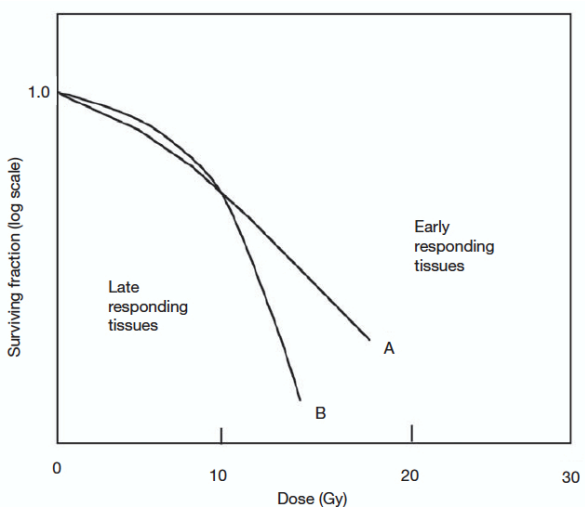

Figure 12 – Linear-quadratic model for early and late responding tissues. A: high *α/β* value; B: low *α/β* value [25].

The Poisson-Linear-Quadratic model may then be applied to calculate the probability of response (P), which is described by the following expression:

$$P = e^{-N_0 s}$$

where N_0 is the number of clonogens in case of tumours or the number of functional sub-units for organs at risk before the irradiation and s is the cellular survival rate calculated by the LQ models [25].

The probability of response may be described by several radiobiological models such as the Lyman and the Relative Seriality (Figure 13). Although, these are similar around the D_{50} value, differences between the models exist at low and high doses.

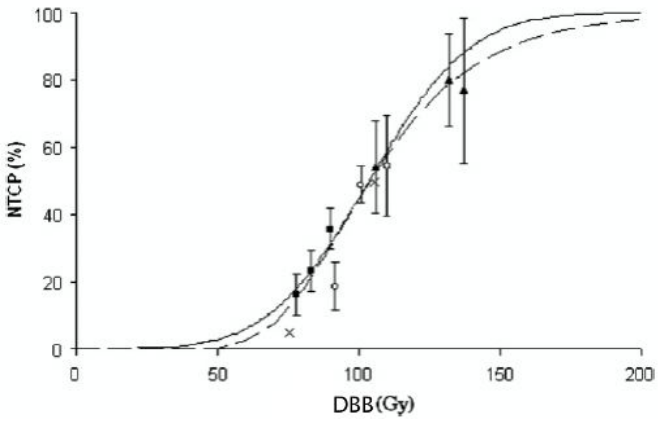

Figure 13 – Dose-response curves for the Lyman (solid line) and Relative Seriality (dashed line) models derived for the breast complications [26].

2.5.1 Lyman's Model

The classical Lyman's model describes the probability of response in normal tissues or tumours, when an organ or tumour is uniformly irradiated. For normal tissues the probability of injury (P_I) as a dose function (D), can be derived through the following integral probability:

$$P_I = \frac{1}{\sqrt{2\pi}} \int_{-\infty}^{t} e^{-t^2/2} \partial t$$

where

$$t = \frac{D - TD_{50}(v)}{m \times TD_{50}(v)}$$

$$v = V/V_{ref}$$

$$D_{50}(v) = D_{50}(1) \times v^{-n}$$

$D_{50}(1)$ is the dose that causes 50% response if the organ was uniformly irradiated, v is the fraction of the organ that was irradiated, V_{ref} is the reference volume for which D_{50} was derived, m is the slope of the curve and n is the volume effect relationship. If $n \approx 1$ the organ can be considered as having a parallel structure however if $n \approx 0$ it will be a serial structure [27-29].

Once this model can only be used for uniformly distributed dose irradiations, in case of a non-uniform distributions, the dose-volume histogram has to be transformed into a single dose value, i.e., equivalent uniform dose (EUD):

$$EUD = \left(\sum_i v_i D_i^{1/n} \right)^n$$

where v_i corresponds to the volume of the dose bin corresponding to the dose D_i and n corresponds to the volume effect of the organ [30,31].

2.5.2 Relative Seriality Model

The Relative Seriality model corresponds to a radiobiological model that describes tissue response to radiation, allowing to calculate the probability of complications for a heterogeneous dose distribution. For normal tissues, the probability of injury (P_I) to a certain organ that is irradiated with a certain dose distribution ($\vec{D}$) can be given by the expression:

$$P_I(\vec{D}) = \left[1 - \prod_{i=1}^{M} P(D_i)^{\Delta v_i}\right]^{\frac{1}{s}} \Leftrightarrow$$

$$\Leftrightarrow P_I(\vec{D}) = \left[1 - \prod_{i=1}^{M} (1 - \exp\left(-\exp\left(e\gamma - \left(\frac{D_i}{D_{50}}\right).(\mathrm{e}\gamma - \ln(\ln(2)))\right)\right)^{s})^{\Delta v_i}\right]^{\frac{1}{s}}$$

where M is the number of voxels, D_i is the dose in each voxel and Δv_i ($=\Delta V_i/V_{ref}$) is the fractional subvolume of an organ that is irradiated with dose D_i.

The parameters of the Relative Seriality model are [28,32]:

- D_{50} - dose related to a 50% probability of complications;
- γ - maximum normalized value of the dose-response gradient, i.e., corresponds to the slope of the curve;
- s - quantifies the volume effect, assuming the values 0 or 1 for a parallel or serial organ, respectively.

2.6 State of Art

Marzi et al. [28], *Shiltra et al.* [33] and *Houwling et al.* [34] have derived dose-response curves for the Relative Seriality model. These studies evaluated salivary flow compared with the pre-treatment one (objective measure) and/or evaluated the complications of the patients using questionnaires (subjective measure). The studies made focused in their majority the severities of complications *G*3 or *G*4.

Marzi et al. [28] used the dose in both parotids in patients treated with *IMRT* and evaluated patient complications *G*3 in the follow-up times of 3, 6 and 12 months (Table 2). *Marzi et al.* [28] and *Houwling et al.* [34] obtained D_{50} values ranging from

38.8Gy to 40Gy, γ values from 0.80 to 0.95 and *s* value close to zero, reinforcing that the parotids are parallel structures.

Table 2 - Summary of dose response parameters for the Seriality Model

References	Follow-up Times	D_{50} [95% *CI*]	γ [95% *CI*]	*s* [95% *CI*]	Additional Information
Schiltra C.	13 wk	37.0 [32.0-46.0]	2.00 [1.00-5.30]	4E-07 [0.00-0.19]	Salivary flow, *3D-CRT*
Marzi S.	3 m	20.0 [16.7-24.1]	0.77 [0.31-1.42]	0.01	*G3*, *RTOG*, *IMRT*
	6 m	26.3 [21.5-32.8]	0.73 [0.15-1.55]	0.01	
	12 m	40.0 [32.0-54.0]	0.80 [0.35-1.62]	0.01	
Houweling A.	12 m	38.8 [36.5-43.5]	0.95 [0.70-1.30]	0.08 [0.00-0.65]	Salivary flow, *IMRT*, *3D-CRT*

Dose-response parameters were also derived for the Lyman's model by several authors as, for example, *Marzi et al.* [28], *Roesink et al*. [29], *Shiltra et al.* [33], *Houwling et al.* [34] and *Dijkema et al.* [35] (Table 3). D_{50} values obtained for both parotids at the follow-up time of 12 months ranged from 39.4Gy to 41.6Gy, *m* values from 0.36 to 0.45 and *n* values rounded the value 1, which in the Lyman's model means that the parotids are parallel structures.

Table 3 - Summary of some of the dose response parameters for the Lyman's Model

References	Follow-up Times	D_{50} [95% *CI*]	*m* [95% *CI*]	*n* [95% *CI*]	Additional Information
Schiltra C.	13 wk	38.0 [33.0-45.0]	0.26 [0.16-0.34]	1.30 [0.30-3.20]	Salivary flow, *3D-CRT*
Roesink J.	6 wk	31.0 [26.0-35.0]	0.54 [0.40-0.78]	1.00	Salivary flow, *RTOG/EORTC*, *3D-CRT*
	6 m	35.0 [30.0-40.0]	0.46 [0.34-0.66]	1.00	
	12 m	39.0 [34.0-44.0]	0.45 [0.33-0.65]	1.00	
Marzi S.	3 m	21.4 [18.4-25.5]	0.57 [0.34-1.37]	1.00	*G3*, *RTOG*, *IMRT*
	6 m	27.8 [23.6-33.7]	0.49 [0.27-1.42]	1.00	
	12 m	41.6 [32.8-56.8]	0.45 [0.27-1.49]	1.00	
Dijkema T.	12 m	40.5 [36.8-44.1]	0.36 [0.28-0.44]	1.00	*G4*, *IMRT*, *dIMRT*, Michigan (also values for Utrech)
Houweling A.	12 m	39.4 [33.8-41.8]	0.42 [0.36-0.58]	1.13 [0.75-1.25]	Salivary flow, *IMRT*, *3D-CRT*

A study made by *Eisbruch et al.* [36] showed that the mean dose that should be delivered to the parotids should not overpass 26Gy, value that was embraced by other authors.

This master thesis is focused in the Relative Seriality Model, although the data from other models was also collected. In this review all the parameters affecting the outcome, as for example the severity of complications studied, the type of follow-up used and the follow-up times studied were stored in an excel database (Appendix A).

CHAPTER 3: Materials & Methods

3.1 Patients

411 patients with head and neck tumours treated at *IPOCFG* from May 2007 to November 2013 were initially included in this study. Criteria for patient exclusion were:

- very small number of follow-up appointments (11 patients);
- *G*2 at the first consult. Such high severity in the first follow-up visit means that the patient already had complications that were not caused by radiation therapy (3 patients);
- *G*4 complications (1 patient);
- short follow-up time: *RT* treatment started after July 2013 (33 patients);
- patients without dose information (25 patients).

After the exclusion of 73 patients, a total of 338 patients remained. Patient's characteristics for this group are shown in Table 4. The population gathered for this study presented an average age of 57.4±11.9 years (from 12 to 88) and average overall treatment time of 46±4.2 days. *rIMRT* (presented in Chapter 3.2) was the most used treatment technique to treat the population, 44%.

Table 4 – Patient's characteristics and number (*n* =338, population included in the study)

Characteristics	*n* (%)
Gender	
Female	56 (16.3)
Male	196 (83.7)
Tumour type	
Oral cavity	72 (21.3)
Oropharynx	68 (19.8)
Larynx	64 (19.2)
Nasopharynx	42 (12.4)
Pharyngeal-Laryngeal	40 (11.5)
Hypopharynx	27 (7.7)
Paranasal sinus	3 (0.9)
Others	22 (7.1)

Characteristics	*n* (%)
T stage	
TX	8 (2.4)
T1-2	155 (46.5)
T3-4	168 (50.5)
N stage	
NX	8 (2.7)
N0-2a	157 (46.8)
N2b-3b	168 (50.5)
Technique	
3D-CRT	36 (11.2)
dIMRT	98 (28.4)
rIMRT	150 (44.4)
IMRT	54 (16.0)

3.2 Treatment

At *IPOCFG* different radiation therapy techniques were used in the treatment of head and neck tumour cases. For each patient treatment selection was made according to the tumour type, tumour stage, age, general health status, etc. Since 2006 the techniques used were:

- 3D Conformal Radiation Therapy (*3D-CRT*) - simple tumour cases (mostly stages I or II) are treated with up to 10 beam directions. In most cases only the primary tumour is outlined and the regional lymphatic nodes are not irradiated;
- Direct IMRT (*dIMRT*) – forward planning using five to seven gantry directions with a total of 15 to 25 beams. In this technique each beam direction delivers at least three segments. The first segment irradiates the total target volume (*PTV*), the second irradiates the left side of the *PTV* sparing the spinal cord from irradiation, and the third one irradiates the right side of the *PTV* also sparing the spinal cord (Figure 14);
- Inverse Planning – *IMRT* normally uses five to nine equidistant fields. It can be separated in two techniques according to the number of segments used:
    - Rapid *IMRT* (*rIMRT*) – uses around 30 to 55 segments;
    - *IMRT* – uses 56 to 80 segments. Requires extensive patient specific quality control limiting the utilization of this technique to most difficult tumour cases.

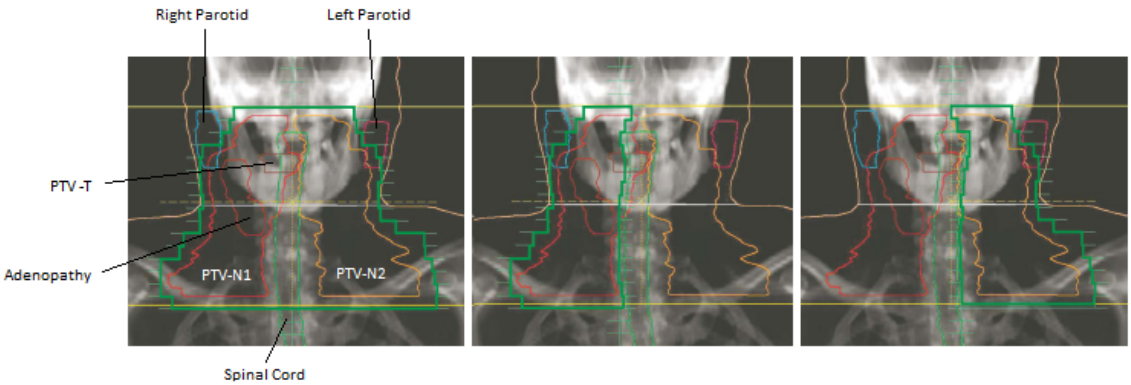

Figure 14 – Example of three segments of a *dIMRT* treatment: the first irradiates the total *PTV* (*PTV-N1*, which includes the *PTV-T* and the adenopathies, and *PTV-N2*); the second and third segments irradiate the left and right side of the *PTV*, respectively, protecting the spinal cord from being irradiated [courtesy of *IPOCFG*].

The commercial treatment planning system used is ONCENTRA (Elekta/Nucletron) and treatment delivery is performed in a Siemens Oncor Avant-Garde linear accelerator.

3.3 Dosimetry

Most radiation therapy treatments were delivered by a sequence of two or three plans, where the total delivered dose is given by the sum of the dose of all plans. However, for radiobiological modelling the total physical dose needs to be converted to an equivalent 2Gy fractionation because all radiobiological models were derived for that fractionation. For that, the structures, plans and dose matrix of all patients were manually exported from the ONCENTRA. Additional patient information was exported from LANTIS (Siemens), the Record & Verify data network, and imported into RESPONSE (*UA*/*IPOCFG*), an electronic health patient information software developed by Aveiro University in collaboration with *IPOCFG*. In cases where the radiation therapy was suspended, total dose was corrected for treatment interruptions.

Total delivered dose was corrected for a 2Gy fractionation using the Biologically Effective Dose concept, *BED*, which converts the 3D dose distribution of each treatment plan into a 2Gy fraction dose for each voxel:

$$BED = \sum_{i}^{N_p} \left[D_i \left(1 + \frac{d_i}{\frac{\alpha}{\beta}} \right) \right] = D_{2Gy} \left(1 + \frac{2}{\frac{\alpha}{\beta}} \right)$$

in this equation N_p is the number of plans, D_i is the physical dose in each voxel of the dose distribution i, d_i is the dose per fraction in each voxel and α/β is the ratio of the Linear-Quadratic model which assumes the value 3 for late effects in normal tissues and 10 for early effects.

The total delivered dose corrected into the 2Gy fractionation allow to calculate dose-volume histograms and dose statistics for all the regions of interest such as mean dose and *DBB*.

The biologically effective uniform dose - $\overline{\overline{D}}$ or *DBB* – is a dose quantity that takes into account the real dose distribution (3D dose matrix) as well as the biological

characteristics of the structure, i.e., their radiosensitivity. Thus this value describes more accurately tissue response to radiation. The *DBB* can be calculated through the following expression [25,37,38]:

$$P(\bar{\bar{D}}) = P(\vec{D}) \leftrightarrow \bar{\bar{D}} = D_{50}\frac{e\gamma - \ln\left(-\ln\left(P(\vec{D})\right)\right)}{e\gamma - \ln(\ln(2))}$$

3.4 Dose-Response Curves

In this study dose-response curves were derived for the Relative Seriality model. The study was made considering the dose delivered into the structures: contralateral parotid, ipsilateral parotid, sum of the parotids and salivary glands (Figure 15). The contralateral parotid corresponds to the parotid in the opposite side of the primary tumour so it receives less dose than the ipsilateral parotid. The sum of the parotids is a structure that includes both parotids. Two groups of salivary glands were created because some patients were operated and did not have one of the submandibular glands:

- Salivary Glands-5 – includes the ipsilateral parotid, contralateral parotid, oral cavity and both submandibular glands;
- Salivary Glands-4 – contains all the above structures except the ipsilateral submandibular gland.

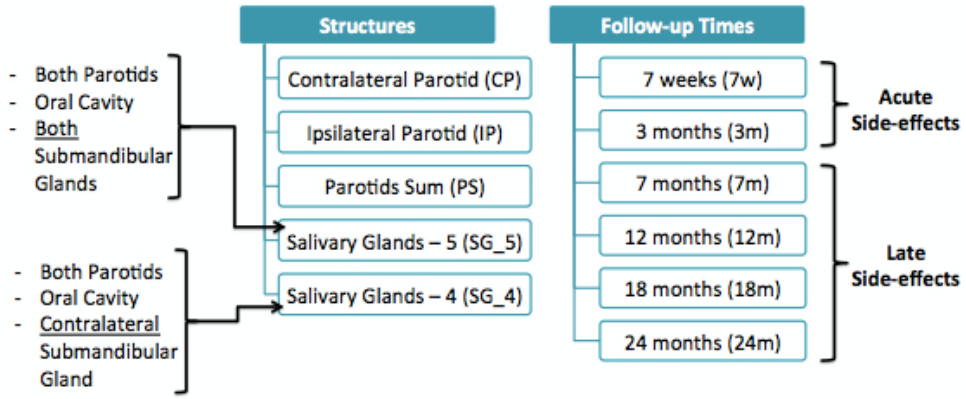

Figure 15 – Structures and follow-up times studied.

Patient's follow-up at *IPOCFG* consists on weekly visits during treatment that take about seven weeks. After that the patients have appointments every three months during two to three years and later every six months. The severity of complications were classified according to *RTOG/EORTC* guidelines (Table 1). Because at *IPOCFG* patients have continuous follow-up appointments, it was possible to derive dose-response curves for different times after the radiation therapy treatment. Periods evaluated were 7 weeks, 3, 7, 12, 18 and 24 months (Figure 15).

3.5 Maximum Likelihood Model

The Maximum Likelihood Model is the method used to find the best combination of radiobiological parameters for, in this case, the Relative Seriality model. The maximum likelihood function (L) is model related so it is calculated in order to D_{50}, γ and s, taking into account the radiosensitivity of the tissue ($\vec{X}$) and the treatment delivered to the patient ($\vec{\theta}$):

$$L\left(\vec{X}\backslash\vec{\theta}\right) = L\left((D_{50},\gamma,s),\left(\vec{D},\vec{V}\right)\right) \Leftrightarrow$$

$$\Leftrightarrow L\left(\vec{X}\backslash\vec{\theta}\right) = \prod_{i=1}^{m} P((D_{50},\gamma,s),(\overrightarrow{D_i},\overrightarrow{V_i}))\times\prod_{j=1}^{n}(1-P\left((D_{50},\gamma,s),(\overrightarrow{D_j},\overrightarrow{V_j})\right))$$

where $\vec{D}$ is the dose delivered during treatment, $\vec{V}$ is the corresponding tissue volume receiving that dose, and m and n are the numbers of patients with and without complications, respectively.

With the values of the maximum likelihood function, the best radiobiological parameters and their confidence intervals can be determined by fitting the normal tissue response probability in order to D_{50} and γ. If all the D_{50} and γ possibilities were calculated that would create a 3D curve where each point would correspond to a combination of parameters (Figure 16). Since in practice not all the possibilities are calculated it is necessary to repeat the fitting process several times using a different set of initial guesses for D_{50} and γ to guarantee that the combination that maximizes L was found (maximum point of the 3D curve) [32,33,39].

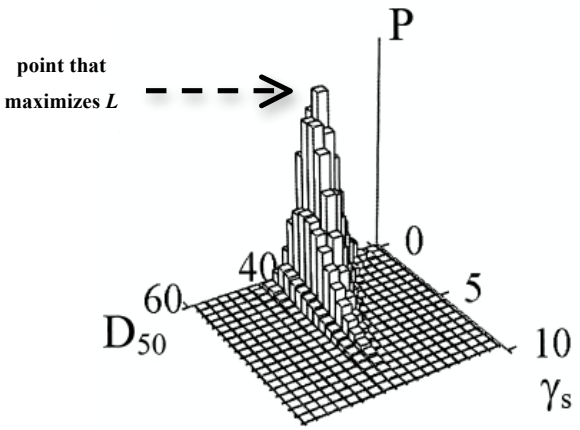

Figure 16 – Example of the curve expected for a probability of injury (*P*) as a function of the parameters D_{50} and γ_s for a fixed *s* value of 0.01 [33].

3.6 Goodness of the Fit

There are several methods that statistically analyse the goodness of the fit. In this study the Receiver Operating Characteristic (*ROC*) curve, the Pearson's X^2-test and the Worst-fit were used.

3.6.1 ROC Curve

A model is considered useful in case it efficiently separates responders (patients with complications) from non-responders (complication-free patients). The Receiver Operating Characteristic curves (*ROC* curves) use the Relative Seriality model parameters to evaluate the reliability of the model through the discrimination between patients with complications and complication-free.

ROC curves can be generated through the plotting of the true positive ratio (*TPR*) versus the false positive ratio (*FPR*) (Figure 17). To calculate the true and false positive ratios the population is sorted by their probability of complications and then the observed responses above the trial cutoffs (P_{cut}) is compared with the number of expected responses. The true positive ratio corresponds to the number of correct positive results above P_{cut} (*TP*) that occur among all positive samples, i.e., sensitivity:

$$TPR = \frac{\sum TP}{\sum Positive\ Samples}$$

The false positive ratio quantifies the number of incorrect positive results above the P_{cut} (*FP*) that occur among all negative samples, i.e., 1-specificity:

$$FPR = \frac{\sum FP}{\sum Negative\ Samples}$$

The plot of true positive ratio versus false positive ratio will create a curve where the Area Under the Curve (*AUC*) will quantify the ability of the test to discriminate responders and non-responders. In case of *AUC*=1 that means that there is an optimal discrimination between complications and complication-free patients. If *AUC*=0.5, which happens when *TPR=FPR*, that means that the prediction is random. For example in Figure 17 *C* corresponds to a random result (*AUC*=0.5), *D* to the ideal situation (*AUC*=1) and *E* is considered worse than guessing (*AUC*<0.5). Thresholds to separate good from very good from reasonable are still discussed among different authors. In this study the evaluation of the area under the curve was made through the following ranges [32,40,41]:

- very good: 0.8 - 0.9;
- good: 0.7 - 0.8;
- reasonable: 0.6 - 0.7;
- poor: <0.5.

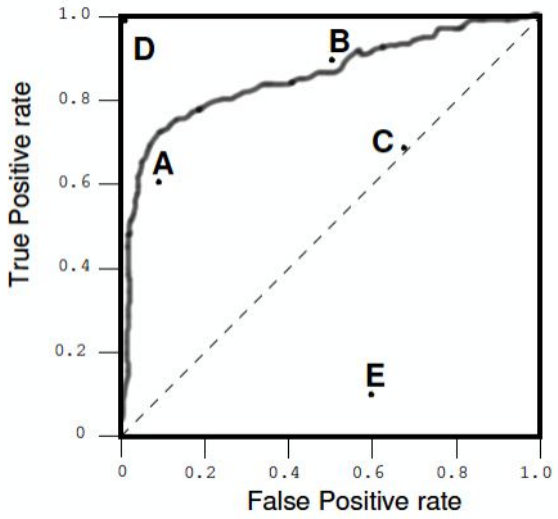

Figure 17 – Example of a *ROC* curve [adapted from 40].

3.6.2 Pearson's X^2-test

Pearson's X^2-test is a statistical method that studies the spread of data points (complications and complication-free). The Pearson's statistical test approaches a X^2 distribution, which can be calculated through the following expression:

$$X^2 = \sum_{i=1}^{n} \frac{(O_i - E_i)^2}{E_i}$$

where E_i is the expected frequency, n is the total number of dose ranges and O_i is the observed frequency.

To execute the Pearson's X^2-test it is necessary to achieve a good approximation of the X^2 distribution, which can be made through the comparison of the value from the X^2 distribution with the degrees of freedom (*df*). The degrees of freedom are calculated through:

$$df = n - (s + 1)$$

where s corresponds to the number of co-variants used in fitting the distribution, which in our case correspond to the three radiobiological parameters, i.e., $df=n-(3+1)$.

The spread can be considered as a good distribution if the X^2 distribution divided by the number of degrees of freedom ($=X^2/df$) is reasonably large, i.e., close to 1. However, if the value is small, that could mean that the data doesn't make a good representation of the distribution or that the theoretical distribution does not estimate well the observed distribution, i.e., actual data [42,43].

3.6.3 Worst-fit

The Worst-fit probability is based on the assumption that the log-likelihood function describes a Gaussian distribution and considers the variance magnitude through the comparison between the mean and maximum values of *ln(L)*. For the goodness of the fit to be considered optimal, a good agreement between the

prediction and clinical results distributions must be achieved through a large probability, i.e., close to 1 [39].

3.6.4 Tolerance Dose

The tolerance dose corresponds to the threshold that separates complication-free patients from patients with complications. This dose value has an odd ratio (*OR*) associated, which represents the risk of patients developing complications in case of the threshold being overpassed.

The odd ratio corresponds to a statistical quantifier of the strength of the association between the complications and complication-free patients. This value can only be considered as statistical significant when the lower limit of the 95% confidence interval (*CI*) is equal or higher than 1. In case of being lower than 1 the association is bad and cannot be considered as significant [32].

CHAPTER 4: Results

4.1 Dose-Volume Histograms Analysis

Dose-volume histograms (*DVH*) show the percentage of the irradiated volume versus the dose delivered in each structure. In clinical practice generally cumulative dose-volume histograms are used for treatment plan evaluation. Using the dose-volume histograms of all treated patients, mean *DVH* for patients treated with different techniques or having different treatment outcomes were calculated. For that different MATLAB functions were developed (Appendix B).

Figure 18 shows the mean dose-volume histograms of the contralateral parotid for patients treated with different techniques. Although it was expected that the mean dose-volume histograms for *IMRT* should present lower dose, this is not seen because this technique is used to treat most difficult tumour cases. By contrary, *3D-CRT* technique has the lowest dose values because it is used to treat the simplest cases. Furthermore, the beam configuration used in *3D-CRT* is completely different than for *IMRT* because of the different *PTV* shapes. Thus, patients treated with *3D-CRT* were excluded from the study (36 patients) to consider only patients that were irradiated similarly. 302 patients were considered as the final population of the study. With *IMRT* and *rIMRT* a smaller volume of the structure is irradiated with higher dose while a larger amount of tissue is irradiated with lower doses.

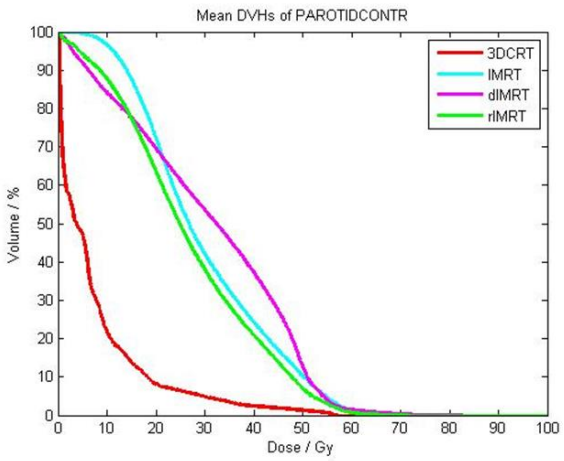

Figure 18 – Mean dose-volume histogram for the contralateral parotid for different treatment techniques.

Figure 19 shows the mean dose-volume histograms for the contralateral parotid 24 months after radiation therapy (thicker curve). The black curves show the *DVH* for each patient. The first, second and third plots display the dose-volume histograms for patients with complications *G*0, *G*1 and *G*2, respectively. N_c shows the number of patients in each group. As expected the mean *DVH* for *G*0, i.e., for the group of patients complication-free, had lowest dose values when compared to the other two. However, mean curves for *G*1 and *G*2 are almost overlapped. Thus, two studies were made where patients were grouped as showed in Figure 20.

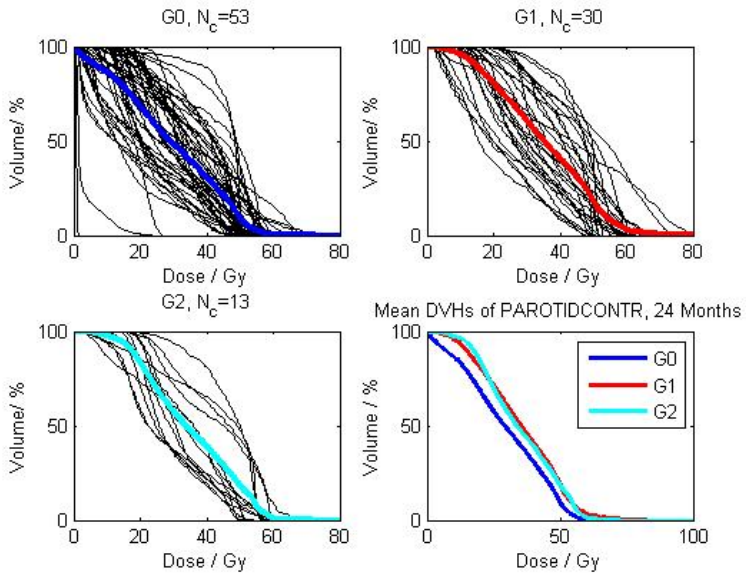

Figure 19 – Mean dose-volume histograms calculated for patients with endpoints *G*0, *G*1 and *G*2 for the contralateral parotid, twenty-four months after the radiation therapy treatment.

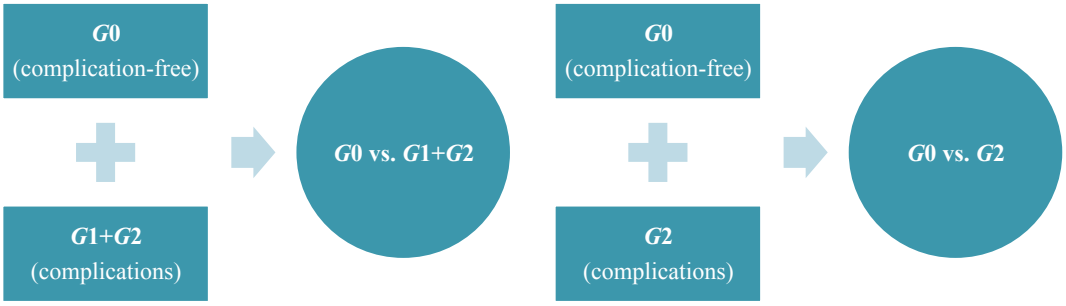

Figure 20 – Both ways of grouping the patients: *G*0 vs. *G*1+*G*2 and *G*0 vs. *G*2.

4.2 *G*0 vs. *G*2

Figure 21 to 27 show some of the dose-response curves derived for xerostomia *G*2 when the dose in the parotid glands was considered, as well as the correspondent *ROC* curves. Dose-response curves were derived for all structures and follow-up times, as well as the respective *ROC* curves for the group *G*0 vs. *G*2 can be seen in Appendix C.1.

In the left side of the Figure 21 the *DRC* derived for the ipsilateral parotids 12 months after radiation therapy (solid line), as well as their 68% confidence interval (both dashed lines) are presented. The crosses correspond to patients with complications and the circles correspond to the patients without complications. The squares show the percentage of patients with xerostomia *G*2 in each dose range and the error bars represent the dose standard deviation. For example, 55% of the ipsilateral parotids irradiated with around 48Gy reported complications *G*2. Since the discrepancy between the clinical points and the model is not that big that means that the model represents well the clinical data. In the right side of the Figure 21 the *ROC* curve derived for this *DRC* is shown. The area under the curve is 0.69 indicating a model of reasonable quality (range 0.6 to 0.7).

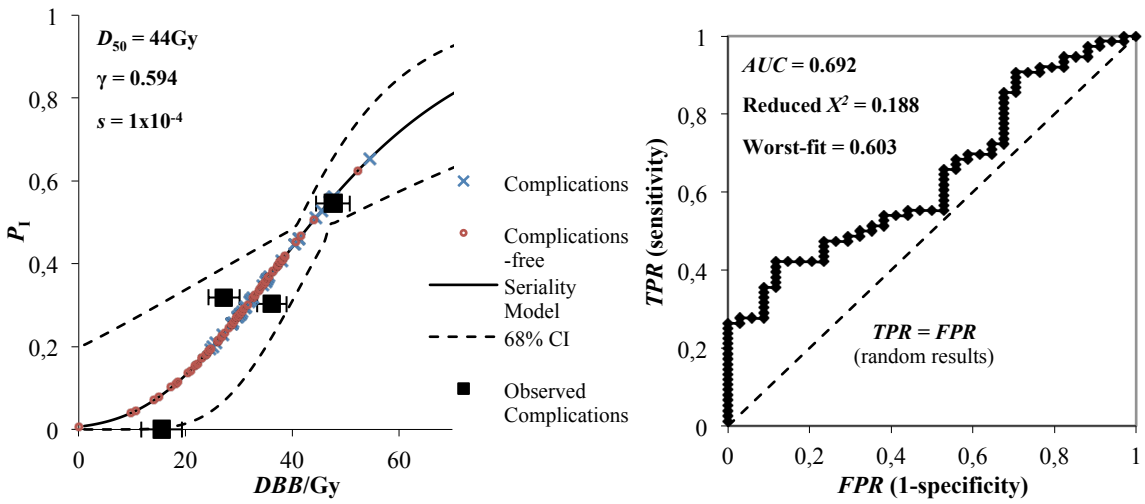

Figure 21 - *DRC* (left) and correspondent *ROC* curve (right) for the ipsilateral parotid 12 months after the *RT* for the group *G*0 vs. *G*2.

Figure 22 to 27 show the *DRC* and respective *ROC* curves for all the follow-up times studied when the structure under analysis was the contralateral parotid. From these figures it can be shown that in general the model follows very closely the clinical points. Supporting the quality of de model are the values of *AUC* ranging from 0.620 to 0.715 and the values of the Worst-fit ranging from 0.601 to 0.611 (Table 6 and 7, respectively). However, some discrepancies were obtained. For the follow-up time 7 weeks although the model follows very closely the clinical data, the model estimate a probability of complications of 25% for patients that were not irradiated (Figure 22). This questions the quality of the model for very low doses since patients that started treatment already with complications were excluded from the study. This may mean that the algorithm that optimizes the radiobiological parameters was trapped in a local maximum and the maximum of the *L* function was not reached. The low γ value indicates that this may have happened. In Figure 24 the clinical point corresponding to 40Gy is outside the confidence interval of the *DRC*. This may be related to the low number of patients included in this point (*N*=2), leading to the conclusion that the point is not very reliable.

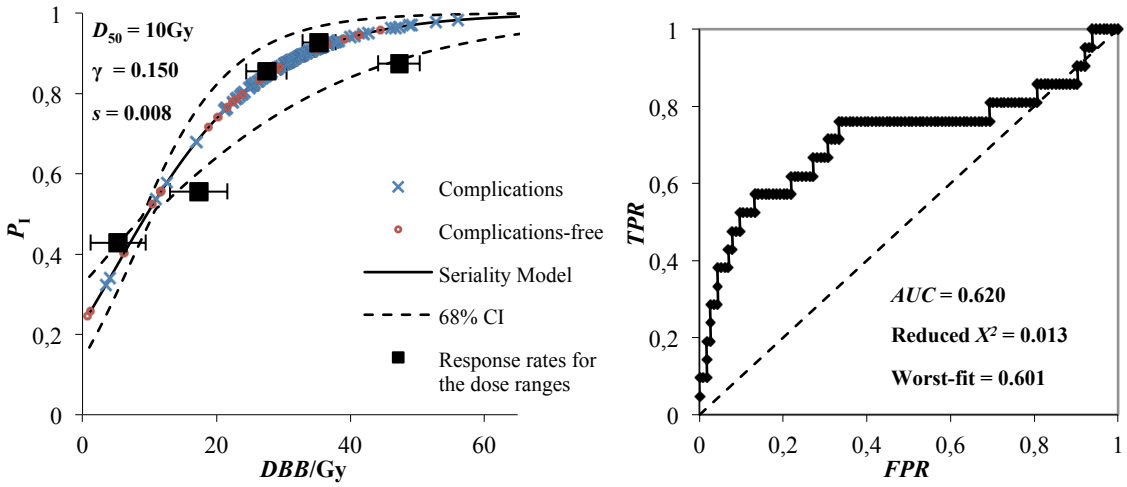

Figure 22 – *DRC* (left) and correspondent *ROC* curve (right) for the contralateral parotid 7 weeks after the *RT*, for the group *G*0 vs. *G*2.

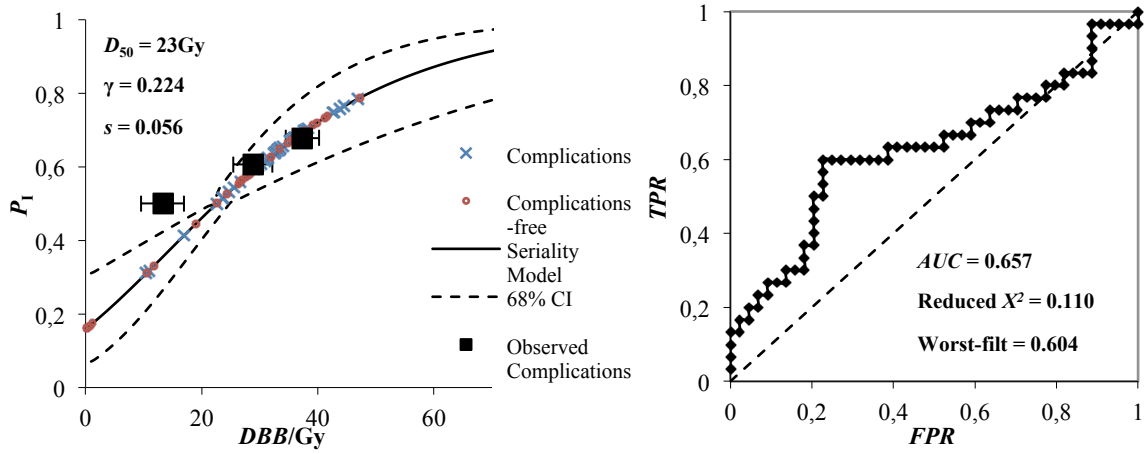

Figure 23 - *DRC* (left) and correspondent *ROC* curve (right) for the contralateral parotid 3 months after the *RT* for the group *G*0 vs. *G*2.

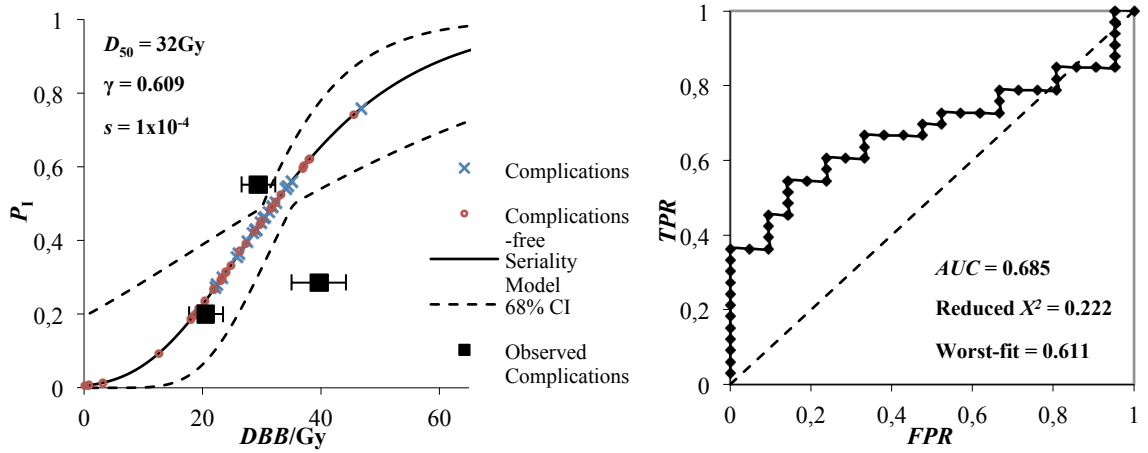

Figure 24 - *DRC* (left) and correspondent *ROC* curve (right) for the contralateral parotid 7 months after the *RT* for the group *G*0 vs. *G*2.

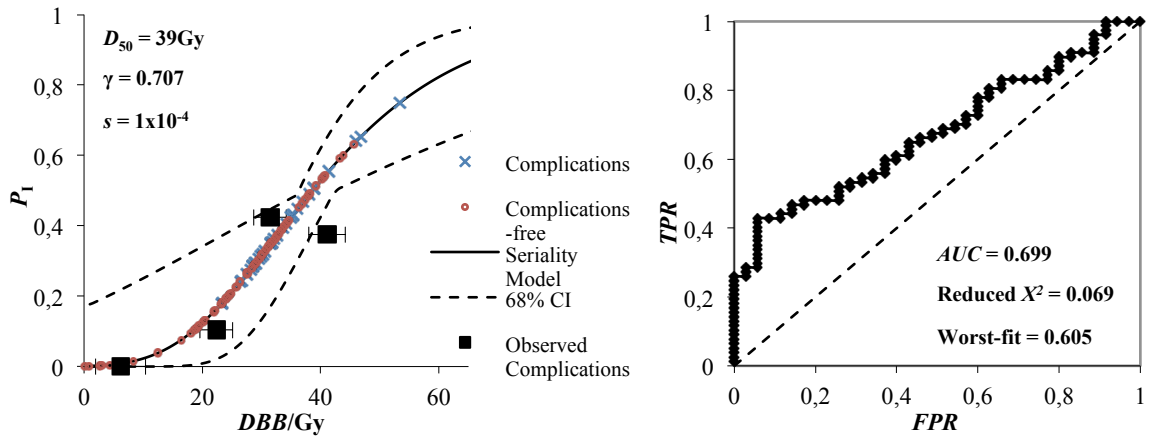

Figure 25 - *DRC* (left) and correspondent *ROC* curve (right) for the contralateral parotid 12 months after the *RT* for the group *G*0 vs. *G*2.

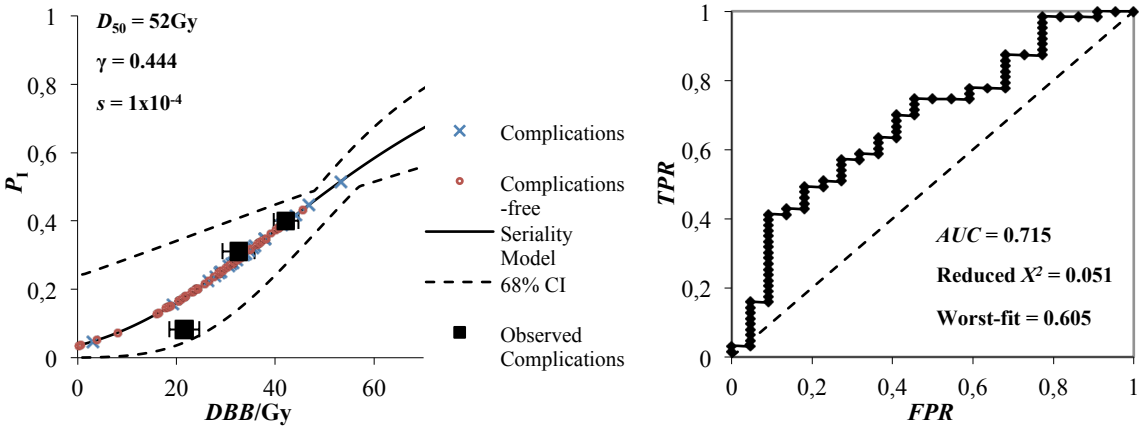

Figure 26 – *DRC* (left) and correspondent *ROC* curve (right) for the contralateral parotid 18 months after the *RT* for the group *G*0 vs. *G*2.

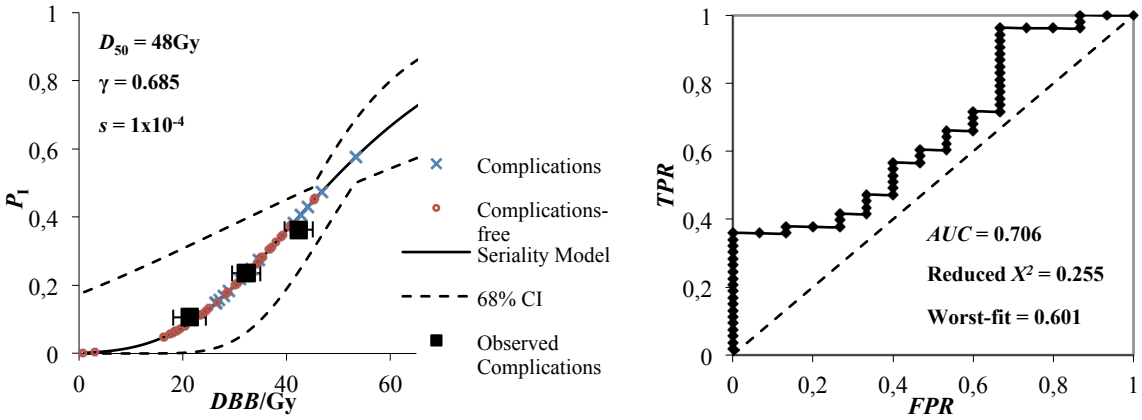

Figure 27 - *DRC* (left) and correspondent *ROC* curve (right) for the contralateral parotid 24 months after the *RT* for the group *G*0 vs. *G*2.

The radiobiological parameters, D_{50}, γ and s, calculated for *G*0 vs. *G*2 for the contralateral parotid for increasing follow-up time can be compared in Table 5. The same results for all structures showed and follow-up times are in Appendix D.1. As the follow-up time increases also the D_{50} value does. This is because there is a decrease of the complications with time (Figure 28) due to the capacity of regeneration of the healthy tissues with time after irradiation. For example 23% of patients at the 24th month of follow-up remained with xerostomia *G*2 compared to 78% at the 7th week.

Table 5 – Relative Seriality model parameters for the contralateral parotids, *G*0 vs. *G*2

Follow-up Times	Nb. Patients	D_{50} [68% *CI*] (Gy)	γ [68% *CI*]	*s*
7 wk	135	9.6 [8.6-10.6]	0.150 [0.045-0.225]	0.008
3 m	74	22.6 [20.3-35.6]	0.224 [0.067-0.381]	0.056
7 m	54	32.2 [29.0-35.4]	0.609 [0.183-1.035]	$1x10^{-4}$
12 m	112	38.6 [34.7-42.5]	0.707 [0.212-1.202]	$1x10^{-4}$
18 m	85	51.7 [46.5-56.9]	0.444 [0.133-0.755]	$1x10^{-4}$
24 m	68	48.3 [43.5-53.1]	0.685 [0.206-1.165]	$1x10^{-4}$

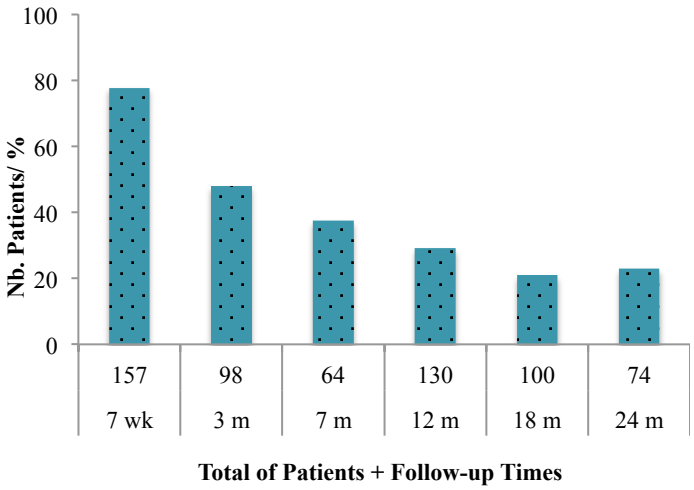

Figure 28 - Evolution of the number of patients (%) in the complications group (*G*2) through the follow-up time.

A recurrent problem in this study was the low γ value obtained for the dose-response curves of the salivary glands (including 4 and 5 structures) at the 3rd month after the radiation therapy treatment. This may be related to the fact that although some patients were irradiated with low *DBB* values they developed complications. The low γ values may be related to the clinical history of these patients, e.g. a previously disease leading to a higher radiosensitivity of the patient and so to a higher damage of the healthy tissues, preventing the recovery of the complications developed with the radiation therapy treatment. Due to this low γ values further analysis of these models were not made.

The last radiobiological parameter of the model, *s*, is approximately zero confirming that the parotids are parallel organs, i.e., that a small part of the parotids may be irradiated with a dose above the tolerance dose and organ functionality is not lost if the remaining organ is protected.

Table 6 and 7 summarizes the values obtained for the *AUC* and Worst-fit for all dose-response curves, respectively. The goodness of the fit evaluated using the methods: *ROC* curves, Pearson's X^2-test and Worst-fit are in Appendix E.1 for every structure and follow-up time. Considering *AUC* values, the best dose-response parameters are those derived for the follow-up times 12, 18 and 24 months when considering the dose in the contralateral parotid and parotids sum. Using the Worst-fit model to test the goodness of the fit (Table 7), values around 0.60 were obtained for all cases. This means that the dose-response curves are of reasonable quality.

Table 6 – *AUC* values (%) for the *DRC* derived for *G*0 vs. *G*2.

Follow-up Times	Contralateral Parotid	Ipsilateral Parotid	Parotids Sum	Salivary Glands_4	Salivary Glands_5
7w	62.01	64.41	62.81	65.13	63.66
3m	65.74	66.10	65.93	- *	- *
7m	68.47	67.40	67.94	67.43	65.46
12m	69.93	69.18	69.37	67.24	66.28
18m	71.45	68.51	70.25	68.48	67.32
24m	70.64	67.11	69.14	65.75	64.63

*Due to the poor quality of the γ value, these models were rejected in this study.

Table 7 – Worst-fit values (%) for the *DRC* derived for *G*0 vs. *G*2.

Follow-up Times	Contralateral Parotid	Ipsilateral Parotid	Parotids Sum	Salivary Glands_4	Salivary Glands_5
7w	60.11	60.11	60.11	60.11	60.11
3m	60.37	61.30	61.02	- *	- *
7m	61.08	60.96	61.70	60.45	60.19
12m	60.54	60.31	60.48	60.22	60.15
18m	60.49	60.12	60.23	60.44	60.32
24m	60.11	60.11	60.11	60.11	60.11

*Due to the poor quality of the γ value, these models were rejected in this study.

The mean *DBB* used to plot all dose-response curves from this study, in the contralateral parotid and sum of the parotids for patients with complications and complication-free was calculated (Figure 29). The mean *DBB* values for the other structures may be seen in Appendix F.1. Figure 29 shows the mean *DBB* values and standard deviation for patients that developed complications (circles) and those that did not (squares) for all follow-up times studied. The threshold value, above which patients have a higher risk to develop complications, is also presented (stars). Generally, patients that developed complications received a higher dose than those that had no side-effects, dose value that is around 26Gy (confirms the study of *Eisbruch et al.* [27]). For patients with complications mean *DBB* was approximately

33Gy. Considering the dose in both parotids, mean *DBB* values for the group of patients complication-free and with complications received around 28Gy and 34Gy, respectively. To note that the difference between the values of both structures is not that significant as indicated by their standard deviation. The threshold or tolerance dose for the contralateral parotid at the follow-up time of 12 months was 28Gy, i.e., for patients receiving dose higher than 28Gy the risk of developing complications was 3.85 (95% *CI*: 1.19-12.47) times higher than patients that received doses lower than 28Gy. Once the lower value of the confidence intervals was higher than 1, the odd ratio can be considered as statistically significant. The same threshold dose was obtained for a follow-up time of 12 months when considering the dose in the sum of the parotids. However, the risk of developing complications is a bit higher, 4.57 (95% *CI*: 1.60-13.10) times higher than patients that received lower doses.

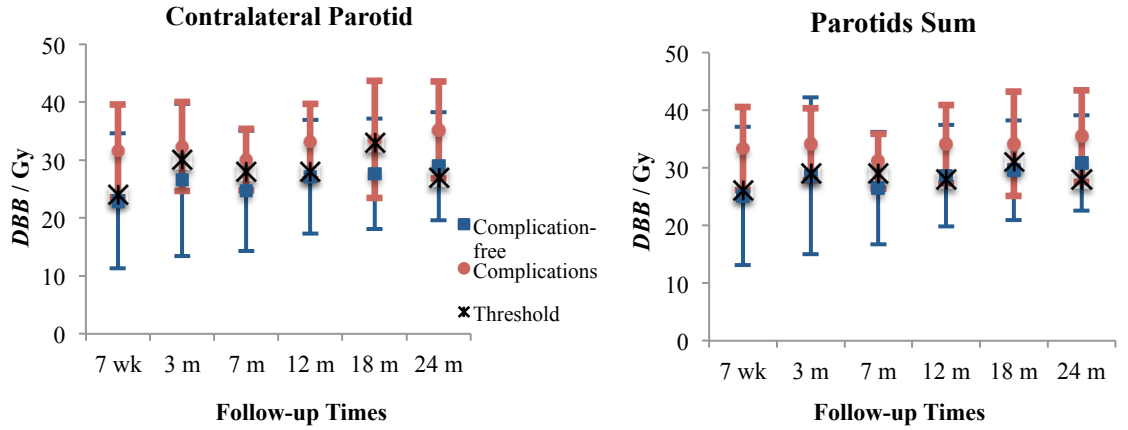

Figure 29 - Mean *DBB* values and respective standard deviation for the complication-free (*G*0) and complications (*G*2) groups for the contralateral parotid (left) and sum of the parotids (right). The threshold dose above which patients had a higher risk to develop complications is also shown.

4.3 *G*0 vs. *G*1+*G*2

Figure 30 to 33 show some of the dose-response curves derived for xerostomia *G*1+*G*2 for different structures 24 months after *RT*, as well as the correspondent *ROC* curves. Dose-response curves and respective *ROC* curves derived for *G*1+*G*2 xerostomia are presented in Appendix C.2 for every structure and follow-up time studied.

In the left side of the Figure 30 the dose-response curve derived for the contralateral parotids at the 24th month of follow-up (solid line) is presented. Qualitatively, the model represents well the clinical data. Quantitatively, if the contralateral parotid is irradiated with 22Gy the model predicts a 27% probability of complications, while the incidence of complications for this dose is 31%. The *ROC* curve is presented above the line that shows random predictions, i.e., where the true positive ratio is equal to the false positive ratio (*TPR=FPR*). The area under the curve in this case was 0.67 what is considered a reasonable model.

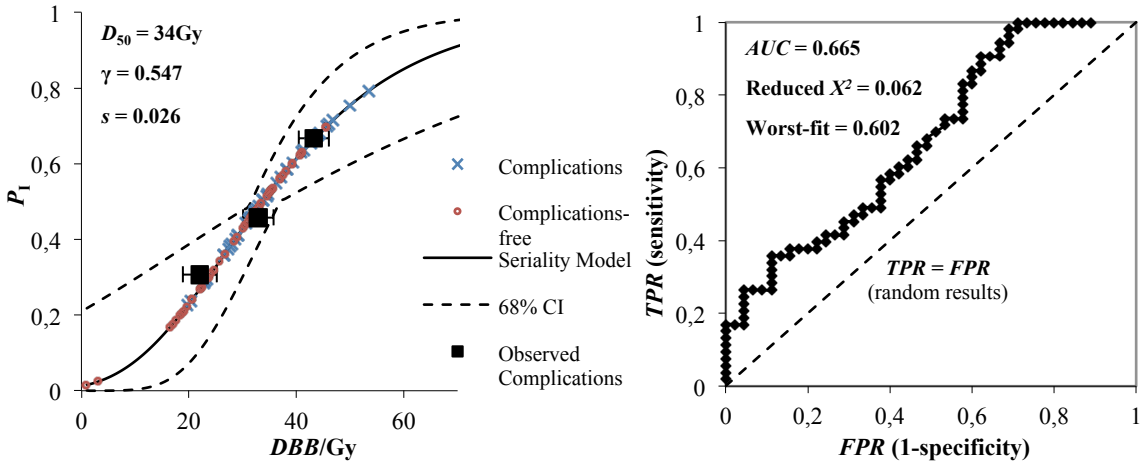

Figure 30 – *DRC* (left) and correspondent *ROC* curve (right) for the contralateral parotids 24 months after the *RT* for the group *G*0 vs. *G*1+*G*2.

Figure 31 to 33 show the *DRC* and respective *ROC* curves derived for the 24th month after the *RT* studied when the structures under analysis were the sum of the parotids and the salivary glands with 4 and 5 structures. From these figures it can be shown that for both salivary glands the models do not follow the clinical points so well and so this situations need to be revaluated.

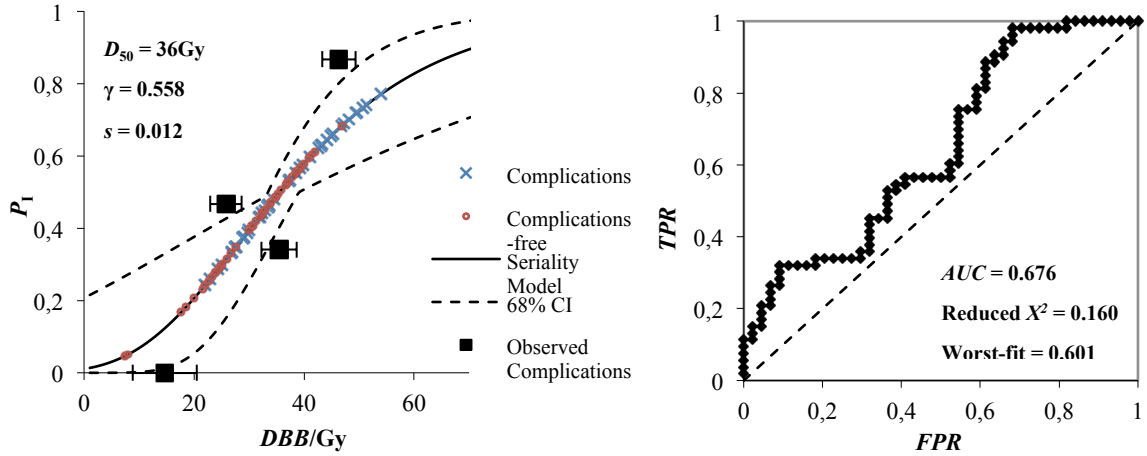

Figure 31 - *DRC* (left) and correspondent *ROC* curve (right) for the parotids sum 24 months after the *RT* for the group *G*0 vs. *G*1+*G*2.

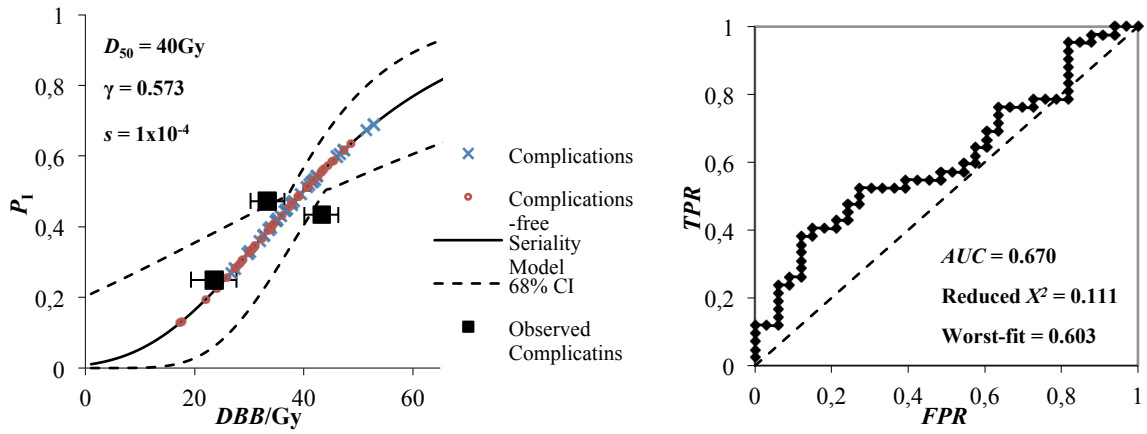

Figure 32 - *DRC* (left) and correspondent *ROC* curve (right) for the salivary glands with 4 structures 24 months after the *RT* for the group *G*0 vs. *G*1+*G*2.

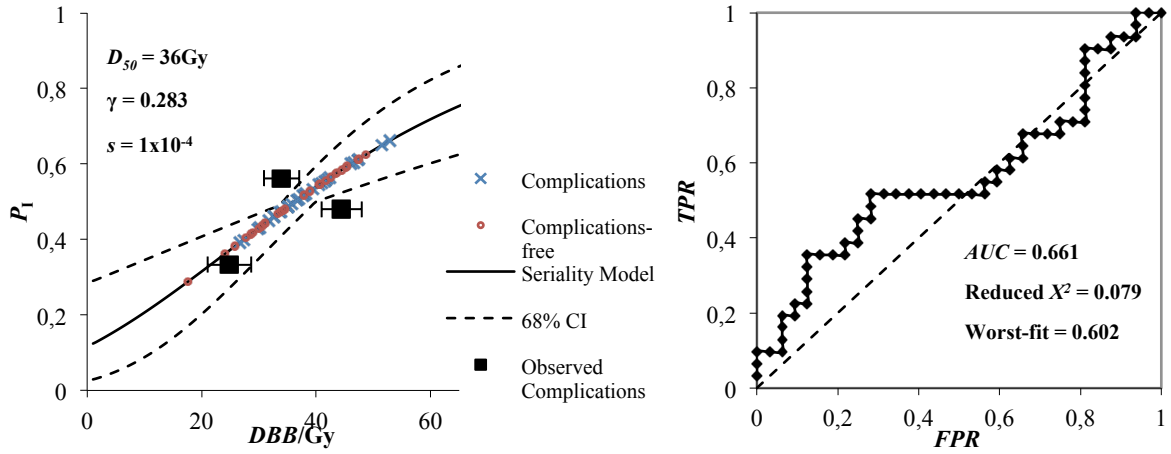

Figure 33 - *DRC* (left) and correspondent *ROC* curve (right) for the salivary glands with 5 structures 24 months after the *RT* for the group *G*0 vs. *G*1+*G*2.

The radiobiological parameters for the contralateral parotid when patients were grouped as *G*0 vs. *G*1+*G*2 are presented on Table 8. The relative seriality parameters, D_{50}, γ and *s*, calculated for *G*1+*G*2 xerostomia for all the structures and follow-up times are presented on the Appendix D.2. As before, D_{50} increases with follow-up time and $s \approx 0$. Models with very low γ values ($\gamma < 1x10^{-2}$) were rejected in this study, i.e., the models for the 7th week and 3rd month of follow-up time of all the structures studied.

Table 8 – Relative Seriality model parameters for the contralateral parotids, *G*0 vs. *G*1+*G*2

Follow-up Times	Nb. Patients	D_{50} [68% *CI*] (Gy)	γ [68% *CI*]	*s*
7 wk	291	4.0 [3.6-4.4]	$1x10^{-4}$ [$0.3x10^{-4}$-$1.7x10^{-4}$]	0.039
3 m	171	7.1 [6.4-7.8]	$1x10^{-4}$ [$0.3x10^{-4}$-$1.7x10^{-4}$]	0.139
7 m	97	20.6 [18.5-22.7]	0.429 [0.129-0.729]	0.026
12 m	188	23.1 [20.8-25.4]	0.247 [0.074-0.420]	$3.3x10^{-4}$
18 m	145	24.8 [22.3-27.3]	0.225 [0.068-0.383]	$1x10^{-4}$
24 m	98	33.6 [30.2-37.0]	0.547 [0.164-0.930]	0.026

Table 9 show the values obtained for the *AUC* for the dose-response curves of *G*1+*G*2 xerostomia. The values quantifying the goodness of the fit for this group is shown in Appendix E.2 for every structure and follow-up time. The best dose-response curves were for the follow-up times of 12, 18 and 24 months when it is considered the dose that reaches the contralateral parotid and parotids sum. However, when comparing these results with those obtained for *G*2 xerostomia it can be noticed that the *AUC* of *G*0 vs. *G*2 were about 0.70 and for the *G*0 vs. *G*1+*G*2 the *AUC* values approximate 0.66. This leads to the conclusion that the models derived for *G*2 xerostomia have a higher prediction ability than for *G*1+*G*2 xerostomia.

Table 9 - *AUC* values (%) for the *DRC* derived for *G*0 vs. *G*1+*G*2.

Follow-up Times	Contralateral Parotid	Ipsilateral Parotid	Parotids Sum	Salivary Glands_4	Salivary Glands_5
7m	64.84	65.73	65.31	65.53	65.53
12m	66.06	66.18	66.19	66.11	65.87
18m	66.03	66.03	66.05	66.04	65.74
24m	66.47	66.97	67.55	66.97	66.13

The mean *DBB* values that differentiate patients with complications from complication-free were calculated and are shown in Figure 34 for the contralateral parotid and sum of the parotids. The corresponding *DBB* values for the other

structures may be seen in Appendix F.2. Complication-free patients had mean *DBB* values in the contralateral parotid around 27Gy and patients with complications received approximately 32Gy. For the sum of the parotids complication-free and complications groups received around 29Gy and 33Gy, respectively. However caution is advised since the difference between the values of both structures is not that significant. The threshold dose for the contralateral parotids 24 months after the *RT* was 26Gy. Patients receiving higher dose values at the contralateral parotids have a risk of developing complications 4.47 (95% *CI*: 1.51-13.24) times higher than patients that received lower doses. This result was statistically significant. In other hand, the threshold dose in the sum of the parotids for the same follow-up time was 39Gy, with a risk of developing complications of 4.14 (95% *CI*: 1.52-11.24) compared to patients receiving lower doses.

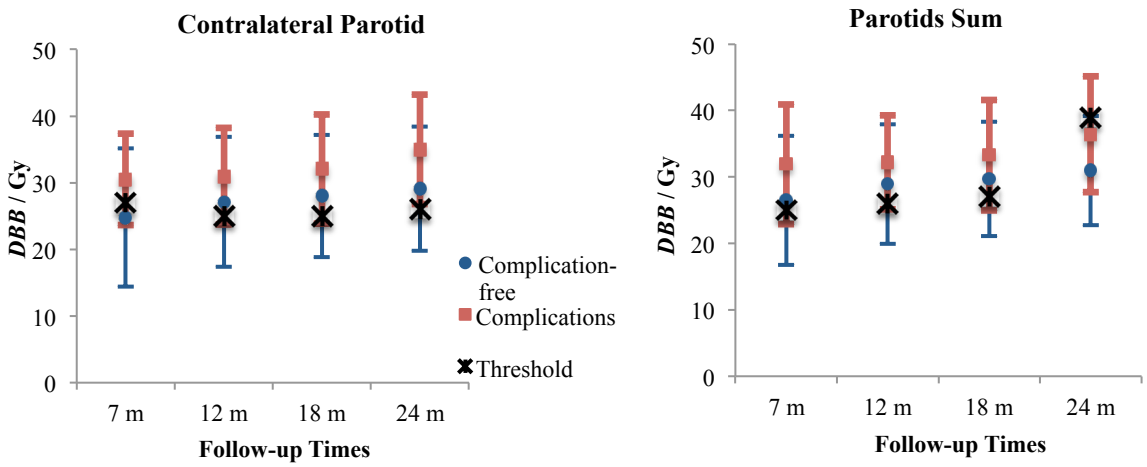

Figure 34 - Mean *DBB* values and respective standard deviation for the complication-free (*G*0) and complications (*G*1+*G*2) groups for the contralateral parotid (left) and sum of the parotids (right). Threshold dose shows the tolerance dose above which patients had a higher risk to develop complications.

4.4 Mean Dose vs. *DBB*

The results reported throughout the study are based on the quantity *DBB*. However, this measure is still not used in daily clinical practice because it is not calculated by any treatment planning system. Commonly the mean dose in the parotids is used because the programs used for planning the radiation therapy

treatment still calculate physical dose in most of the cases. Thus the relation between *DBB* and the mean dose (D_{mean}) in the contralateral parotids was studied (Figure 35) for the follow-up times 12 and 24 months. It can be seen that the relation between *DBB* and mean dose values is almost linear (slope of the curve is approximately 1) but both dose measures are not equal. Both follow-up time's data are overlapped and both linear tendencies have a $R^2 \approx 1$. Due to that, it can be concluded that the *DBB* values are almost proportional to the mean dose values and they are time independent.

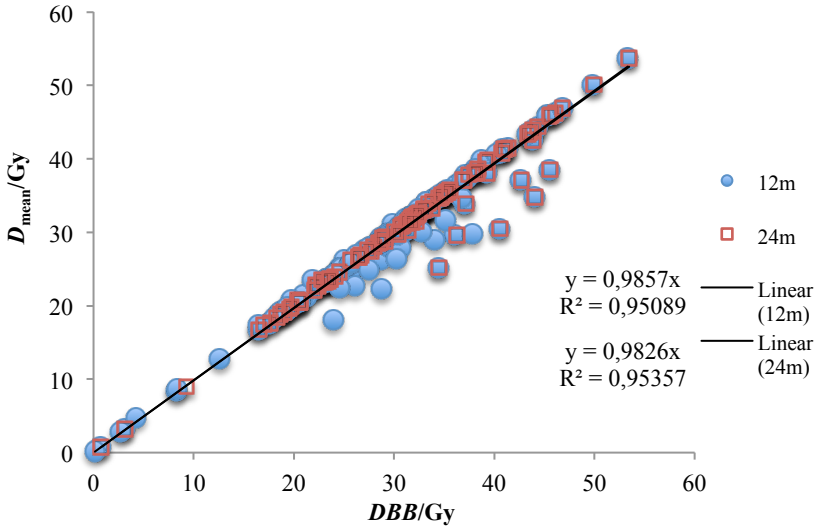

Figure 35 – Comparison of the *DBB* with the mean dose (D_{mean}), for the contralateral parotids, 12 and 24 months after *RT*.

CHAPTER 5: Discussion

5.1 Comparison of Endpoints

Figure 36 shows the dose-response curves derived for the contralateral parotid, sum of the parotids and salivary glands with 4 structures at the 18th month of follow-up, for both the groups *G*0 vs. *G*2 and *G*0 vs. *G*1+*G*2. From the figure, it can be seen that when low severities of complications, e.g. *G*1, are included in the model the curves shift to the left because low severities are related to low dose values received during the radiation therapy treatment. However, Figure 36 show that the radiobiological parameters derived for xerostomia *G*2 are better than the ones derived for xerostomia *G*1+*G*2, since at 0Gy a 0% probability of complications is estimated.

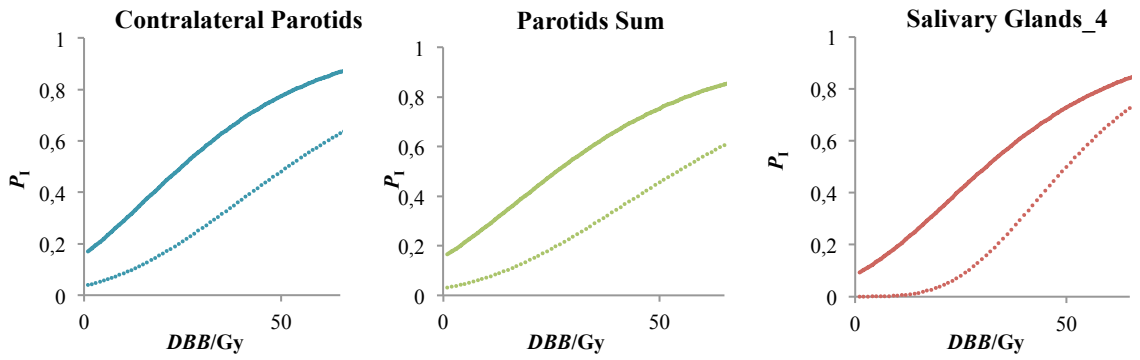

Figure 36 – *DRC* for follow-up time of 18 months: *G*0 vs. *G*1+*G*2 (solid curves) and *G*0 vs. *G*2 (dashed curves).

5.2 *DRC* for Different Structures

Dose-response curves for different structures are compared for different follow-up times in Figure 37. The results for 7 months of follow-up time for the groups *G*0 vs. *G*2 and *G*0 vs. *G*1+*G*2 are shown. It can be noticed that the *DRC* curves from the group *G*0 vs. *G*1+*G*2 are very close. In this case only the parotids may be used to estimate the probability of xerostomia in a patient. However, the models derived for *G*0 vs. *G*2 are different depending on the structure under analysis. The cause of the deviation can be related to the fact that there are too few salivary glands (*SG*)

outlined (32 for the *SG* with 4 structures and 24 for the *SG* with 5 structures), which may affect the *DRC* shape. Further studies are needed to better understand this difference.

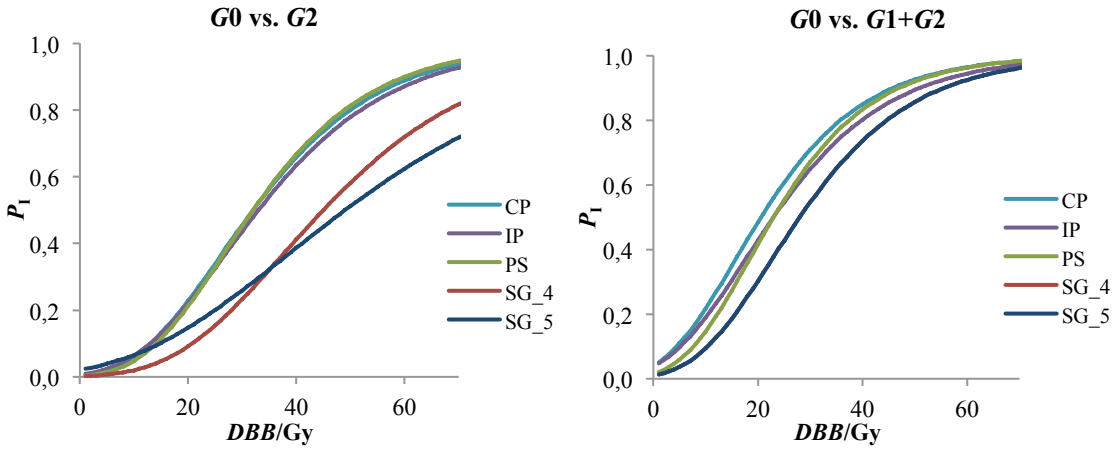

Figure 37 – *DRC* for different structures, 7 months after *RT*. *CP*: contralateral parotids, *IP*: ipsilateral parotids, *PS*: parotids sum, *SG_4*: salivary glands with 4 structures, *SG_5*: salivary glands with 5 structures.

5.3 *DRC* for Different Follow-up Times

In Figure 38 the *DRC* for the parotids sum are presented for *G*0 vs. *G*2 and *G*0 vs. *G*1+*G*2. The dashed lines show acute complications (≤6 months) while solid lines show late complications (>6 months). As also seen in Table 5 (*G*0 vs. *G*2) and Table 8 (*G*0 vs. *G*1+*G*2), the *DRC* shift towards higher dose values with increasing follow-up time (higher D_{50}) and became less steeped (lower γ). This is a consequence of recovery of healthy tissues with time.

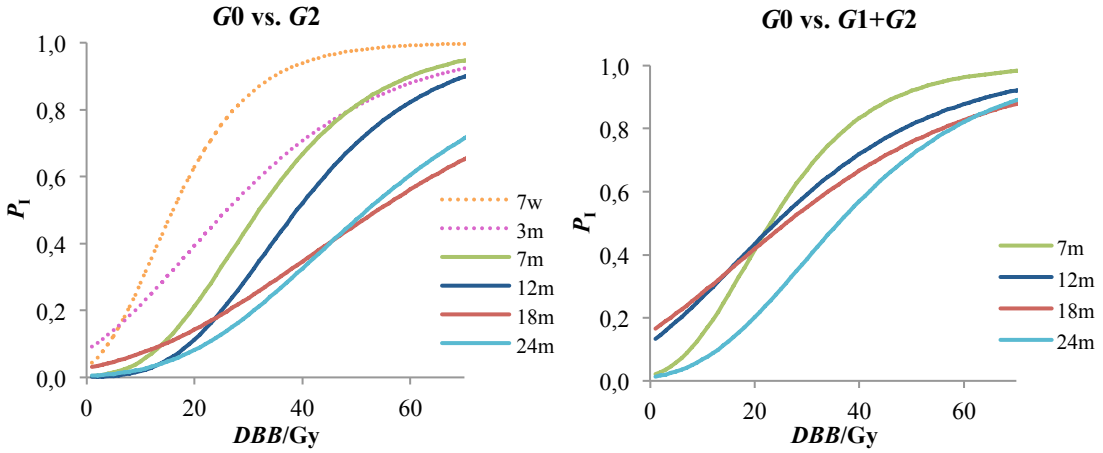

Figure 38 – *DRC* of the parotids sum (ipsilateral + contralateral) for different follow-up times.

5.4 Comparison with Literature

The dose-response curves derived in this study for the Relative Seriality model using *IPOCFG*'s clinical data were compared with the dose-response curves published in the literature. For a fair comparison the results presented in Figure 39 were chosen for the same structure, i.e., the sum of the parotids, similar time periods and severity of complications. Once the published results were mostly related to the severity *G*3 it was decided to compare these results with the dose-response curves derived for *G*2 xerostomia.

The *DRC* for a follow-up of 12 months are very similar. For the 6 and 7 months, it is normal a little detachment between the curves once it is being compared two different but proximal time periods. For the 3rd month of follow-up time a large difference exist between the curves. This may be related to the lack of convergence of the optimization algorithm in the derivation of the dose-response curve for this follow-up time.

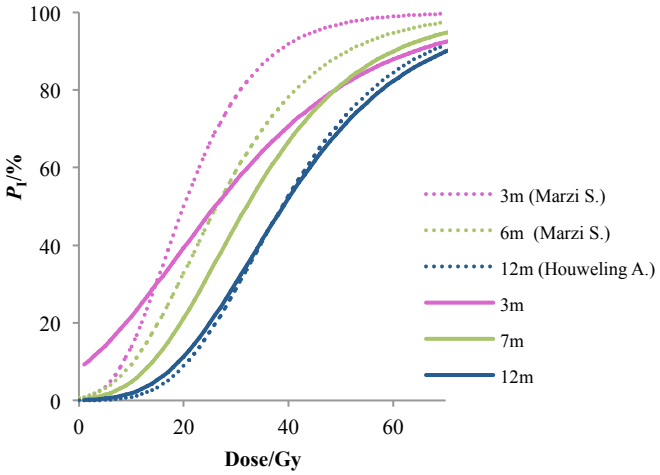

Follow-up Times [Ref.]	D_{50} [68% *CI*]	γ [68% *CI*]	*s*
3m [28]	26.3 [23.7-28.9]	0.34 [0.10-0.58]	0.01
6/7m [28]	32.5 [29.3-35.8]	0.66 [0.20-1.12]	0.001
12m [34]	39.2 [35.3-43.1]	0.73 [0.22-1.24]	$1x10^{-4}$

Figure 39 – Comparison of the published *DRC* for the Relative Seriality Model (dashed lines) with the *DRC* derived in this study for parotids sum of *G*0 vs. *G*2 (solid lines). Radiobiological parameters *Marzi et. al.* etc. (right).

CHAPTER 6: Conclusions

The dose-response parameters that may give the best prediction of the probability of xerostomia were obtained for the follow-up times of 12, 18 and 24 months when considering the dose in the contralateral parotid and/or the sum of the parotids. Furthermore, the predictive ability of the model is better for xerostomia *G*2 than for xerostomia *G*1+*G*2.

As the follow-up time increases, *DRC* move towards high D_{50} values. γ values range from 0.1 to 0.7. The radiobiological parameter *s* confirms the fact that the parotids are parallel structures.

Patients irradiated in the contralateral parotid and in the sum of the parotids with a mean dose values higher than 28Gy have a risk of developing xerostomia *G*2 3.85 and 4.57 times higher than if receiving lower dose values, respectively.

Xerostomia is a consequence of damages in all salivary glands. However, the dose in both parotids may be a good surrogate to estimate the probability of *G*2 xerostomia. Unfortunately, given the small number of patients used to derive the dose-response curves for the salivary glands, further studies may be needed to confirm the results obtained.

Model validation using a different patient population must be made before the model derived in this study may be used clinically.

REFERENCES

[1] James M. Slater, *Ion Beam Therapy: Fundamentals, Technology, Clinical Applications*.: Linz, Ute (Ed.), 2012.

[2] Cancer Research UK. [Online]. http://www.cancerresearchuk.org/cancer-info/cancerandresearch/all-about-cancer/what-is-cancer/treating-cancer/history-of-radiotherapy/radiotherapy3

[3] Linear Accelerators. [Online]. http://hyperphysics.phy-astr.gsu.edu/hbase/particles/linac.html

[4] P. Kallman, B. Lind, E. Eklof, and A. Brahme, "Shaping of arbitrary dose distributions by dynamic multileaf collimation," *Phys. Med. Biol.*, vol. 33, no. 11, pp. 1291-1300, 1988.

[5] Jacob Van Dyk, *The Modern Technology of Radiation Oncology - A Compendium for MEdical Physicists and Radiation Oncologists*. Madison, Wisconsin: Medical Physics Publishing, 1999.

[6] Hans-Georg Menzel, *ICRU 83: Prescribing, Recording and Reporting Photon-Beam Intensity-Modulated Radiation Therapy (IMRT)*. Geneva, Switzerland: Oxford University Press, 2010, vol. 10.

[7] David Hinckley, *ICRU REPORT 62: Prescribing, Recording and Reporting Photon Beam Therapy (Supplement to ICRU Report 50)*. Bethesda, Maryland, USA, 1999.

[8] David Hinckley, *ICRU REPORT 50: Prescribing, Recording, and Reporting Photon Beam Therapy*. Bethesda, Maryland, USA, 1993.

[9] Eugene N. Myers and Robert L. Ferris, *Salivary Gland Disorders*. Pittsburgh, USA, PA: Springer, 2007.

[10] Stephen Gallik. (2009) Histology OLM: The online lab manual for mammalian histology. [Online]. http://histologyolm.stevegallik.org/node/476

[11] Michael Edgar, Colin Dawes, and Denis O'Mullane, *Saliva and oral health*.: Stephen Hancocks Limited, 2012.

[12] Lynne H. Slim and Cheryl Thomas. (1996-2014) dentalcare.com - Trusted Resource. Informed Professionals. Healthier Patients. [Online]. http://www.dentalcare.com/en-US/dental-education/continuing-

education/ce96/ce96.aspx?ModuleName=coursecontent&PartID=7&SectionID=-1

[13] James D. Cox, Joann Stetz, and Thomas F. Pajak, "Toxicity criteria of the Radiation Therapy Oncology Group (RTOG) and the European Organizationfor Research and Treatment of Cancer (EORTC)," *Int. J. Radiation Oncology Biol. Phys.*, vol. 31, no. 5, pp. 1341 - 1346, 1995.

[14] Anders Brahme, "Development of Radiation Therapy Optimization," Department of Medical Radiation Physics, Karolinska Institutet and Stockholm University, Stockholm, Acta Oncologica 2000.

[15] James M. Galvin, "Alternative Methods for Intensity-Modulated Radiation Therapy Inverse Planning and Dose Delivery," *Seminars in Radiation Oncology*, vol. 16, pp. 218-223, 2006.

[16] Thomas Bortfeld, "IMRT: a review and preview," *Phys. Med. Biol.*, vol. 51, pp. 363-379, 2006.

[17] S. Webb, "The physical basis of IMRT and inverse planning," *The British Journal of Radiobiology*, pp. 678-689, October 2003.

[18] P. C. Williams, "IMRT: delivery techniques and quality assurance," *The British Journal of Rdiobiology*, pp. 766-776, November 2003.

[19] Werner Bar et al., "A comparison of forward and inverse treatment planning for intensity modulated radiotherapy of head and neck cancer," *Radiotherapy and Oncology*, vol. 69, pp. 251-258, August 2003.

[20] A. Taylor and M E B Powell, "Intensity-modulated radiotherapy - what is it?," *e-med*, vol. 4, pp. 68-73, 2004.

[21] Don Carlson, "Intensiy Modulation Using Multileaf Collimators: Current Status," *Medical Dosimetry*, vol. 26, no. 2, pp. 151–156, 2001.

[22] Essa Mayyas et al., "Evaluation of multiple image-based modalities for image-guided radiation therapy (IGRT) of prostate carcinoma: A prospective study," *Medical Physics*, vol. 40, no. 4, March 2013.

[23] David A. Jaffray, "Emergent Technologies for 3-Dimensional Image-Guided Radiation Delivery," *Seminars in Radiation Oncology*, vol. 15, pp. 208-216, 2005.

[24] Predrag Sukovic. (2004) American Association of Dental Maxillofacial Radiographic Technicians. [Online]. http://www.aadmrt.com/article-1---2004.html

[25] Michael Joiner and Albert van der Kogel, *BAsic Clinical Radiobiology*.: Edward Arnold, 2009, vol. 4.

[26] M. A. R. Alexander, W. A. Brooks, and S. W. Blake, "Normal tissue complication probability modelling of tissue fibrosis following breast radiotherapy," *Phys. Med. Biol.*, vol. 52, pp. 1831-1843, 2007.

[27] C. Burman, G. J. Kutcher, B. Emani, M. Goitein, "Fitting of normal tissue tolerance data to an analytic function," *Int. J. Radiation Oncology Biol. Phys.*, vol. 21, pp. 123-135, 1991.

[28] Simona Marzi et al., "Analysis of salivary flow and dose-volume modeling of complication incidence in patieents with head-and-neck cancer receiving intensity-modulated radiotherapy," *Int. J. Radiation Oncology Biol. Phys.*, vol. 73, no. 4, pp. 1252-1259, 2009.

[29] Judith M. Roesink, Marinus A. Moerland, Jan J. Battermann, Gerrit Jan Horduk, and Chris H. J. Terhaard, "Quantitative dose-volume response analysis of changes in parotid gland function after radiotherapy in the head-and-neck region," *Int. J. Radiation Oncology Biol. Phys.*, vol. 51, no. 4, pp. 938-946, 2001.

[30] Mohsen Bakhshandeh et al., "Norma tissue complication probability modeling of radiation-induced hypothyroidism after head-and-neck radiation therapy," *Int. J. Radiation Oncol. Biol. Phys.*, vol. 85, no. 2, pp. 514-521, 2013.

[31] Angel I. Blanco et al., "Dose-volum modeling of salivary function in patients with head-and-neck cancer receiving radiotherapy," *Int. J. Radiation Oncology Biol. Phys.*, vol. 62, no. 4, pp. 1005-1069, 2005.

[32] Panayiotis Mavroidis et al., "Statistical methods for clinical verification of dose-response parameters related to esophageal stricture and AVM obliteration from radiotherapy," *Physics in Medicine and Biology*, vol. 49, pp. 3797-3816, 2004.

[33] C. Schilstra and H. Meertens, "Calculation of the Uncertainty in Complication Probability for various Dose–Response Models, Applied to the Parotid Glands," *Int. J. Radiation Oncology Biol. Phys.*, vol. 50, no. 1, pp. 147–158, 2001.

[34] Antonetta C. Houwling et al., "A comparison of dose-response models for the parotid gland in a large group of had-and-neck cancer patients," *Int. J. Radiation Oncology Biol. Phys.*, vol. 76, no. 4, pp. 1259-1265, 2010.

[35] Tim Dijkema et al., "Parotid gland function after radiotherapy: the combined Michigan and Utrech experience," *National Institute of Health*, vol. 78, no. 2, pp. 449-453, October 2010.

[36] Avraham Eisbruch, Randall K. Ten Haken, Hyungin M. Kim, Lon H. Marsh, and Jonathan A. Ship, "Dose, volume, and function relationships in parotid salivary glands following conformal and intensity-modulated irradiation of head and neck cancer," *Int. J. Radiation Oncology Biol. Phys.*, vol. 45, no. 3, pp. 577-587, 1999.

[37] Brígida C. Ferreira, Maria do Carmo Lopes Lopes, Josefina Mateus, Miguel Capela, and Panayiotis Mavroidis, "Radiobiological evaluation of forward and inverse IMRT using different fractions for head and neck tumours," *Radiation Oncology*, 2010.

[38] Panayiotis Mavroidis, Bengt K. Lind, and Anders Brahme, "Biologically effective uniform dose (D) for specification, report and comparison of dose response relations and treatment plans," *Physics in Medicine and Biology*, vol. 46, no. 10, 2001.

[39] Panayiotis Mavroidis et al., "Dose-response relations for anal sphincter regarding fecal leakage and blood or phlegm in stools after radiotherapy for prostate cancer," *Strahlentherapie und Onkologie*, vol. 181, no. 5, pp. 293-306, 2005.

[40] Tom Fawcett, "ROC Graphs: Notes and Practical Considerations for Data Moning Researchers," Intelligent Enterprise Technologies LAboratory, 2003.

[41] Tom Fawcett, An introduction to ROC analysis, December 2005.

[42] Gianna Boero, Jeremy Smith, and Kenneth F. Wallis, "Decompositions of Pearson's chi-squared test," *Journal of Econometrics*, vol. 123, pp. 189-193, 2004.

[43] Ling. (2008) Tutorial: Pearson's chi-square test for independence. [Online]. http://www.ling.upenn.edu/~clight/chisquared.htm

APPENDIXES

Appendix A – Review from the Literature

Summary of the papers related to the salivary glands that report xerostomia as a complication.

APPENDIXES

Papers	Score	Scoring Criteria	*Guideline*	Population		Tumour	*Follow up*			Prescribed Dose		Planning				Other treatments		
				Nº of Patients (N)	Age	Sublocation	Duração	Assessment		Total dose (Gy)	Dose/fraction (Gy)	Technique	Fields	Energy (MV)	TPS	Pre-RT Treatments	Concomitant chemotherapy	Date of treatments
					Mean			Objective	Subjective									
1		0: no effect on speech or swallowing; 1: speech requires some effort; smallowing requires some effort but without need to be supported by fluid intake; 2: discomfort in speaking and swallowing with need for fluid intake; 3: need for fluid intake for regular conversation; 4: dry oral mucosa		25	52,4	Oropharynx, nasopharynx, lynphoma (Waldeyer's ring)	2,3-36,6 months	Scintigraphy (measurement of salivary flow)		30-70	2,3-2,5	3DCRT	opposed lateral fields or 3 fields					
2	4	Severe=decrease in stimulated salivary flow <25% of the pre-RT value	RTOG	88	55	Oral cavity, oropharynx, nasopharynx, larynx, salivary glands, skin, others	1 year after RT	measurement of salivary flow		64 (57,6–72)	1,8-2	3DCRT, IMRT	3DCRT: 7 to 8 fields, sometimes are used electron irradiation fields for the posterior cervical	6, 15, 9 MeV and 12 MeV	U-Mplan	Surgery, Chemotherapy		March of 1994 to Augost of 1997
3		decrease in stimulated salivary flow to <25% of the pre-RT value		15			until the 13th week after RT	measurements of salivary excretion fraction by saliva collection		46 - 70	2	3DCRT	2 laterally opposed fields and an AP field	6	Helax TMS	Surgery		
4		decrease in stimulated salivary flow to <25% of the pre-RT value	RTOG/EORTC Late Effects Consensus Conference	108	57	Larynx, oropharynx, oral cavity, nasopharynx, nose, hipopharynx, unknown, others	6 weeks after RT 6 months after RT 1 year after RT	measurement of salivary flow		46-70	2	3DCRT	Opposed lateral fields with spinal cord protection up to 40-46 Gy; electron fields for boost in the posterior neck region; supraclavicular regions irradiated with hemi-previous field	6	Plato	No	No	
5	2		RTOG	23		Oral cavity, oropharynx, nasopharynx, larynx, hipopharynx	14,8 months (8-26 months)	Measurment of the salivary flow with and without estimulation		50 (PTV1), 10 to 20 (PTV2)	2	IMRT	7 to 8 fields and 1-15 segments by field (step and shoot)	6,15	Helax TMS	Surgery		April 2000 to December 2001
6				65	57	Oral cavity, oropharynx, nasopharynx, larynx, pharynx, others	up to 1 year after RT	measurment of the salivary flow	questionaires	50,4 to 72	1,8 to 2	3DCRT, IMRT			CMS (RTC-3D), Peacock Planner (IMRT)	Surgery, chemotherapy	Yes	February 1997 to September 2000
7	4	Decrease in stimulated salivary flow to <25% of the pre-RT value		52	56	Larynx, Floor of mouth/oral cavity, Oropharynx, Nasal cavity, Hypopharynx, Nasopharynx, Other	57 months (44–72)	stimulated parotid saliva using Lashley cups placed over the orifice of the parotid duct		66 (40–70)		3DCRT	Opposing lateral fields and anterior field for the supraclavicular regions, electron beams used to boost the posterior neck region		PLATO RTS	Surgery		
8	ΔF ≤ 50%	Reduction of the relative excretion rate (ΔF) of >50%		33	58,4	Oropharynx, nasopharynx, larynx, paranasal sinus, lymphoma	6 weeks after completing radiotherapy and then in 3-month intervals within the first year	clinical examination; CT or MRI exam, post-therapeutic salivary gland scintigraphy was performed 3 months after RT			1,8 - 2	RT	Lateral opposing fields, anterior and lateral wedged fields	6 MV, diferent electron energy			yes (24%)	
	ΔF ≤ 75%	Reduction of the relative excretion rate (ΔF) of >75%																
	ΔF ≤ 50%	Reduction of the relative excretion rate (ΔF) of >50%		23	55,3						1,8 - 2	RT (+Amifostine)	Lateral opposing fields, anterior and lateral wedged fields	6 MV, diferent electron energy			yes (30%)	
	ΔF ≤ 75%	Reduction of the relative excretion rate (ΔF) of >75%																
	ΔF ≤ 50%	Reduction of the relative excretion rate (ΔF) of >50%		19	54					70 (52+18)	1,8 - 2,2	IMRT		6, 15	KonRad/Virtuos (Siemens)		yes (32%)	
	ΔF ≤ 75%	Reduction of the relative excretion rate (ΔF) of >75%																
9	4	Decrease in stimulated salivary flow to <25% of the pre-RT value	RTOG/EORTC	157	58	Larynx, Hypopharynx, Oropharynx, Nasopharynx, Oral cavity, Nasal cavity, Unknown primary, Other		stimulated parotid saliva measurements using Lashley cups		46-70	2	3DCRT	Opposing lateral fields and anterior field for the supraclavicular regions, eletron beams to boost the posterior neck region	6	PLATO RTS 2,0		No	
				64	60	Hypopharynx, Oropharynx, Nasopharynx, Unknown primary				54-69	1,8-2,3	IMRT	five equidistant beams ans seven beams	6	PLATO ITP, 1,1		Yes	1996-2007
10	3	0 = none; 1 = slight dryness of mouth, good response to stimulation; 2 = moderate dryness of mouth, poor response to stimulation; 3 = complete dryness of mouth, no response to stimulation; 4 = fibrosis	RTOG	59	57,5	Nasopharynx, oropharynx, hypopharynx, oral cavity	12,8 months after RT (2,8–29,3)	measurements of salivary excretion fraction by scintigraphy or saliva collection	quality-of-life questionnaires (the patient's subjective perception of xerostomia)	70		IMRT	5 to 7 fields, ensuring, whenever achievable, that each parotid did not receive a mean dose >32 Gy		Cadplan; Eclipse	Surgery	yes	
11	4	Complication for each individual gland was defined as a stimulated parotid flow eatio <25% on the pre-RT flow rate		92	54	Larynx, Hypopharynx, Oropharynx, Nasopharynx, Oracl cavity, Nasalcavity, Salivary Glands, Unknown n primary, Other	1 year after RT	measurement of simulated individual parotid gland flow rates before and after RT using Lashley cups after applying citric acid solution (2-5%) on the mobile part of the tongue		60-75	1,8-2,0	Forward-planned, inverse-planned and beamlet IMRT				Surgery: Y/N		1994-2005
				130	58					50-70 , 69-70	2 , 2,0-2,3	CRT (opposing lateral beams), inverse-planned IMRT						1996-2007
				222														
12		stimulated salivary flow to <25% of pre-RT value		347			1 year after RT	stimulated salivary flow rates measurement using Lashley cups				IMRT, 3DCRT	Inversed planned IMRT or Opposed lateral beams					
13	4	fow ratio <25% of the pre-RT flow rate	RTOG/EORTC	151	60	Larynx, Hypopharynx, Oropharynx, Nasopharynx, Oracl cavity, Unknown primary	1 year after RT	stimulated salivary flow rates measurement using Lashley cups			69-70						Surgery: Y/N	1999-July 2012

NTCP Calculation																														References		
Model	Dose-volume histogram				Fitting parameters			Model Parameters																						Authors	Publication	Year
	Organ delimitation	Dosimetric parameters	α/β (Gy)	Sensitivity	Method	χ2	p	D50	95% CI		s	95% CI		γ	95% CI		m	95% CI		n	95% CI		k	95% CI		Other parameters	XX Axis	NTCP plot			
									-	+		-	+		-	+		-	+		-	+		-	+							
Logistic	Parotid glands	D mean (sum of parotids)			t student			< 33																					Kaneko et al,	Oral Oncol 1998;34:140 –146,	1998
								40-55																							
LKB	Parotid glands	V7, V15, V30 e V45, D mean			Maximum likelihood			28,4	25	34,7							0,18	0,1	0,33	1									Eisbruch et al,	Int, J,Radiat, Oncol, Biol, Phys, 45 577–87	1999
Lyman	Parotid glands				Maximum likelihood			38	33	45							0,26	0,16	0,34	1,3	0,3	3,2					Schilstra_2001	Schiltra	Volume 58, Issue 1, 1 January 2004, Pages 175–184, Vol, 50, No, 1, pp, 147–158, 2001	2001
Seriality								37	32	46	####	0	0,19	2	1	5,3															
Critical Volume (Probit)								38	15	55				4,4	> 0,5																
Lyman					Maximum likelihood			31	26	35							0,54	0,40	0,78	1						D mean		Roesink J, et al,	Int, J, Radiation Oncology Biol, Phys,, Vol, 51, No, 4, pp, 938–946	2001
								35	30	40							0,46	0,34	0,66	1											
								39	34	44							0,45	0,33	0,65	1											
Lyman	Parotid glands and submandibular	D mean	3		Maximum likelihood		0.002	46.6									0.13									EUD		Scrimger et al,	Int, J, Radiation Oncology Biol, Phys,, Vol, 60, No, 1, pp, 178–185	2004
Mean dose-exponential; EUD-exponential ; Parallel-exponential; Exponential-sigmoid; Exponential-sigmoid Comp-mean; Exponential-sigmoid Comp-max																													Blanco et al,	Int J Radiat Oncol Biol Phys 2005;62	2005
Lyman	Parotid glands	Mean dose					0,018	34	30	40							0,37	0,28	0,5	1					n fixed at 1	Mean dose parotid gland		Braam et al,	Int, J, Radiat, Oncol, Biol, Phys, 62 659–64	2005
							0,018	40	35	46							0,33	0,25	0,46	1											
							0,182	42	37	50							0,37	0,28	0,51	1											
								46	39	60							0,53	0,44	0,69	1											
Log Logistic	Parotid and submandibular glands	Mean dose			maximum likelihood			34,2	22	46,4													2,3	0,9	3,7		D (Gy)	Munter_2006	Münter	Int, J, Radiation Oncology Biol, Phys,, Vol, 67, No, 3, pp, 651–659, 2007	2007
	Parotid gland only							36,4	20,5	52,3													2,2	0,4	4						
	Parotid and submandibular glands							50,3	45,8	54,8													3,8	2,3	5,3						
	Parotid gland only							55,7	50,7	60,7													3,4	1,4	5,4						
	Parotid and submandibular glands							46,3	44	48,6													6,1	4,8	7,4						
	Parotid gland only							44,3	41,1	47,5													5,5	3,9	7,1						
	Parotid and submandibular glands							54,1	50	58,2													3,4	2,4	4,4						
	Parotid gland only							49,8	44,6	55													3,1	1,8	4,4						
	Parotid and submandibular glands							36,8	33,9	39,7													5	3,9	6,1						
	Parotid gland only							35	31,5	38,5													6,5	4,4	8,6						
	Parotid and submandibular glands							42,5	39,4	45,6													5,3	4	6,6						
	Parotid gland only							41	35,7	46,3													4,9	3,2	6,6						
Lyman	Parotid glands	Mean dose			maximum likelihood		0,01	32	29	34							0,51	0,42	0,64	1					n fixed at 1	Mean dose; Dose		Dijkema, et al,	Int, J, Radiation Oncology Biol, Phys,, Vol, 72, No, 4, pp, 1101–1109	2008
							0,007	36	33	39							0,45	0,38	0,59	1											
							0,12	40	37	44							0,46	0,37	0,59	1											
							0,01	26	22	29							0,59	0,46	0,79	1											
							0,007	31	26	35							0,63	0,61	0,85	1											
							0,12	38	35	42							0,33	0,23	0,49	1											
LKB	parotid glands	Dmean	3	α/β =4,5 Gy; similar results as α/β=3 Gy	maximum likelihood			21,4	18,4	25,5							0,57	0,34	1,37	1						Dmean parotids	Marzi_2009	Marzi	Int J Radiat Oncol Biol Phys, 2009 Mar 15;73(4):1252-9	2009
Seriality								20	16,7	24,1	0,01			0,77	0,31	1,42														
LKB								27,8	23,6	33,7							0,49	0,27	1,42	1										
Seriality								26,3	21,5	32,8	0,01			0,73	0,15	1,55														
LKB								41,6	32,8	56,8							0,45	0,27	1,39	1										
Seriality								40	32	54	0,01			0,8	0,35	1,62														
LKB	parotid glands	Dmean			Maximum Likelihood	Delta= 340,6	0,68	40,5	36,8	44,1							0,36	0,28	0,44	1						Mean Dose		Dijkema, et al,	Int J Radiat Oncol Biol Phys, 2010 October 1; 78(2): 449-453	2010
								39,7	37	43,3							0,44	0,35	0,54	1										
						Delta= 340,6	0,68	39,4	33,8	41,8							0,42	0,36	0,58	1,13	0,75	14,3									
						Delta= 339,2	<0,0001	39,9	37,3	42,8							0,4	0,34	0,51	1					n value was fixed at 1						
LKB	left and right parotid glands were delineated on a contrast-enhanced computed tomography (CT)		between 3 and 10		maximum likelihood			39,4	33,8	41,8							0,42	0,36	0,58	1,13	0,75	14,3				Mean dose; Mean BED	NR	Houweling et al,	International Journal of Radiation Oncology Biology Physics; Volume 76, Issue 4, 15 March 2010, Pages 1259–1265	2010
mean dose								39,9	37,3	42,8							0,4	0,34	0,51	1										
Seriality								38,8	36,5	43,5	0,08	0	0,65	0,95	0,7	1,3														
Critical Volume (Probit)																									α=0,03;No=1; λ=0,65;NFSU=21					
Parallel FSU								37	32	44							0,35	0,3	0,6				2,75	0,5	4,5	D50 = 30,5					
VDth model (dose treshold)																	0,48	0,35	0,65							Dth=30,5; rdV50=0,68					
LKB		Dmean				Maximum Likelihood	<0,05	22,7	11,7	37,1	55						1,57	0,87	3,14							D mean submandibular glands			Submandibular gland dose-response relationships after radiotherapy for h&n cancer	
								35	27,8	41,5							0,44	0,28	0,65											

Appendix B – MATLAB Codes

- **Function that imports the dose-volume information from the text files and saves in a matrix the information related to each file.**

```
function [dose, volume]=plot_DVH(filename,dvh)
%------------------------------------------------------------------------
% done by Claudia Xavier in 7-10-2013
%------------------------------------------------------------------------
%function [dose, volume]=plot_DVH(filename, dvh)
%."dvh" includes: color, linestyle, linewidth, x_max,y_max, y_label
%------------------------------------------------------------------------
A=load(filename); %read the file (2 columns)
dose=A(:,1); %gives a name to column 1
volume=A(:,2); %same for the 2nd
clear A

plot(dose,volume,'Color',dvh.color,'LineStyle',dvh.linestyle,'LineWidth',dvh.line
width) %for each patient
hold on
axis([0 dvh.x_max 0 dvh.y_max])
xlabel('Dose / Gy'), ylabel(dvh.y_label)
title('Dose-Volume Histogram')
```

- **Function that runs the function *plot_DVH* and creates the mean dose-volume curve of that group of dose-volume histograms. It saves the dose values, mean volume values and the total number of *DVH* used to calculate the mean curve.**

```
function
[dose,mean_volume,k]=plot_DVH_allpatients(patientlist,filename,directory_resp
onse,dvh,dvh_mean)
```

```
%------------------------------------------------------------------------
% done by Claudia Xavier in 7-10-2013
%------------------------------------------------------------------------
%[dose,mean_volume]=plot_DVH_allpatients(patientlist,filename,directory_resp
onse,dvh,dvh_mean)
%."dvh" includes: color, linestyle, linewidth, x_max,y_max, y_label
%------------------------------------------------------------------------
dose = [];
mean_volume = [];
if strfind(filename, 'cum')
   dvh.y_label='Volume/ %';
   dvh.y_max=100;
elseif strfind(filename, 'dif')
   dvh.y_label='Volume';
   dvh.y_max=10;
end

k=0; %counts
matrix_volume=[];
for i=1:numel(patientlist)
   dir_patient = int2str(patientlist(i)); %RID=patient directory
   if exist([directory_response dir_patient], 'dir')
      allfilename= [directory_response dir_patient '\' filename];
      %if the patient directory exists it creates a new one with the hole information
of
% the files of the patient
      if exist(allfilename, 'file')
         [dose,volume]=plot_DVH(allfilename,dvh);
         if ~isempty(volume)
            k=k+1; %number of columns (different patients)
            matrix_volume(:,k)=volume; %matrix of the volume only if the volume
%exists for a certain file
         end
      end
```

```
   end
end
clear volume

if ~isempty(matrix_volume) %in the case of existing a matrix volume
   mean_volume=mean(matrix_volume,2); %mean volume is calculated for each
%volume of all patients
   plot(dose,mean_volume,'Color',dvh_mean.color,
'LineStyle',dvh_mean.linestyle,...
      'LineWidth',dvh_mean.linewidth) %plot the means
end
```

- **Main function that reads the excel file with the data related to each patient in order to create the *DVH*. It creates several subplots in the same figure where each subplot runs the function *plot_DVH_allpatients* and the last subplot corresponds to the mean curves of the previous ones.**

```
function difer_patients_vector_parotid(filename,sheet,column,time)
%--------------------------------------------------------------------------
% done by Claudia Xavier in 7-10-2013
%--------------------------------------------------------------------------
%function difer_patients_vector(filename,sheet,column)
% .to RUN this function -> insert it on the command window and
change"filename" by the name of the file which
% DVH you want to plot (don't forget the extention), “sheet" by the name of the
excel sheet and "column" by the
% letter(s) of the column of  interestt
% .Analyze the complications that patients developed (numbers...UPDATED)
%--------------------------------------------------------------------------
directory_response =
'C:\Users\Administrator\Desktop\correrMatlab\PatientData\DVH\';
excel_directory    = 'C:\Users\Administrator\Desktop\correrMatlab\';
excel_directory    = [excel_directory 'Book15_population_without3D-CRT.xlsx'];
```

```
patients_nb       = 386; %number of patients in the excel sheet (in RID)
last_line         = patients_nb +3;%+3 because excel file starts in line 4

% FOR ALL PATIENTS:
figure(1);
dvh.color     = 'k';
dvh.linestyle = '-';
dvh.linewidth = 1;
dvh.x_max     = 80;
dvh_mean.y_label='Volume / %';
dvh_mean.linestyle= dvh.linestyle;
dvh_mean.linewidth= dvh.linewidth+2;
patientlist=xlsread(excel_directory, sheet, ['A4:A' int2str(last_line)]); %read
numbers
%in the excel sheet

% DIVIDED:
[column,~]=xlsread(excel_directory, sheet, [column int2str(4) ':' column
int2str(last_line)]); % read strings in the
% excel sheet
[~,name]=fileparts(filename); %cut strings and return only part of it
[~,name]=fileparts(name);

variable=unique(column); %find ONCE the different variables in hole column
index=find(~isnan(variable));
variable = variable(index);

color='brcmgy'; %don't need to be a cell because it's only one letter
linestyle={'-' '--' ':' '-.' '.' '*' '+' 'o' '>' 'x' '^' 'v' '<' 'p' 'h'}; %cell
line_nb=2;
column_nb=2;
subplot_nb=line_nb*column_nb; %in this case its allways 6 (2x3)
close all %close all windows (e.g.figures) before running the figures below
```

```
figure_nb=1; %so we can start at the 2nd one [mod(1/6)=1]
k=1; %counts the number of plots
k1=1; %counts the mean plots
for i=1:numel(variable)
   if mod(i,subplot_nb)==1 %i/6, if i is multiple of 6, the rest is 0
        %but we want it to open a new figure in 7, 13,... so the ==1
      figure_nb=figure_nb+1; %when rest==1 it creates a new figure
      k=1; %when a new figure is created, k returns to 1
   end
   figure(figure_nb) %make the new figure
   dvh_mean.color=color(k); %colors returns to the beginning when k=1
   dvh_mean.linestyle=linestyle{figure_nb-1}; %linestyle returns to the
beginning
%when k=1
   [dose,mean_volume,N_c]=subplot_DVH_allpatients(variable(i),column,
patientlist,filename, ,...
      directory_response, dvh, dvh_mean,line_nb, column_nb,k);
   k=k+1; %counts the k values until 7(when k=[1-6] creates 6 plots in the figure
and
%when k=7 creates a new one)
   if ~isempty(dose) %in the case of having dose values
      figure(2)
      subplot(line_nb,column_nb,4)
      plot(dose,mean_volume,dvh_mean.color,'LineStyle',...
         dvh_mean.linestyle,'LineWidth',2.5) %plots all the mean values in a single
%plot
      legend_variable{k1}=['G' int2str(variable(i))]; %creates a new cell only with
the
%tumours that were ploted
      k1=k1+1; %number of mean plots
      hold on
      xlabel('Dose / Gy'), ylabel(dvh_mean.y_label)
      title(['Mean DVHs of ' name ', ' time])
```

```
    end
end

figure(2),legend(legend_variable) %calls this figure, in the end, to put the legend
in it
function
[dose,mean_volume,N_c]=subplot_DVH_allpatients(variableX,column,patientlist
,filename,...
    directory_response,dvh,dvh_mean,line_nb, column_nb,position) %creates the
%subplots and saves the dose
%and mean_volume data

index=find(column==variableX); %finds a certain variable in the column and
save
%the correspondent RIDs
if ~isempty(index) %in the case of having a list of RIDs for a tumortype(e.g.)
    patientlist=patientlist(index); %patient list will corresponde to that
    subplot(line_nb,column_nb,position)
    [dose,mean_volume,N_c]=plot_DVH_allpatients(patientlist,filename,...
    directory_response,dvh,dvh_mean); %N=length(index); %counts the number
of
%patients in each plot (to add nb. of patients)
    title(['G' int2str(variableX) ', N_c=' int2str(N_c)])
    clear patientlist index
else
    dose=[];
    mean_volume = [];
end
```

Appendix C – *DRC* and *ROC* curves

Appendix C.1 – *G*0 vs. *G*2

- IPSILATERAL PAROTID

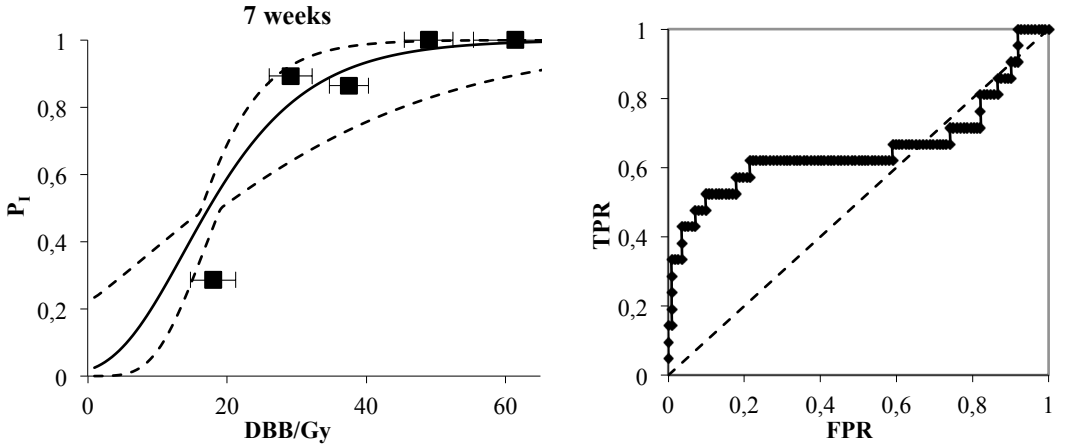

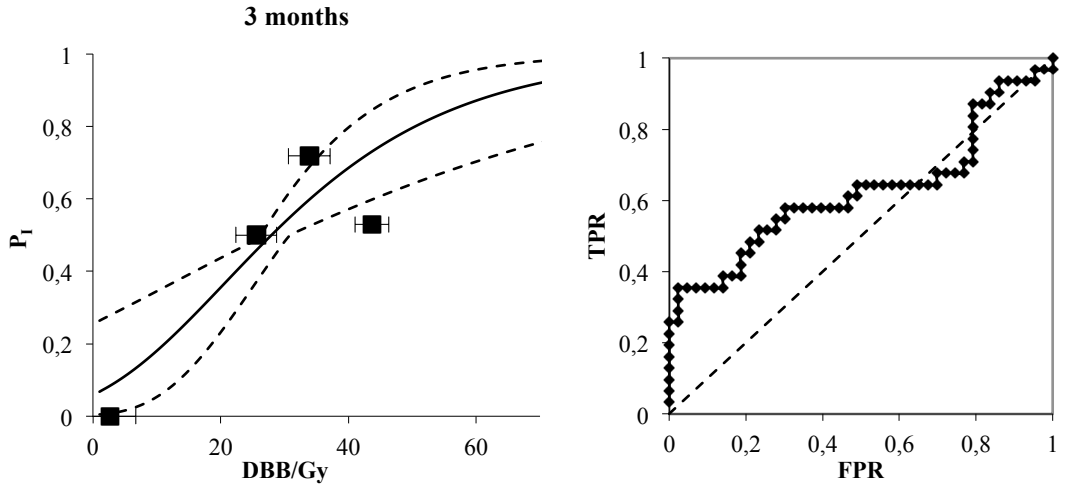

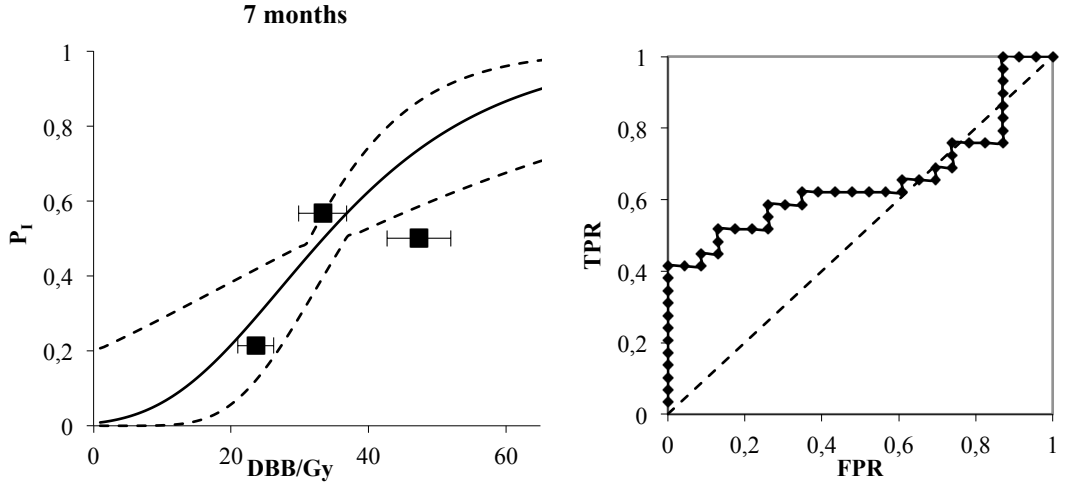

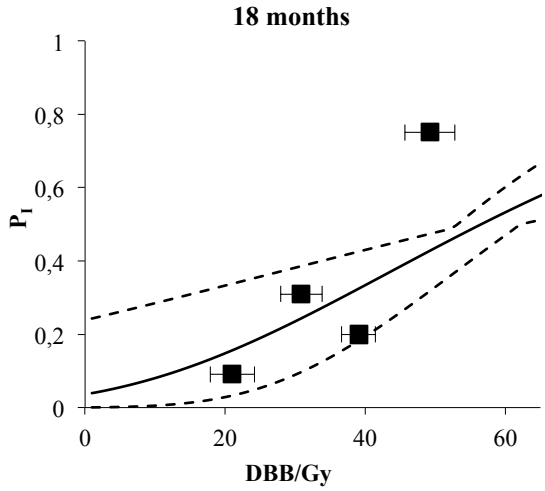

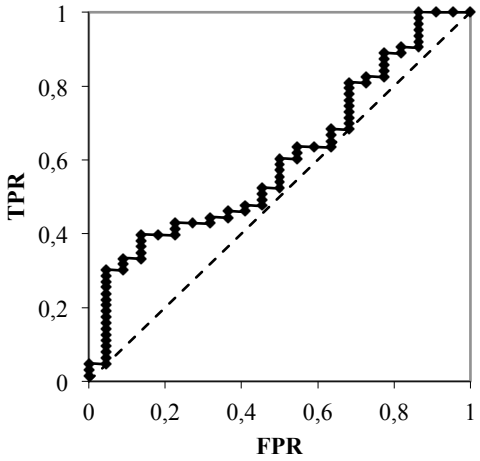

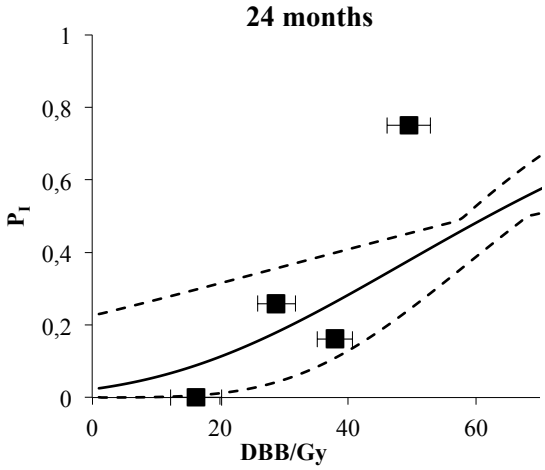

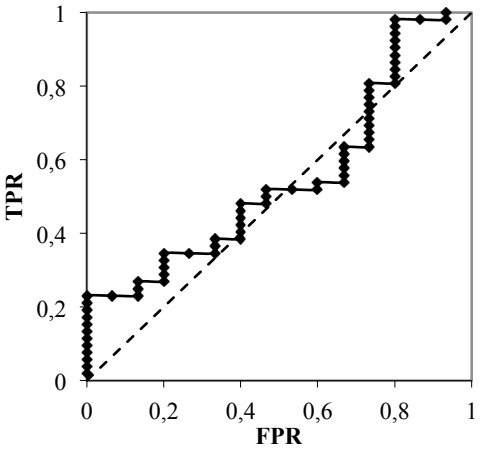

- PAROTIDS SUM

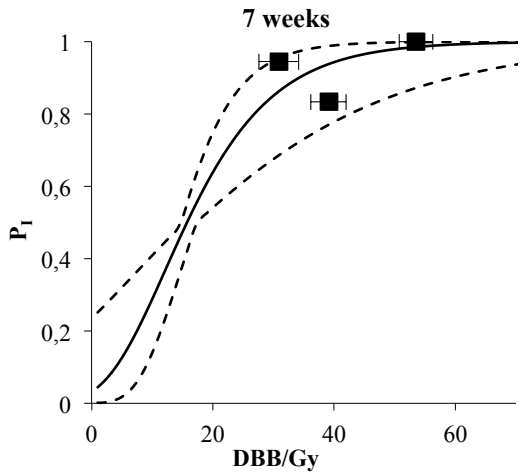

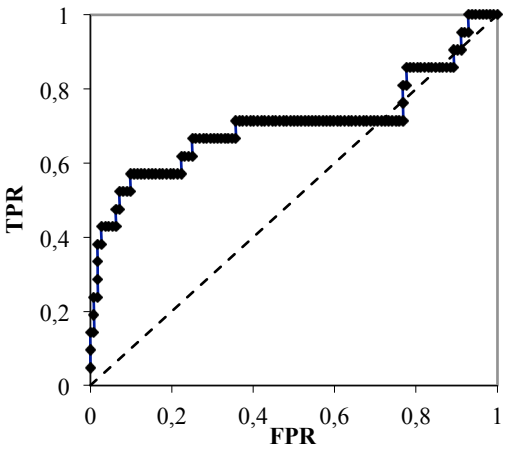

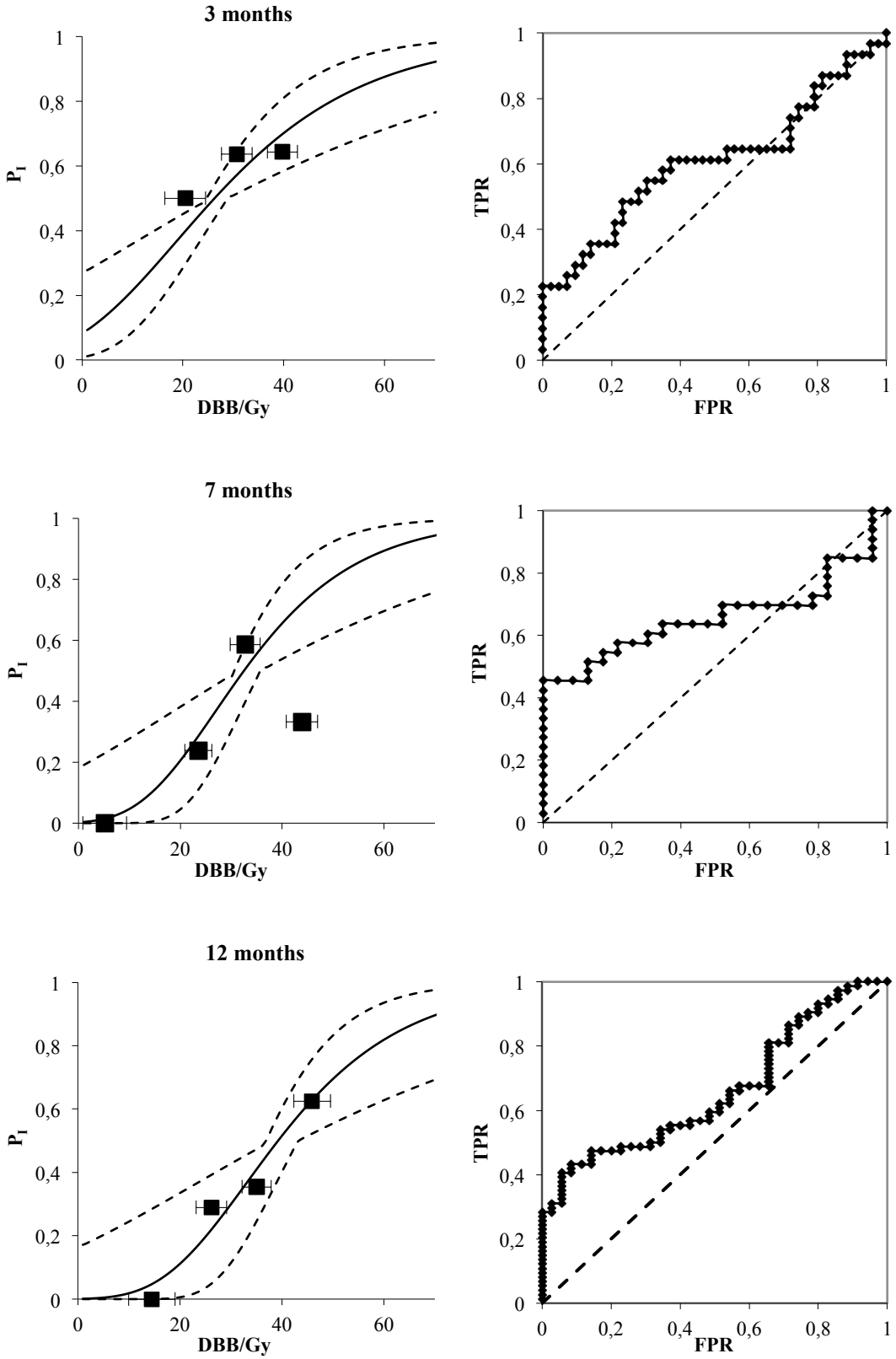
3 months
P_I
DBB/Gy
TPR
FPR
7 months
P_I
DBB/Gy
TPR
FPR
12 months
P_I
DBB/Gy
TPR
FPR

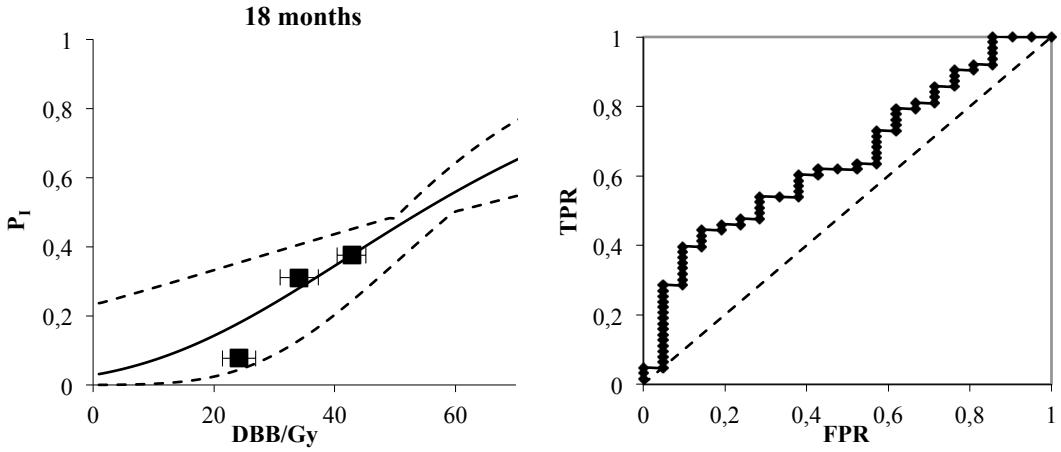

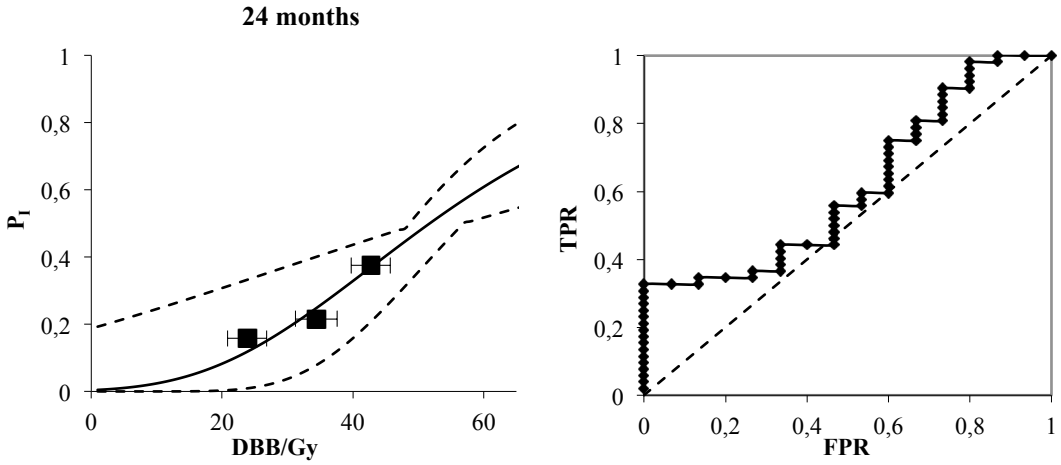

- SALIVARY GLANDS – 4 structures

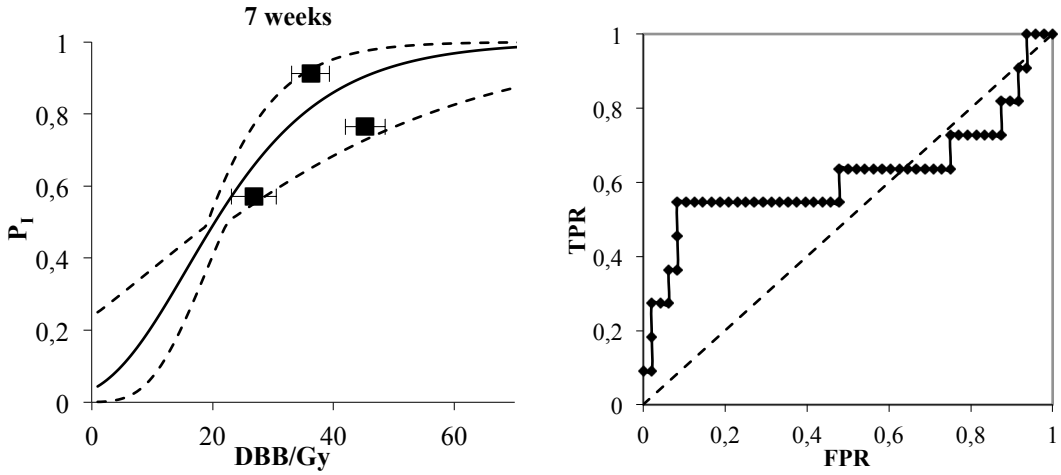

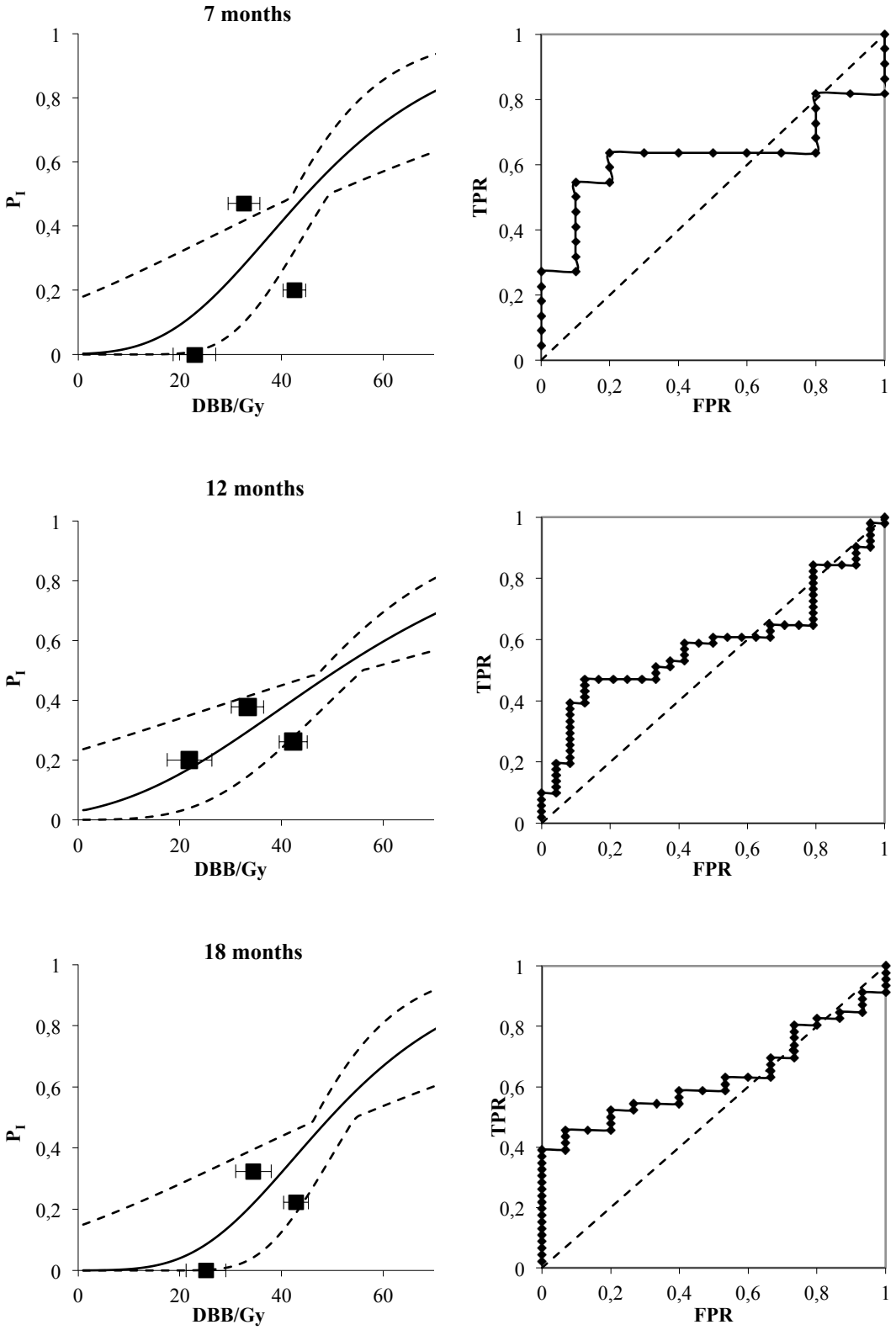
7 months
P_I
DBB/Gy
TPR
FPR
12 months
P_I
DBB/Gy
TPR
FPR
18 months
P_I
DBB/Gy
TPR
FPR

- SALIVARY GLANDS – 5 structures

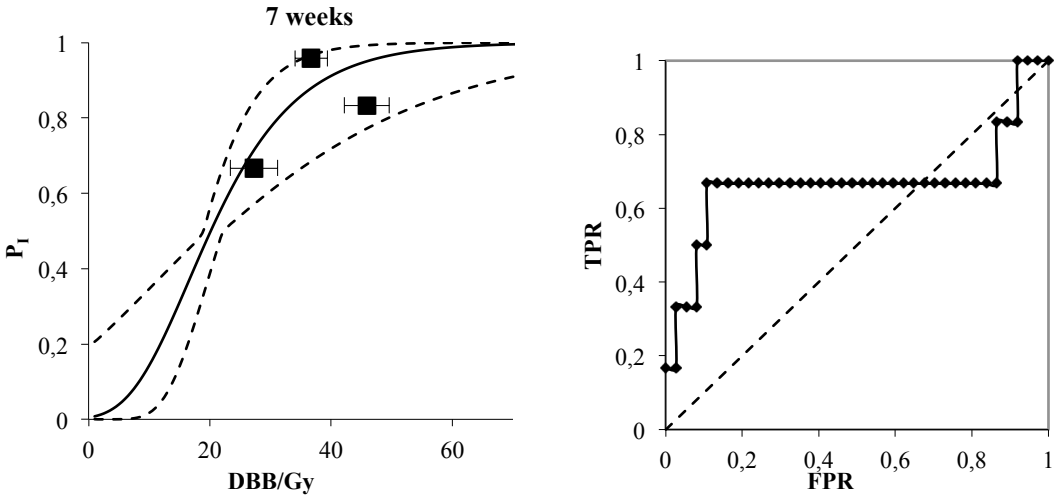

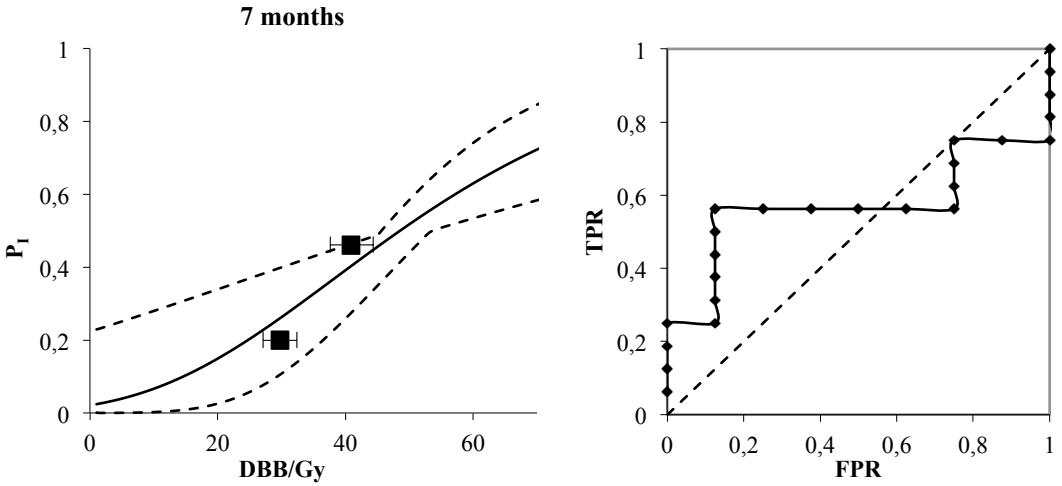

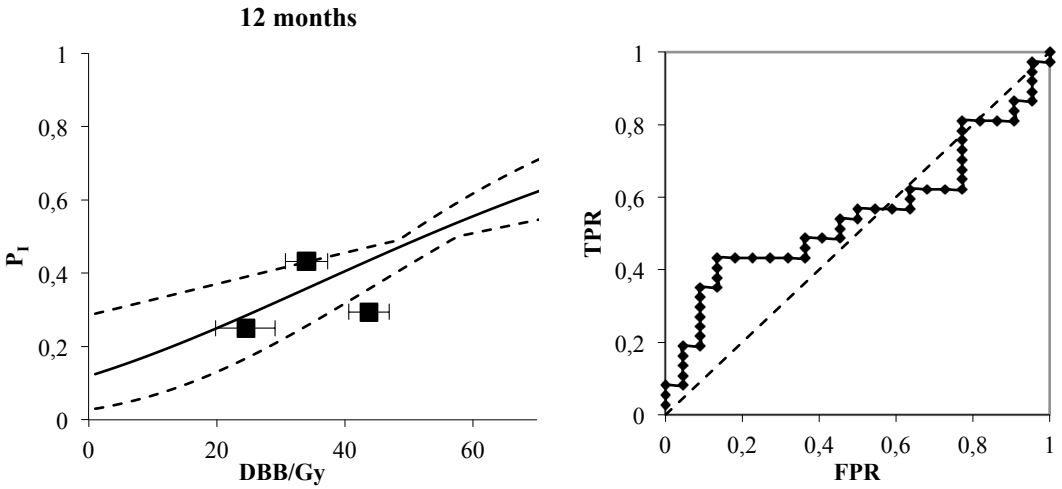

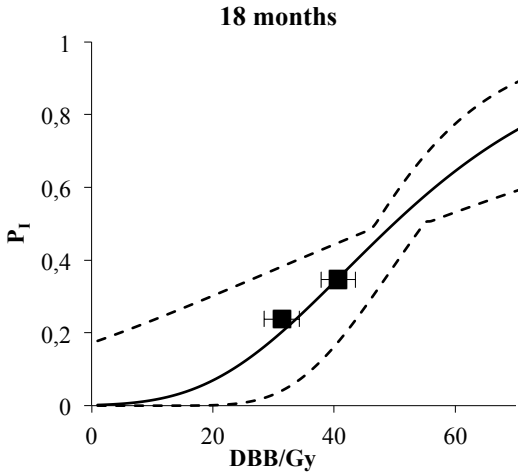

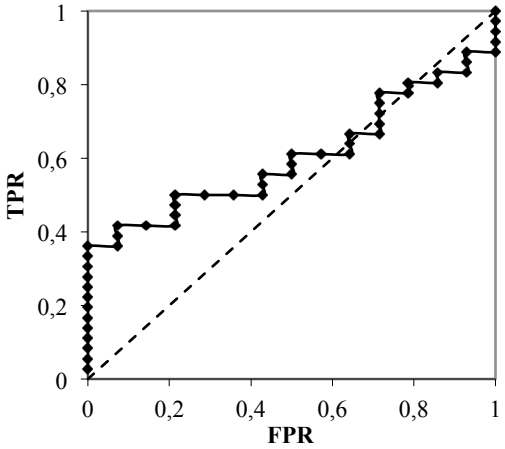

Appendix C.2 – *G*0 vs. *G*1+*G*2

- CONTRALATERAL PAROTID

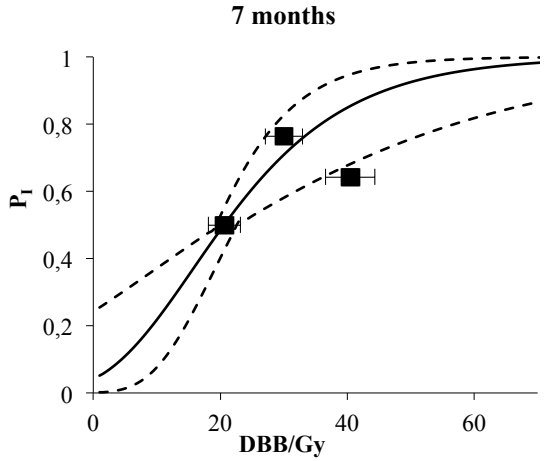

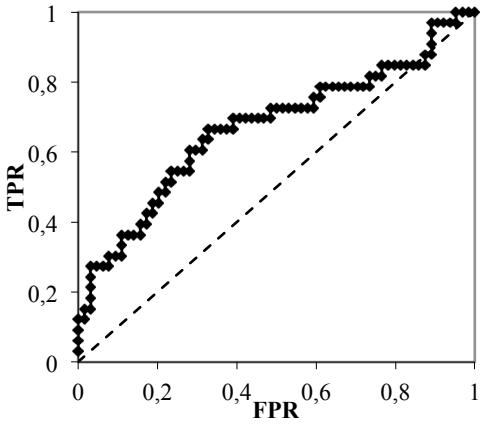

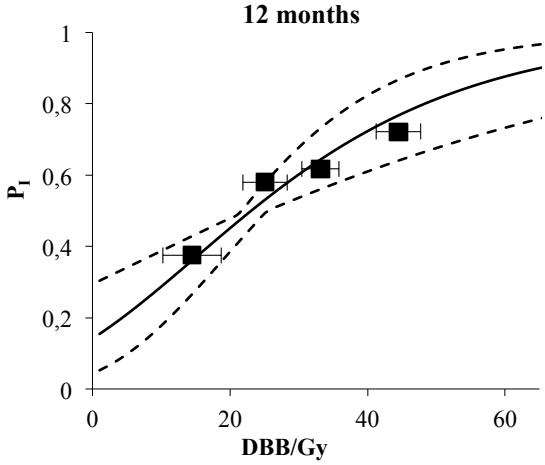

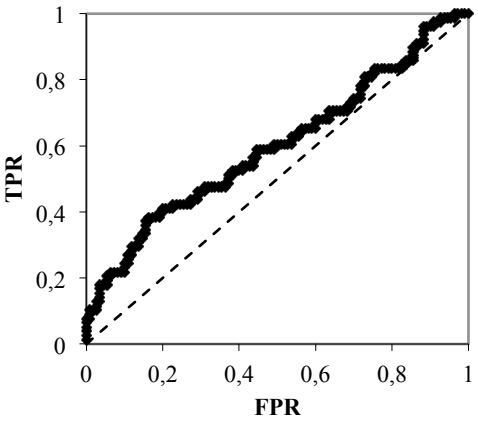

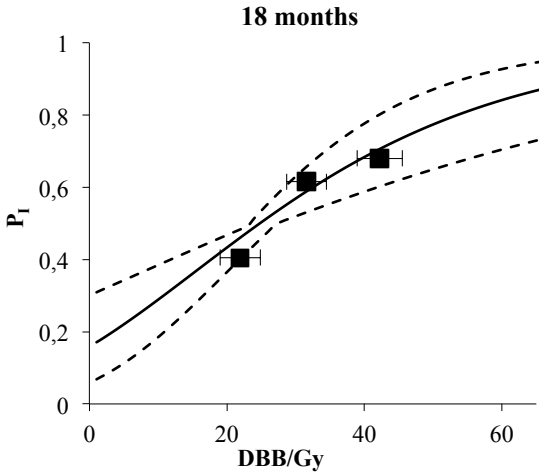

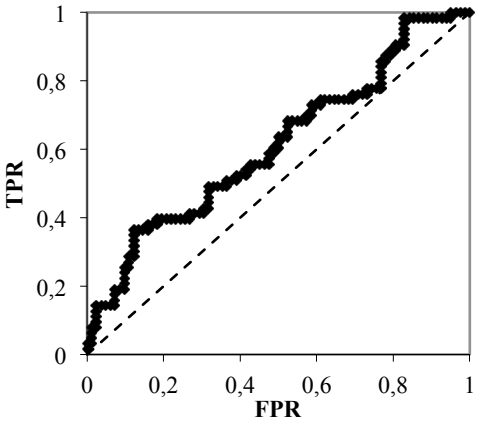

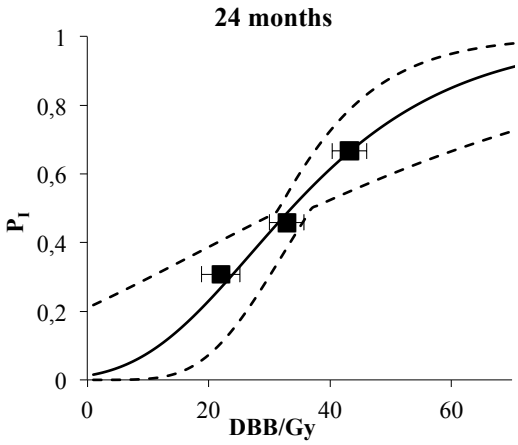

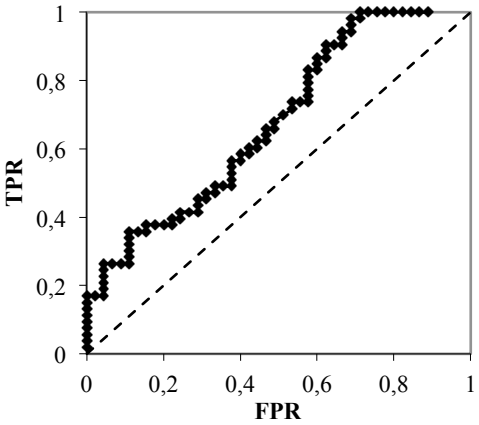

- IPSILATERAL PAROTID

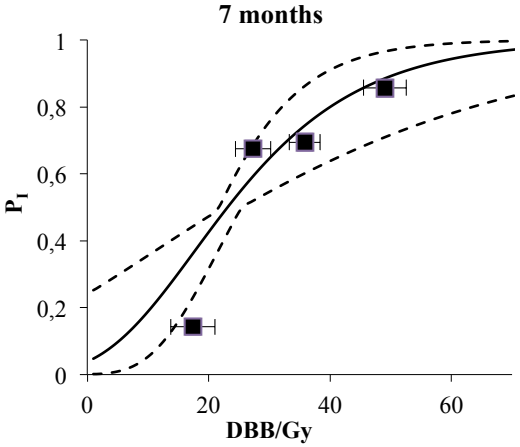

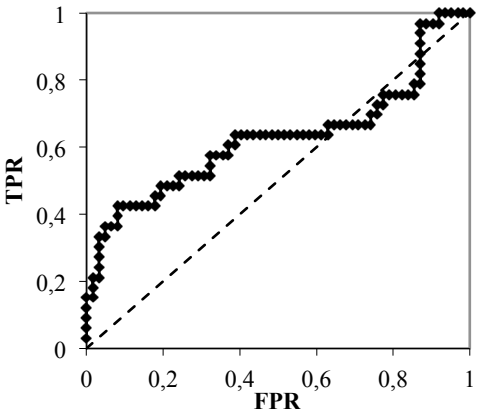

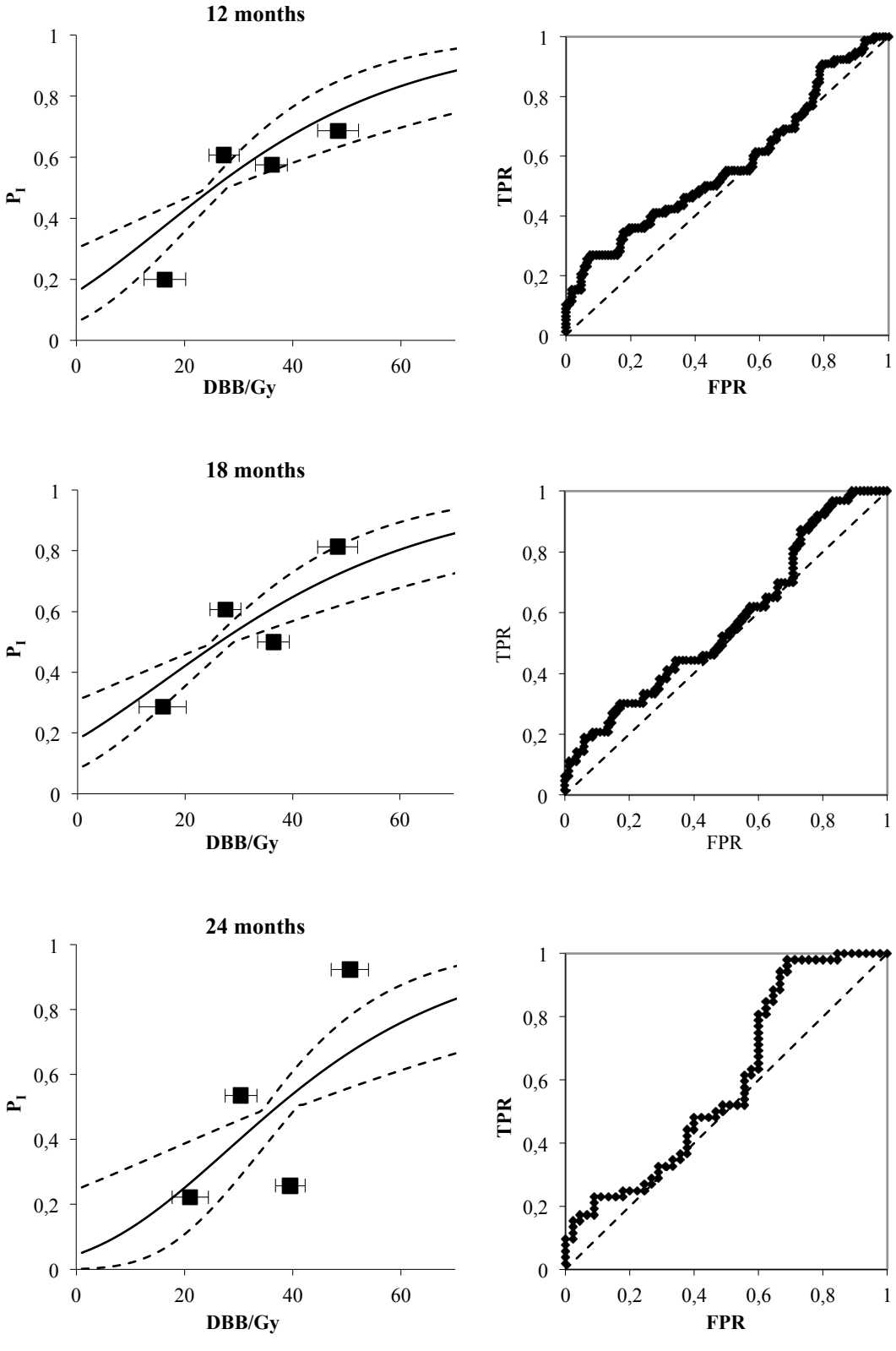
12 months
P_I
DBB/Gy
TPR
FPR
18 months
P_I
DBB/Gy
TPR
FPR
24 months
P_I
DBB/Gy
TPR
FPR

- PAROTIDS SUM

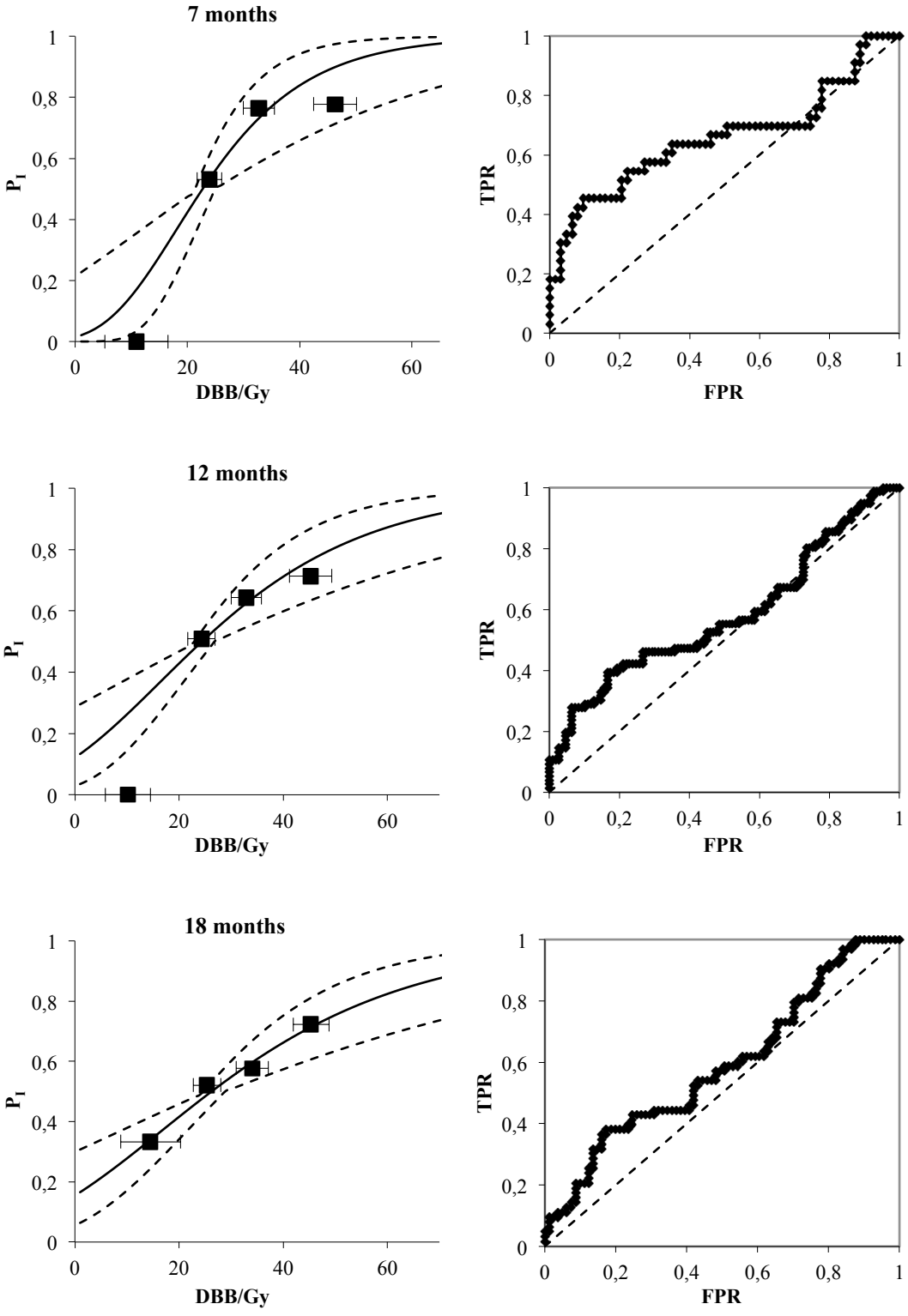

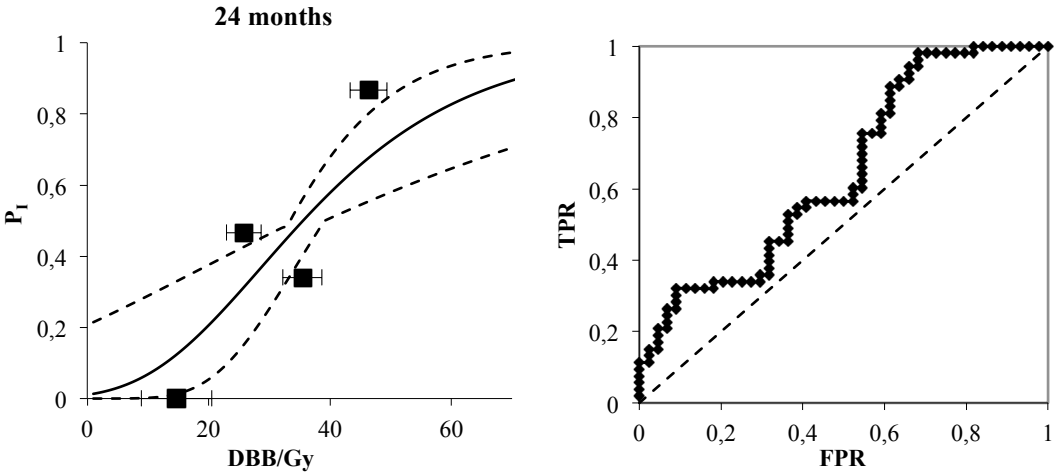

- SALIVARY GLANDS – 4 structures

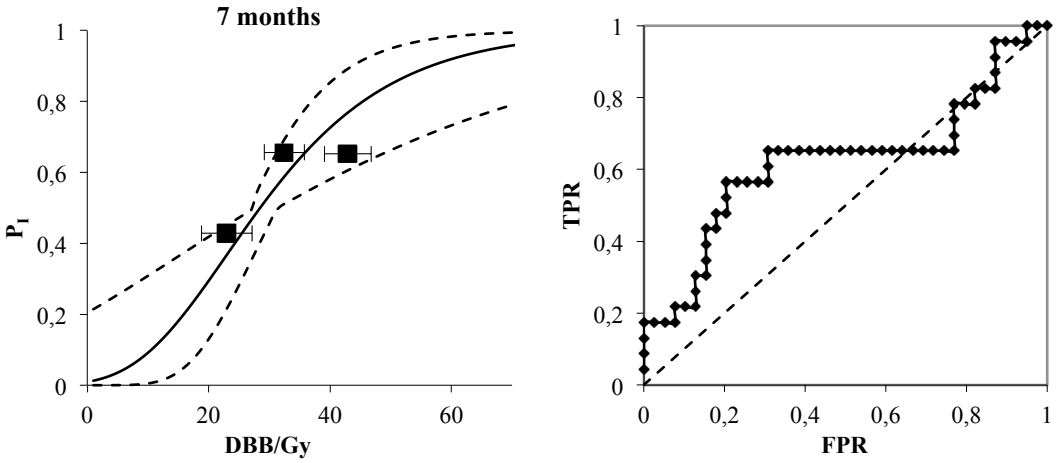

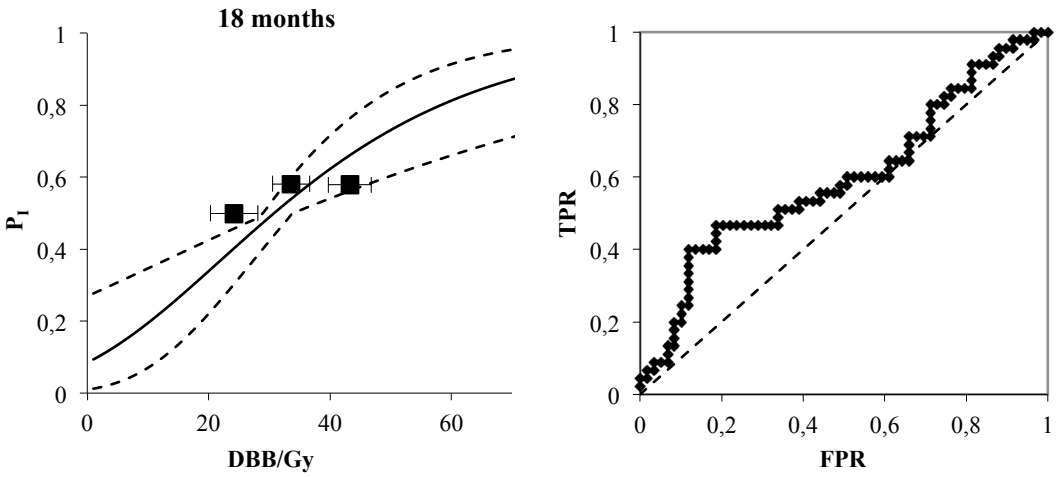

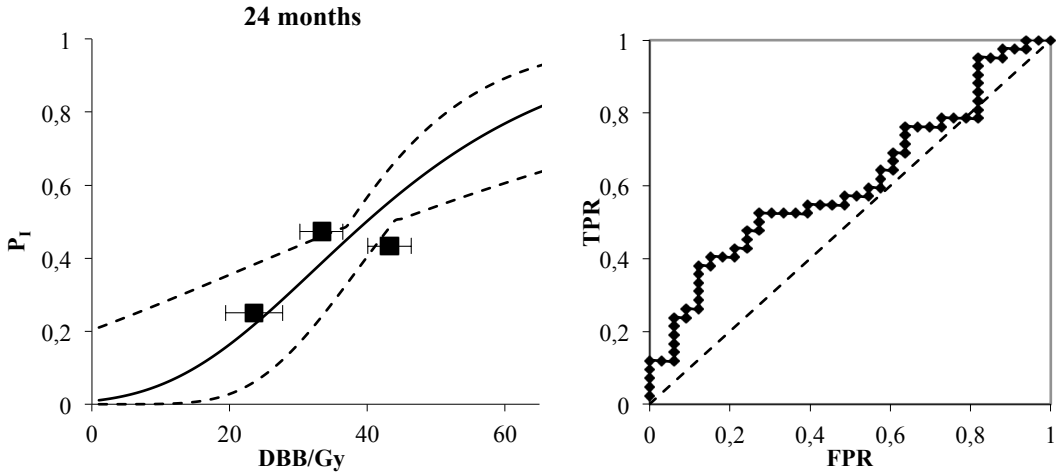

- SALIVARY GLANDS - 5 structures

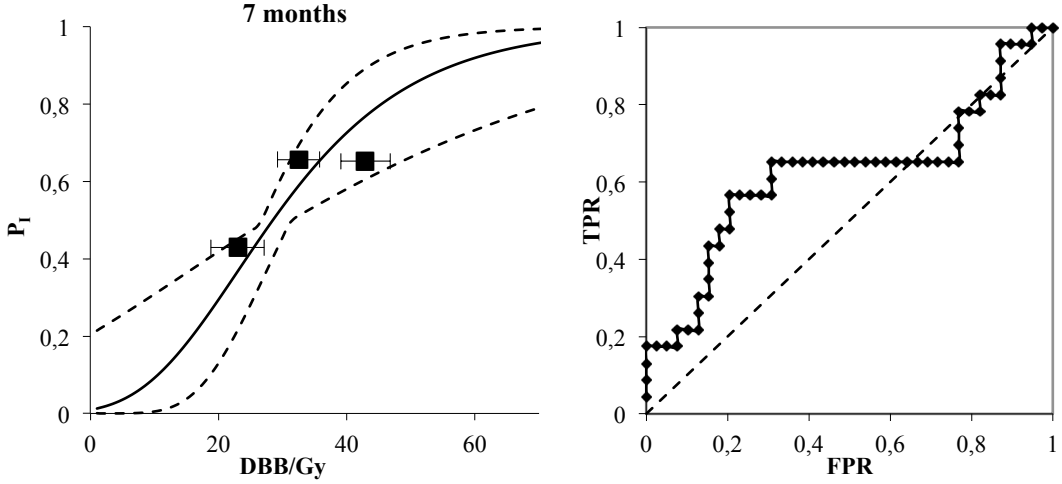

Appendix D – Seriality Model Parameters

Appendix D.1 – *G*0 vs. *G*2

	CONTRALATERAL PAROTID					
Follow-up Time	**7 weeks**	**3 months**	**7 months**	**12 months**	**18 months**	**24 months**
Nb. Patients	135	74	54	112	85	68
D_{50} (Gy) [68% CI]	9.6 [8.6-10.6]	22.6 [20.3-35.6]	32.2 [29.0-35.4]	38.6 [34.7-42.5]	51.7 [46.5-56.9]	48.3 [43.5-53.1]
γ [68% CI]	0.150 [0.045-0.225]	0.224 [0.067-0.381]	0.609 [0.183-1.035]	0.707 [0.212-1.202]	0.444 [0.133-0.755]	0.685 [0.183-1.165]
s	0.008	0.056	$1x10^{-4}$	$1x10^{-4}$	$1x10^{-4}$	$1x10^{-4}$

	IPSILATERAL PAROTID					
Follow-up Time	**7 weeks**	**3 months**	**7 months**	**12 months**	**18 months**	**24 months**
Nb. Patients	133	74	52	110	85	67
D_{50} (Gy) [68% CI]	17.4 [15.7-19.1]	27.9 [25.1-30.7]	33.4 [30.1-36.7]	43.7 [39.3-48.1]	56.5 [50.9-62.2]	61.9 [55.7-68.1]
γ [68% CI]	0.518 [0.155-0.881]	0.383 [0.115-0.651]	0.593 [0.179-1.012]	0.594 [0.178-1.010]	0.442 [0.133-0.751]	0.489 [0.147-0.831]
s	$1x10^{-4}$	0.005	$1x10^{-4}$	$1x10^{-4}$	$1x10^{-4}$	$1x10^{-4}$

	PAROTIDS SUM					
Follow-up Time	**7 weeks**	**3 months**	**7 months**	**12 months**	**18 months**	**24 months**
Nb. Patients	133	74	56	109	84	67
D_{50} (Gy) [68% CI]	15.7 [14.1-17.3]	26.3 [23.7-28.9]	32.5 [29.3-35.8]	39.2 [35.3-43.1]	54.2 [48.8-59.6]	51.7 [46.5-56.9]
γ [68% CI]	0.456 [0.137-0.775]	0.338 [0.101-0.575]	0.655 [0.197-1.114]	0.730 [0.219-1.241]	0.468 [0.140-0.796]	0.633 [0.190-1.076]
s	$1x10^{-4}$	0.006	0.001	$1x10^{-4}$	$1x10^{-4}$	$1x10^{-4}$

	SALIVARY GLANDS_4					
Follow-up Time	**7 weeks**	**3 months**	**7 months**	**12 months**	**18 months**	**24 months**
Nb. Patients	59	26	32	75	61	53
D_{50} (Gy) [68% CI]	20.4 [18.4-22.4]	21.2 [19.1-23.3]	44.9 [40.4-49.4]	50.9 [45.8-56.0]	49.5 [44.6-54.5]	87.7 [78.9-96.5]
γ [68% CI]	0.448 [0.134-0.762]	$1x10^{-4}$ [$3x10^{-5}$-$2x10^{-4}$]	0.685 [0.206-1.165]	0.468 [0.140-0.796]	0.812 [0.244-1.380]	0.411 [0.123-0.699]
s	$1x10^{-4}$	$1x10^{-4}$	$1x10^{-4}$	0.001	$4x10^{-4}$	$1x10^{-4}$

	SALIVARY GLANDS_5					
Follow-up Time	**7 weeks**	**3 months**	**7 months**	**12 months**	**18 months**	**24 months**
Nb. Patients	43	22	24	59	50	41
D_{50} (Gy) [68% CI]	20.1 [18.1-22.1]	16.9 [15.2-18.6]	48.5 [43.7-53.4]	52.4 [47.2-57.6]	49.8 [44.8-54.8]	140.7 [126.6-154.8]
γ [68% CI]	0.618 [0.185-1.051]	$1x10^{-4}$ [$3x10^{-5}$-$2x10^{-4}$]	0.497 [0.149-0.845]	0.278 [0.083-0.473]	0.693 [0.208-1.178]	0.218 [0.065-0.371]
s	$1x10^{-4}$	$1x10^{-4}$	$1x10^{-4}$	0.008	$5x10^{-4}$	$5x10^{-4}$

Appendix D.2 – *G*0 vs. *G*1+*G*2

	CONTRALATERAL PAROTID					
Follow-up Time	**7 weeks**	**3 months**	**7 months**	**12 months**	**18 months**	**24 months**
Nb. Patients	291	171	97	188	145	98
D_{50} (Gy) [68% CI]	3.9 [3.6-4.4]	7.1 [6.4-7.8]	20.6 [18.5-22.7]	23.1 [20.8-25.4]	24.8 [22.3-27.3]	33.6 [30.2-37.0]
γ [68% CI]	$1x10^{-4}$ [$3x10^{-5}$-$2x10^{-4}$]	$1x10^{-4}$ [$3x10^{-5}$-$2x10^{-4}$]	0.429 [0.129-0.729]	0.247 [0.074-0.420]	0.225 [0.068-0.383]	0.547 [0.164-0.930]
s	0.039	0.139	0.026	$3.3x10^{-4}$	$1x10^{-4}$	0.026

	IPSILATERAL PAROTID					
Follow-up Time	**7 weeks**	**3 months**	**7 months**	**12 months**	**18 months**	**24 months**
Nb. Patients	289	171	95	185	145	97
D_{50} (Gy) [68% CI]	4.5 [4.1-5.0]	8.6 [7.7-9.5]	23.1 [20.8-25.4]	25.4 [22.9-27.9]	26.4 [23.8-29.0]	37.1 [33.4-40.8]
γ [68% CI]	$1x10^{-4}$ [$3x10^{-5}$-$2x10^{-4}$]	0.017 [0.005-0.029]	0.435 [0.131-0.740]	0.225 [0.068-0.383]	0.200 [0.060-0.340]	0.416 [0.125-0.707]
s	$1x10^{-4}$	0.010	0.002	$1x10^{-4}$	$1x10^{-4}$	0.021

	PAROTIDS SUM					
Follow-up Time	**7 weeks**	**3 months**	**7 months**	**12 months**	**18 months**	**24 months**
Nb. Patients	288	171	96	185	144	97
D_{50} (Gy) [68% CI]	4.2 [3.8-4.6]	8.9 [8.0-9.8]	22.7 [20.4-25.0]	24.4 [22.0-26.8]	26.2 [23.6-28.8]	35.5 [32.0-39.1]
γ [68% CI]	$1x10^{-4}$ [$3x10^{-5}$-$2x10^{-4}$]	0.035 [0.011-0.060]	0.528 [0.158-0.898]	0.275 [0.083-0.468]	0.230 [0.069-0.391]	0.558 [0.167-0.949]
s	$1x10^{-4}$	0.015	0.003	$1x10^{-4}$	$1x10^{-4}$	0.012

	SALIVARY GLANDS_4					
Follow-up Time	**7 weeks**	**3 months**	**7 months**	**12 months**	**18 months**	**24 months**
Nb. Patients	123	71	62	116	104	75
D_{50} (Gy) [68% CI]	5.7 [5.1-6.3]	7.9 [7.1-8.7]	28.5 [25.7-31.4]	30.0 [27.0-33.0]	30.8 [27.7-33.9]	39.9 [35.9-43.9]
γ [68% CI]	$1x10^{-4}$ [$3x10^{-5}$-$2x10^{-4}$]	$1x10^{-4}$ [$3x10^{-5}$-$2x10^{-4}$]	0.567 [0.170-0.964]	0.284 [0.085-0.483]	0.333 [0.099-0.566]	0.573 [0.172-0.974]
s	$1x10^{-4}$	$1x10^{-4}$	$1x10^{-4}$	0.004	0.008	$1x10^{-4}$

	SALIVARY GLANDS_5					
Follow-up Time	**7 weeks**	**3 months**	**7 months**	**12 months**	**18 months**	**24 months**
Nb. Patients	100	57	49	97	88	63
D_{50} (Gy) [68% CI]	4.8 [4.3-5.3]	7.5 [6.8-8.3]	25.8 [23.2-28.4]	23.7 [21.3-26.1]	24.5 [22.1-27.0]	36.3 [32.7-39.9]
γ [68% CI]	$1x10^{-4}$ [$3x10^{-5}$-$2x10^{-4}$]	$1x10^{-4}$ [$3x10^{-5}$-$2x10^{-4}$]	0.341 [0.102-0.580]	0.126 [0.038-0.214]	0.109 [0.033-0.185]	0.283 [0.085-0.481]
s	$1x10^{-4}$	$1x10^{-4}$	$1x10^{-4}$	0.016	0.029	$1x10^{-4}$

Appendix E – Goodness of the fit

Appendix E.1 – *G*0 vs. *G*2

	CONTRALATERAL PAROTID					
Follow-up Time	**7 wk**	**3 m**	**7 m**	**12 m**	**18 m**	**24 m**
P_I Expected (%)	84.39	59.35	38.63	31.15	25.91	22.10
P_I Observed (%)	84.44	59.46	38.89	31.25	25.88	22.06
Probability of Worst-fit	0.601	0.604	0.611	0.605	0.605	0.601
Reduced X^2	0.013	0.110	0.222	0.069	0.051	0.255
$P_x(X^2_\nu,\nu)$	1	0.954	0.637	0.999	0.995	0.858
Area Under the Curve (AUC)	0.620	0.657	0.685	0.699	0.714	0.706

	IPSILATERAL PAROTID					
Follow-up Time	**7 wk**	**3 m**	**7 m**	**12 m**	**18 m**	**24 m**
P_I Expected (%)	83.87	57.70	44.03	30.89	25.87	22.38
P_I Observed (%)	84.21	58.11	44.23	30.91	25.88	22.39
Probability of Worst-fit	0.601	0.613	0.610	0.603	0.601	0.601
Reduced X^2	0.023	0.167	0.522	0.188	0.166	0.204
$P_x(X^2_\nu,\nu)$	1	0.919	1	0.988	0.956	0.893
Area Under the Curve (AUC)	0.644	0.661	0.674	0.692	0.685	0.671

	PAROTIDS SUM					
Follow-up Time	**7 wk**	**3 m**	**7 m**	**12 m**	**18 m**	**24 m**
P_I Expected (%)	84.03	57.80	40.77	32.08	25.01	22.43
P_I Observed (%)	84.21	58.11	41.07	32.11	25.00	22.39
Probability of Worst-fit	0.601	0.610	0.617	0.605	0.602	0.601
Reduced X^2	0.029	0.119	0.437	0.142	0.086	0.250
$P_x(X^2_\nu,\nu)$	1	0.949	0.646	0.995	0.987	0.861
Area Under the Curve (AUC)	0.628	0.659	0.679	0.694	0.702	0.691

	SALIVARY GLANDS_4					
Follow-up Time	**7 wk**	**3 m**	**7 m**	**12 m**	**18 m**	**24 m**
P_I Expected (%)	81.18	60.89	31.09	31.95	24.53	18.89
P_I Observed (%)	81.36	61.54	31.25	32.00	24.59	18.87
Probability of Worst-fit	0.601	0.603	0.604	0.602	0.604	0.601
Reduced X^2	0.128	0.351	0.454	0.229	0.260	0.307
$P_x(X^2_\nu,\nu)$	0.879	0.553	0.635	0.876	0.771	0.579
Area Under the Curve (AUC)	0.651	0.668	0.674	0.672	0.685	0.657

	SALIVARY GLANDS_5					
Follow-up Time	**7 wk**	**3 m**	**7 m**	**12 m**	**18 m**	**24 m**
P_I Expected (%)	85.86	66.54	33.25	37.25	27.93	24.36
P_I Observed (%)	86.05	68.18	33.33	37.29	28.00	24.39
Probability of Worst-fit	0.601	0.605	0.602	0.601	0.603	0.601
Reduced X^2	0.040	0.332	1.990	0.322	0.356	0.303
$P_x(X^2_\nu,\nu)$	0.997	0.565	0.158	0.725	0.551	0.876
Area Under the Curve (AUC)	0.637	0.703	0.655	0.663	0.673	0.646

Appendix E.2 – *G*0 vs. *G*1+*G*2

	CONTRALATERAL PAROTID					
Follow-up Time	**7 wk**	**3 m**	**7 m**	**12 m**	**18 m**	**24 m**
P_I Expected (%)	92.11	80.46	65.78	58.42	56.56	45.95
P_I Observed (%)	92.78	80.70	65.98	58.51	56.55	45.92
Probability of Worst-fit	0.603	0.601	0.604	0.604	0.602	0.602
Reduced X^2	0.011	0.033	0.027	0.033	0.093	0.061
$P_x(X^2_\nu,\nu)$	1	1	0.999	1	0.999	0.999
Area Under the Curve (AUC)	0.602	0.650	0.648	0.661	0.660	0.665

	IPSILATERAL PAROTID					
Follow-up Time	**7 wk**	**3 m**	**7 m**	**12 m**	**18 m**	**24 m**
P_1 Expected (%)	92.54	80.48	65.00	57.76	56.53	46.47
P_1 Observed (%)	92.73	80.70	65.26	57.84	56.55	46.49
Probability of Worst-fit	0.601	0.601	0.604	0.603	0.601	0.601
Reduced X^2	0.089	0.039	0.095	0.070	0.048	0.160
$P_x(X^2_\nu,\nu)$	1	1	0.993	1	1	0.977
Area Under the Curve (AUC)	0.624	0.657	0.657	0.662	0.660	0.670

	PAROTIDS SUM					
Follow-up Time	**7 wk**	**3 m**	**7 m**	**12 m**	**18 m**	**24 m**
P_1 Expected (%)	92.62	80.48	65.34	58.81	56.26	45.45
P_1 Observed (%)	92.71	80.70	65.63	58.92	56.25	45.36
Probability of Worst-fit	0.601	0.601	0.604	0.604	0.601	0.601
Reduced X^2	0.011	0.046	0.081	0.170	0.002	0.160
$P_x(X^2_\nu,\nu)$	1	1	0.995	0.999	1	0.987
Area Under the Curve (AUC)	0.611	0.654	0.653	0.662	0.660	0.675

	SALIVARY GLANDS_4					
Follow-up Time	**7 wk**	**3 m**	**7 m**	**12 m**	**18 m**	**24 m**
P_1 Expected (%)	90.97	84.46	62.68	56.84	56.71	43.93
P_1 Observed (%)	91.06	85.92	62.90	56.90	56.73	44.00
Probability of Worst-fit	0.601	0.601	0.601	0.602	0.601	0.603
Reduced X^2	0.013	0.046	0.180	0.089	0.057	0.110
$P_x(X^2_\nu,\nu)$	1	0.987	0.837	0.999	0.999	0.954
Area Under the Curve (AUC)	0.631	0.726	0.655	0.661	0.660	0.670

	SALIVARY GLANDS_5					
Follow-up Time	**7 wk**	**3 m**	**7 m**	**12 m**	**18 m**	**24 m**
P_1 Expected (%)	93.96	85.75	62.68	61.82	60.22	50.76
P_1 Observed (%)	95.00	87.72	62.90	61.86	60.23	50.79
Probability of Worst-fit	0.601	0.601	0.602	0.601	0.601	0.602
Reduced X^2	0.004	0.078	0.178	0.043	0.110	0.078
$P_x(X^2_\nu,\nu)$	1	0.924	0.837	0.999	0.979	0.924
Area Under the Curve (AUC)	0.616	0.776	0.655	0.659	0.657	0.661

Appendix F – Dose values

Appendix F.1 – *G*0 vs. *G*2

	CONTRALATERAL PAROTID					
Follow-up Time	**7 weeks**	**3 months**	**7 months**	**12 months**	**18 months**	**24 months**
Nb. Patients	135	74	54	112	85	68
***DBB* Complications (Gy)**	31.59±8.03	32.29±7.68	30.04±5.30	33.17±6.51	33.51±10.11	35.20±8.40
***DBB* Complication-free (Gy)**	22.95±11.64	26.58±13.16	24.65±10.35	27.11±9.81	27.60±9.51	28.92±9.32
Threshold (Gy)	24	30	28	28	33	27
Odd Ratio [95% CI]	8.8 [3.17–24.42]	4.00 [1.49–10.73]	3.85 [1.19–12.47]	5.27 [1.85–15.01]	3.25 [1.19–8.89]	3.94 [0.80–19.30]

	IPSILATERAL PAROTID					
Follow-up Time	**7 weeks**	**3 months**	**7 months**	**12 months**	**18 months**	**24 months**
Nb. Patients	133	74	52	110	85	67
***DBB* Complications (Gy)**	34.58±7.27	35.66±6.02	34.09±8.19	35.04±7.54	34.77±8.32	35.88±8.15
***DBB* Complication-free (Gy)**	27.39±12.16	30.04±14.38	28.18±10.15	30.15±9.07	31.05±8.75	32.60±7.93
Threshold (Gy)	30	27	30	28	29	47
Odd Ratio [95% CI]	5.38 [2.01–14.38]	23.10 [2.79–191.54]	4.01 [1.22–13.17]	4.38 [1.40–13.2]	3.40 [0.90–12.76]	12.75 [1.22–133.55]

	PAROTIDS SUM					
Follow-up Time	**7 weeks**	**3 months**	**7 months**	**12 months**	**18 months**	**24 months**
Nb. Patients	133	74	56	109	84	67
***DBB* Complications (Gy)**	33.36±7.20	34.10±6.24	31.14±4.76	34.14±6.80	34.18±9.08	35.54±7.97
***DBB* Complication-free (Gy)**	25.15±12.03	28.64±13.62	26.48±9.74	28.67±8.82	29.58±8.63	30.86±8.30
Threshold (Gy)	26	29	29	28	31	28
Odd Ratio [95% CI]	10.15 [3.59–28.72]	2.42 [1.00–7.39]	3.52 [1.14–10.88]	4.57 [1.60–13.10]	2.93 [1.01–8.53]	2.12 [0.53–8.49]

	SALIVARY GLANDS_4					
Follow-up Time	**7 weeks**	**3 months**	**7 months**	**12 months**	**18 months**	**24 months**
Nb. Patients	59	26	32	75	61	53
***DBB* Complications (Gy)**	38.14±6.15	-	36.36±3.96	36.63±4.62	37.84±3.46	36.69±4.51
***DBB* Complication-free (Gy)**	33.92±10.10	-	32.98±8.66	34.61±7.85	34.39±8.00	35.25±7.95
Threshold (Gy)	31	-	33	33	36	35
Odd Ratio [95% CI]	13.2 [2.75–63.27]	-	7.00 [1.18–41.36]	3.38 [1.09–10.44]	3.27 [0.91–11.81]	4.19 [0.80–22.06]

	SALIVARY GLANDS_5					
Follow-up Time	**7 weeks**	**3 months**	**7 months**	**12 months**	**18 months**	**24 months**
Nb. Patients	43	22	24	59	50	41
***DBB* Complications (Gy)**	38.32±6.49	-	36.80±4.17	36.63±4.84	37.87±3.59	36.59±4.54
***DBB* Complication-free (Gy)**	31.99±11.50	-	34.57±8.53	35.37±8.04	35.16±7.87	36.11±7.77
Threshold (Gy)	32	-	33	32	33	35
Odd Ratio [95% CI]	16.00 [2.19–117.09]	-	9.00 [0.89–91.26]	3.43 [0.85–13.80]	4.29 [0.83–22.03]	2.49 [0.54–11.44]

Appendix F.2 – *G*0 vs. *G*1+*G*2

	CONTRALATERAL PAROTID					
Follow-up Time	**7 weeks**	**3 months**	**7 months**	**12 months**	**18 months**	**24 months**
Nb. Patients	291	171	97	188	145	98
***DBB* Complications (Gy)**	-	-	30.49±6.84	30.97±7.28	32.05±8.19	35.01±8.22
***DBB* Complication-free (Gy)**	-	-	24.76±10.36	27.12±9.76	28.01±9.17	29.09±9.31
Threshold (Gy)	-	-	27	25	25	26
Odd Ratio [95% CI]	-	-	3.93 [1.62–9.53]	2.99 [1.53–5.87]	3.35 [1.51–7.46]	4.47 [1.51–13.24]

	IPSILATERAL PAROTID					
Follow-up Time	**7 weeks**	**3 months**	**7 months**	**12 months**	**18 months**	**24 months**
Nb. Patients	289	171	95	185	145	97
***DBB* Complications (Gy)**	-	-	33.19±7.70	33.29±7.74	34.26±8.83	37.40±9.74
***DBB* Complication-free (Gy)**	-	-	28.16±9.95	30.23±9.03	30.61±9.41	32.84±7.87
Threshold (Gy)	-	-	25	25	25	44
Odd Ratio [95% CI]	-	-	5.79 [2.03–16.49]	4.01 [1.72–9.35]	2.41 [0.93–6.23]	11.29 [2.40–53.08]

	PAROTIDS SUM					
Follow-up Time	**7 weeks**	**3 months**	**7 months**	**12 months**	**18 months**	**24 months**
Nb. Patients	288	171	96	185	144	97
***DBB* Complications (Gy)**	-	-	31.90±9.01	32.21±7.09	33.26±8.30	36.40±8.73
***DBB* Complication-free (Gy)**	-	-	26.49±9.73	28.93±9.00	29.70±8.60	30.94±8.20
Threshold (Gy)	-	-	25	26	27	39
Odd Ratio [95% CI]	-	-	5.73 [2.09–15.73]	3.30 [1.66–6.53]	2.97 [1.37–6.35]	4.14 [1.52–11.25]

	SALIVARY GLANDS_4					
Follow-up Time	**7 weeks**	**3 months**	**7 months**	**12 months**	**18 months**	**24 months**
Nb. Patients	123	71	62	116	104	75
***DBB* Complications (Gy)**	-	-	36.74±6.51	36.74±6.10	37.21±6.67	38.40±6.48
***DBB* Complication-free (Gy)**	-	-	32.81±8.50	34.61±7.93	34.54±7.66	35.03±7.83
Threshold (Gy)	-	-	31	33	31	31
Odd Ratio [95% CI]	-	-	5.04 [1.62–15.64]	2.66 [1.22–5.82]	4.51 [1.67–12.17]	4.03 [1.19–13.66]

	SALIVARY GLANDS_5					
Follow-up Time	**7 weeks**	**3 months**	**7 months**	**12 months**	**18 months**	**24 months**
Nb. Patients	100	57	49	97	88	63
***DBB* Complications (Gy)**	-	-	36.74±6.51	36.97±6.13	37.10±6.99	38.25±6.55
***DBB* Complication-free (Gy)**	-	-	32.81±8.50	35.38±8.03	35.38±7.38	36.25±7.84
Threshold (Gy)	-	-	31	30	31	35
Odd Ratio [95% CI]	-	-	5.04 [1.62–15.64]	2.80 [0.96–8.19]	3.43 [1.19–9.88]	2.35 [0.84–6.55]